uOttawa

L'Université canadienne
Canada's university

FACULTÉ DES ÉTUDES SUPÉRIEURES ET POSTOCTORALES

uOttawa

L'Université canadienne
Canada's university

FACULTY OF GRADUATE AND POSDOCTORAL STUDIES

Kessiri Kongmanas
AUTEUR DE LA THÈSE / AUTHOR OF THESIS

M.Sc. (Biochemistry)
GRADE / DEGREE

Department of Biochemistry, Microbiology and Immunology
FACULTÉ, ÉCOLE, DÉPARTEMENT / FACULTY, SCHOOL, DEPARTMENT

Significance of Sulfogalactosylglycerolipid in Male Fertility:
Studies Using Cgt Heterozygous Mice

TITRE DE LA THÈSE / TITLE OF THESIS

Nuch Tanphaichitr
DIRECTEUR (DIRECTRICE) DE LA THÈSE / THESIS SUPERVISOR

CO-DIRECTEUR (CO-DIRECTRICE) DE LA THÈSE / THESIS CO-SUPERVISOR

EXAMINATEURS (EXAMINATRICES) DE LA THÈSE / THESIS EXAMINERS

Ajoy Basak

Xiaochui Zha

Gary W. Slater
Le Doyen de la Faculté des études supérieures et postdoctorales / Dean of the Faculty of Graduate and Postdoctoral Studies

SIGNIFICANCE OF SULFOGALACTOSYLGLYCEROLIPID IN MALE FERTILITY: STUDIES USING *Cgt* HETEROZYGOUS MICE

by

Kessiri Kongmanas

Thesis submitted to the Department of Biochemistry, Microbiology and Immunology in partial fulfillment to the requirements for the degree of Master of Science

University of Ottawa

Ottawa, Ontario, Canada

© copyright
© 2008, Kessiri Kongmanas, Ottawa, Ontario, Canada

Library and Archives Canada

Published Heritage Branch

395 Wellington Street
Ottawa ON K1A 0N4
Canada

Bibliothèque et Archives Canada

Direction du Patrimoine de l'édition

395, rue Wellington
Ottawa ON K1A 0N4
Canada

Your file Votre référence
ISBN: 978-0-494-50896-1
Our file Notre référence
ISBN: 978-0-494-50896-1

NOTICE:
The author has granted a non-exclusive license allowing Library and Archives Canada to reproduce, publish, archive, preserve, conserve, communicate to the public by telecommunication or on the Internet, loan, distribute and sell theses worldwide, for commercial or non-commercial purposes, in microform, paper, electronic and/or any other formats.

The author retains copyright ownership and moral rights in this thesis. Neither the thesis nor substantial extracts from it may be printed or otherwise reproduced without the author's permission.

AVIS:
L'auteur a accordé une licence non exclusive permettant à la Bibliothèque et Archives Canada de reproduire, publier, archiver, sauvegarder, conserver, transmettre au public par télécommunication ou par l'Internet, prêter, distribuer et vendre des thèses partout dans le monde, à des fins commerciales ou autres, sur support microforme, papier, électronique et/ou autres formats.

L'auteur conserve la propriété du droit d'auteur et des droits moraux qui protège cette thèse. Ni la thèse ni des extraits substantiels de celle-ci ne doivent être imprimés ou autrement reproduits sans son autorisation.

In compliance with the Canadian Privacy Act some supporting forms may have been removed from this thesis.

While these forms may be included in the document page count, their removal does not represent any loss of content from the thesis.

Conformément à la loi canadienne sur la protection de la vie privée, quelques formulaires secondaires ont été enlevés de cette thèse.

Bien que ces formulaires aient inclus dans la pagination, il n'y aura aucun contenu manquant.

Canada

ACKNOWLEDGEMENTS

First of all, I would like to thank my supervisor, Dr. Nongnuj Tanphaichitr, for her supervision of this project. Her thoughtful guidance has helped me develop many skills that are important for my career in science. I would also like to express my appreciation to all my thesis advisory committee members, Drs. Vas Mezl, Mike Wade, Euridice Carmona and Richard Bergeron for their valuable guidance. I would also like to acknowledge Dr. Kym Faull at University of California, Los Angeles, U.S.A. for his collaboration with respect to the mass spectrometry work.

I also thank my past and present colleagues for their support and encouragement during my studies. My special thanks go to Hongbin Xu, a Ph.D. student in our lab, for his assistance with the *in vitro* fertilization experiments, and Drs. Maroun Bou Khalil and Wattana Weerachatyanukul, former members in our lab, for their dedication in training me in the lipid work.

I gratefully acknowledge the Development and Promotion of Science and Technology Talents Project (DPST) Scholarship from the Institute for the Promotion of Teaching Science and Technology, Ministry of Science, Royal Thai government for their support of my basic stipend and tuition and fees at the University of Ottawa.

Finally, I would like to thank my family including my parents, my brother and my sister, whose love and understanding have enabled me to complete this work.

ABSTRACT

Sulfogalactosylglycerolipid (SGG) is a sulfoglycolipid present specifically at a substantial level in mammalian male germ cells. It has been shown to function as an adhesion molecule important for sperm-egg interaction and a structural lipid involved in formation of sperm lipid rafts during capacitation *in vitro*. Due to the unique characteristics and functions, SGG can potentially serve as a biomarker for sperm fertility as well as a target for development of a non-hormonal contraceptive. To confirm the *in vivo* roles of SGG, we sought for transgenic mice with reduced amounts of sperm SGG. *Cgt* knockout male mice, transgenetically deficient in UDP-galactose:ceramide galactosyltransferase (CGT), an enzyme involved in SGG synthesis, are infertile due to spermatogenesis disruption. However, the $Cgt^{+/-}$ males can still produce sperm and sire offspring. We hypothesized that $Cgt^{+/-}$ males, expected to have reduced SGG amounts, would have compromised fertilizing ability and could serve as *in vivo* models for studying roles of SGG in fertilization and spermatogenesis. Unexpectedly, our results revealed that $Cgt^{+/-}$ males exhibited unimpaired spermatogenesis and fecundity. Moreover, the levels of SGG as well as lipid profiles of sperm and testes of $Cgt^{+/-}$ mice were similar to those of the wild type, suggesting that compensatory mechanisms must have occurred to maintain SGG levels in the $Cgt^{+/-}$ mice. Although these results revealed that $Cgt^{+/-}$ mice could not be used as the animal models, they implicated significance of normal testis and sperm SGG levels in maintaining normal spermatogenesis and fertility. The possible compensatory mechanisms regulating SGG levels were further investigated in $Cgt^{+/-}$ mice. As expected, only half of *Cgt* mRNA expression level of the wild type was transcribed in the $Cgt^{+/-}$ testes; however, testicular CGT polypeptides as well as their enzymatic activities in the $Cgt^{+/-}$ mice were found at a comparable level to those of the wild type. On the other hand, no change was found in terms of mRNA levels, polypeptide levels or enzymatic activities of arylsulfatase A (ASA), the enzyme responsible for SGG degradation in the testis. In conclusion, the compensatory mechanisms for SGG level adjustment in $Cgt^{+/-}$ mice occurred through the biosynthetic pathway, rather than the degradation pathway, by increasing the CGT polypeptide expression level. Therefore, identification of specific spermatogenic cell stages, contributing to normal expression levels of CGT and SGG in the $Cgt^{+/-}$ testes warrants further studies, as these studies should provide useful information regarding CGT and SGG importance during male

germ cell development. In addition, a new approach to produce the animal models that can produce sperm with reduced SGG levels should be attempted. The RNA interference (RNAi) techniques may be tried to achieve this goal.

TABLE OF CONTENTS

Acknowledgments.....ii

Abstract.....iii

Table of Contents.....v

List of Figures.....viii

List of Tables.....x

List of Abbreviations.....xi

CHAPTER ONE

Introduction

1.1 Overview.....1

1.2 Spermatogenesis.....2

1.3 Spermatogenic stage and cycle.....13

1.4 Sertoli cell-germ cell interactions during spermatogenesis.....15

1.5 Epididymal sperm maturation.....17

1.6 Capacitation.....19

1.7 Acrosome reaction and sperm-ZP interaction.....21

1.8 Sulfogalactosylglycerolipid (SGG).....22

1.8.1 Biosynthesis of SGG.....24

1.8.2 Synthetic sites and cellular localization of SGG.....26

1.8.3 Degradation of SGG during spermatogenesis.....28

1.8.4 Roles of SGG in male reproduction.....29

1.9 Statements of problems.....32

1.10 Hypothesis.....32

1.11 Specific aims.....32

CHAPTER TWO

Materials and Methods

2.1 Animals.....33

2.2 Mating study.....34

2.3 *In Vitro* Fertilization (IVF).....34
2.4 Collection of sperm and testes for biochemical and histological work....36
2.5 Lipid extraction.....36
2.6 SGG quantification by Azure A assay.....37
2.7 Electrospray ionization mass spectrometry (ESI-MS).....38
2.8 High Performance Thin Layer Chromatography (HPTLC).....38
2.9 Histological analyses of testes.....39
2.10 RNA extraction and reverse transcription.....40
2.11 Quantitative real-time PCR.....41
2.12 Production of anti-CGT antibody.....43
2.13 Immunoblotting and densitometric analysis.....44
2.14 CGT enzymatic activity assay.....45
2.15 ASA enzymatic activity assay.....46
2.16 Statistical analyses.....47

CHAPTER THREE

Results

3.1 Genotyping of *Cgt* transgenic mice.....48
3.2 Fecundity of $Cgt^{+/-}$ mice.....48
3.3 Spermatogenesis status of $Cgt^{+/-}$ mice.....50
3.4 Lipid profiles of testes and sperm of $Cgt^{+/-}$ and wild type mice.....54
3.5 Quantification of SGG in sperm and testes of $Cgt^{+/-}$ and wild type mice.57
3.6 *Cgt* mRNA expression levels in $Cgt^{+/-}$ mice.....61
3.7 CGT polypeptide levels in $Cgt^{+/-}$ mice.....61
3.8 Enzymatic activity of CGT in $Cgt^{+/-}$ mice.....63
3.9 Levels of SGG degradation mediated by arylsulfatase A in $Cgt^{+/-}$ mice...66

CHAPTER FOUR

Discussion

4.1 Fertility status and sperm SGG levels of $Cgt^{+/-}$ mice.....71

4.2 Spermatogenesis status and testis SGG levels of *Cgt*$^{+/-}$ mice.....71
4.3 Compensatory mechanisms to adjust SGG levels in *Cgt*$^{+/-}$ mice.....73
4.4 Future directions.....78
4.5 Alternative approaches to study *in vivo* functions of SGG.....80
4.6 Potential translation of CGT and SGG in male contraceptives.....81

REFERENCES.....84

APPENDIX I.....95
APPENDIX II.....98

LIST OF FIGURES:

FIGURE	DESCRIPTION	PAGE
1.1	Seminiferous tubules	3
1.2	Spermatogenesis	5
1.3	Meiosis phase of spermatogenesis	7
1.4	Spermiogenesis	8
1.5	Spermatid and Sertoli cell interactions	11
1.6	Mammalian spermatozoon	12
1.7	Spermatogenic cycles of rat and mouse	14
1.8	Hormonal regulation of spermatogenesis	16
1.9	Sperm-egg interactions	18
1.10	Chemical structures of SGG and SGC	23
1.11	Biosynthetic pathway of SGG/SGC	25
3.1	Genotyping of *Cgt* transgenic mice	49
3.2	*In vitro* fertilizing ability of wild type and $Cgt^{+/-}$ sperm	51
3.3	Average litter size obtained from females mated with $Cgt^{+/-}$ and wild type mice	52
3.4	Light microscopy of testis sections from adult $Cgt^{+/-}$ and wild type mice	53
3.5	Total numbers of sperm from $Cgt^{+/-}$ and wild type mice	55
3.6	HPTLC of sperm and testis lipids from $Cgt^{+/-}$ and wild type mice	56
3.7	Azure A assay and ESI-MS	58
3.8	Quantification of SGG in $Cgt^{+/-}$ and wild type sperm	59
3.9	Quantification of SGG in $Cgt^{+/-}$ and wild type testes	60
3.10	*Cgt* mRNA expression levels in $Cgt^{+/-}$ vs wild type testes	62
3.11	Expression level of CGT polypeptides in $Cgt^{+/-}$ and wild type testes	64
3.12	CGT enzymatic activities at various time points	65
3.13	Enzymatic activity of CGT in $Cgt^{+/-}$ and wild type testes	67

FIGURE	DESCRIPTION	PAGE
3.14	Expression level of *ASA* mRNA in $Cgt^{+/-}$ and wild type testes	69
3.15	Polypeptide expression and enzymatic activity of ASA in $Cgt^{+/-}$ and wild type testes	70
4.1	Compensation of other ceramide-based lipids in the *Cgt* knockout mice	77
4.2	Biosynthesis pathway of glycosphingolipids	83

LIST OF TABLE:

TABLE	DESCRIPTION	PAGE
1	SGG/SGC binding molecules	31

LIST OF ABBREVIATIONS:

ABBREVIATION	DESCRIPTION
ASA	Arylsulfatase A
Cer	Ceramide
Chol	Cholesterol
CGT	UDP-galactose:ceramide galactosyltransferase (protein)
Cgt	UDP-galactose:ceramide galactosyltransferase (gene)
CST	Cerebroside sulfotransferase (protein)
Cst	Cerebroside sulfotransferase (gene)
FSH	Follicle stimulating hormone
GC	Galactosylceramide
GG	Galactosylglycerolipid
GnRH	Gonadotropin releasing hormone
LH	Luteinizing hormone
MLD	Metachromic leukodystrophy
NCS	*p*-nitrocatechol sulfate
PC	Phosphatidylcholine
PE	Phosphatidylethanolamine
PUFA	Polyunsaturated fatty acid
SGC	Sulfogalactosylceramide
SGG	Sulfogalactosylglycerolipid
SM	Sphingomyelin
STDs	Sexually transmitted diseases
T	Testosterone
ZP	Zona pellucida

CHAPTER ONE

INTRODUCTION

1.1 Overview

Many advances have been made in the field of reproductive technology; however, the perfect solutions to male infertility and contraception remain elusive. The most common cause of infertility is sperm dysfunction, diagnosed through semen analysis using sperm concentration, motility, and morphology as the identifying criteria. However, these criteria can only provide limited prognostic and diagnostic information for infertile couples. New biomarkers of sperm function are in need, especially those involved in key physiological processes, e.g. capacitation and sperm-egg interaction. In terms of contraception, none of the present commonly used methods is ideal: reliable, safe, and reversible. Female hormonal contraceptives (e.g., pill, patch), the most commonly used, are reliable in preventing pregnancy but they can have adverse side effects and cannot prevent sexually transmitted diseases (STDs). The common barrier contraceptives, i.e., condoms are safer because they can prevent pregnancy as well as STDs. However, they are less popular than the female contraceptives because they reduce sensation for both partners. Consequently, new contraceptives must be developed to meet this critical need.

Concerning these problems, one should look for the molecule, which is selectively present in spermatogenic cells and sperm with significant function in fertilization, as a potential target for a non-hormonal contraceptive and/or a biomarker of sperm fertilizing ability. Based on these criteria, our lab has been interested in sulfogalactosylglycerolipid (SGG), a sulfoglycolipid present specifically and abundantly in male germ cells. It is also evolutionally conserved among several mammalian species. To date, we have shown that SGG has dual functions as: 1) an adhesion molecule, involved in sperm-ZP binding and

sperm-egg plasma membrane binding *in vitro*, and 2) a structural lipid, involved in the formation of capacitated sperm lipid rafts, which are the sperm surface platforms for ZP binding (Bou et al., 2006; Tanphaichitr et al., 2007). Moreover, studies by Japanese researchers of knockout mice lacking enzymes responsible for SGG synthesis reveal that SGG is essential for spermatogenesis (Fujimoto et al., 2000; Honke et al., 2002). Due to the unique properties and significant roles in male fertility, SGG may serve as a reliable biomarker of sperm function and as a potential target for developing a non-hormonal male contraceptive. However, a comprehensive understanding of the cellular and molecular mechanisms of SGG in the male reproduction is required, as is a confirmation of *in vivo* roles of SGG in male fertility.

1.2 Spermatogenesis

The spermatogenesis process takes place in the seminiferous tubule of the testes. Each seminiferous tubule consists of the seminiferous epithelium with the seminiferous lumen in the center, into which mature spermatozoa generated by spermatogenesis are released. The seminiferous epithelium contains two cell populations: 1) Sertoli cells, somatic columnar epithelial cells which extend from the basal to the apical surface of the seminiferous tubule, and 2) Spermatogenic cells including spermatogonia, primary and secondary spermatocytes, round and elongated spermatids (Figure 1.1A).

In mammals, spermatogenesis is composed of three phases: **the proliferative phase** during which the diploid spermatogonia undergo several mitotic divisions; **the meiotic phase** during which primary spermatocytes give rise to secondary spermatocytes which themselves divide into haploid spermatids; and **the final phase**, spermiogenesis, which

Figure 1.1 Seminiferous tubules. A) Spermatogenesis occurs in the seminiferous tubules of the testis. Each seminiferous tubule is composed of a lumen lined by a specialized epithelium. The seminiferous epithelium contains two cell populations: Sertoli cells and spermatogenic cells (spermatogonia, spermatocytes, and spermatids) **B)** Blood-testis barrier is formed by joining of two occluding junctions of adjacent Sertoli cells. It prevents proteins including antibodies, from reaching developing spermatogenic cells and divides seminiferous epithelium into two compartments: 1) basal compartment, below the junctions, where spermatogonia are located and 2) adluminal compartment, above the junctions, where spermatocytes and spermatids reside.

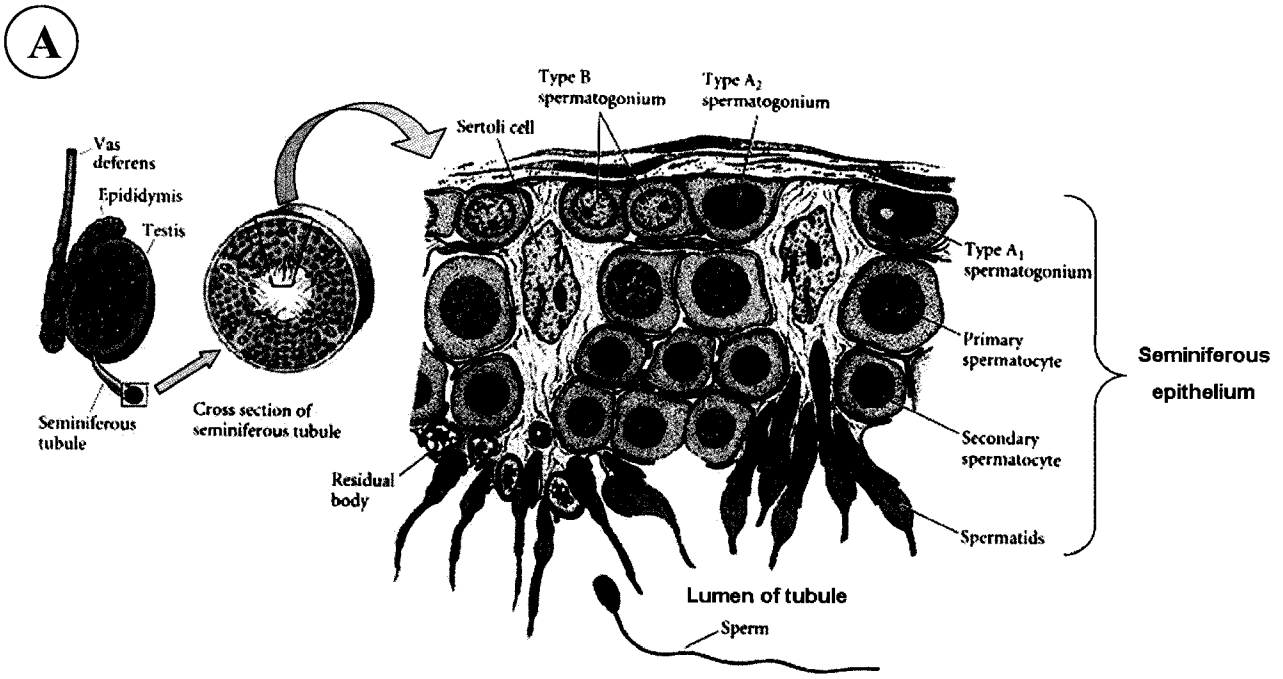

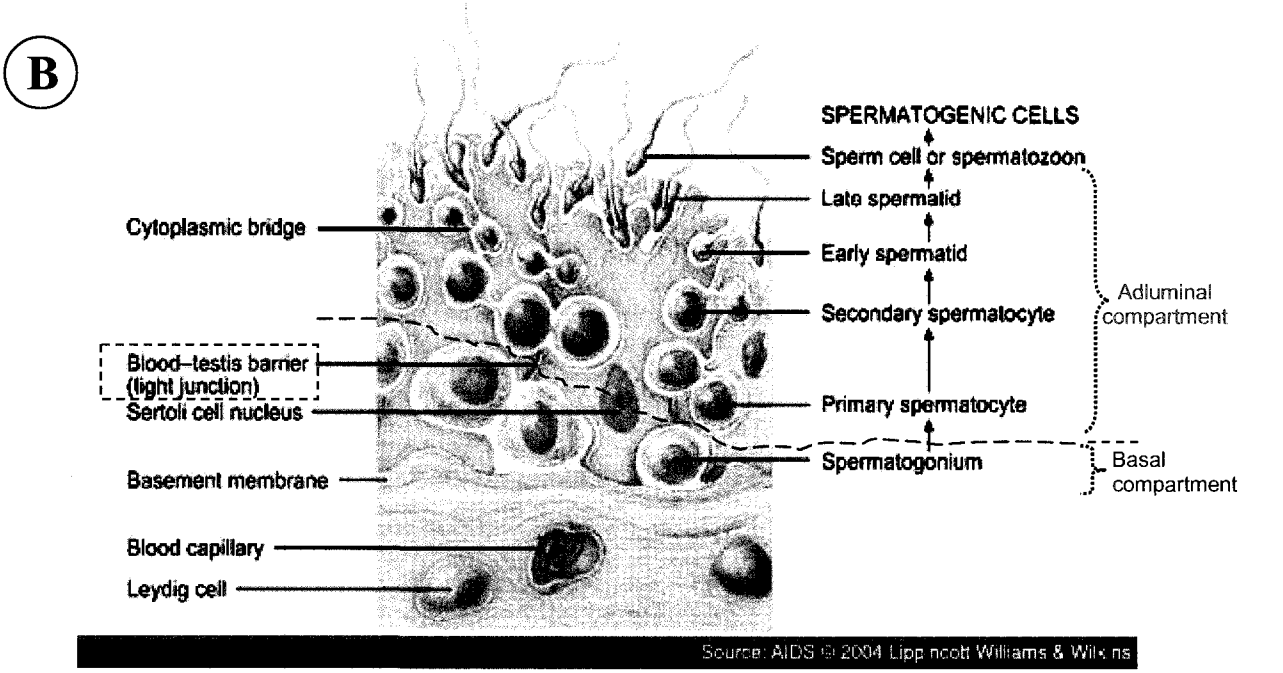

Source: AIDS © 2004 Lippincott Williams & Wilkins

corresponds to the metamorphosis of spermatids into spermatozoa (Figure 1.2) (Alberts et al., 2002; de Kretser and Kerr, 1994). Details of events in each phase are described below:

1) The proliferative phase. The spermatogonial type A stem cells proliferate to produce two types of cells: differentiating spermatogonia and spermatogonial stem cells for the next spermatogenesis cycle. The differentiating cells, which are intermediate (In) and type B spermatogonia, divide and give rise to the more specialized meiotic spermatocytes, but they do not divide to produce new stem cells. In rodents, type A spermatogonia can be further divided into four subtypes: types A_1, A_2, A_3, and A_4. The type A_1 spermatogonial cells subsequently go through six mitoses, generating A_2, A_3, A_4, In, and B spermatogonia, and preleptotene spermatocytes (Dym, 1977; Dym, 1994).

2) The meiotic phase. The first meiotic division is characterized by a long prophase, which can be divided into substages including leptotene, zygotene, pachytene, diplotene and diakinesis. During the prophase of first meiosis, the primary spermatocytes are actively engaged in DNA synthesis. Following the DNA replication, each chromosome of primary spermatocytes appears as a pair of chromatids, having the total DNA content representing twice of that in diploid somatic cells (4C) (de Kretser and Kerr, 1994). Each chromosome, consisting of two sister chromatids, pairs to its homologous chromosome by synapsis to form bivalents. Each member of the bivalent pair subsequently moves to the daughter cells termed secondary spermatocytes. At this step, the secondary spermatocytes contain half the number of chromosomes (haploid number), but actual total DNA content is equivalent to that of somatic cells (2C). The second meiotic division occurs shortly after the first one and during this process, the chromatids of each chromosome separate to daughter cells, termed spermatids, by mechanisms similar to those of a mitotic division. The spermatids contain a

Figure 1.2 Spermatogenesis. Three phases of mammalian spermatogenesis: 1) proliferative phase (mitosis of spermatogonia), 2) meiotic phase, and 3) spermiogenesis (differentiation of spermatids into spermatozoa) (modified from Alberts et al., 2002).

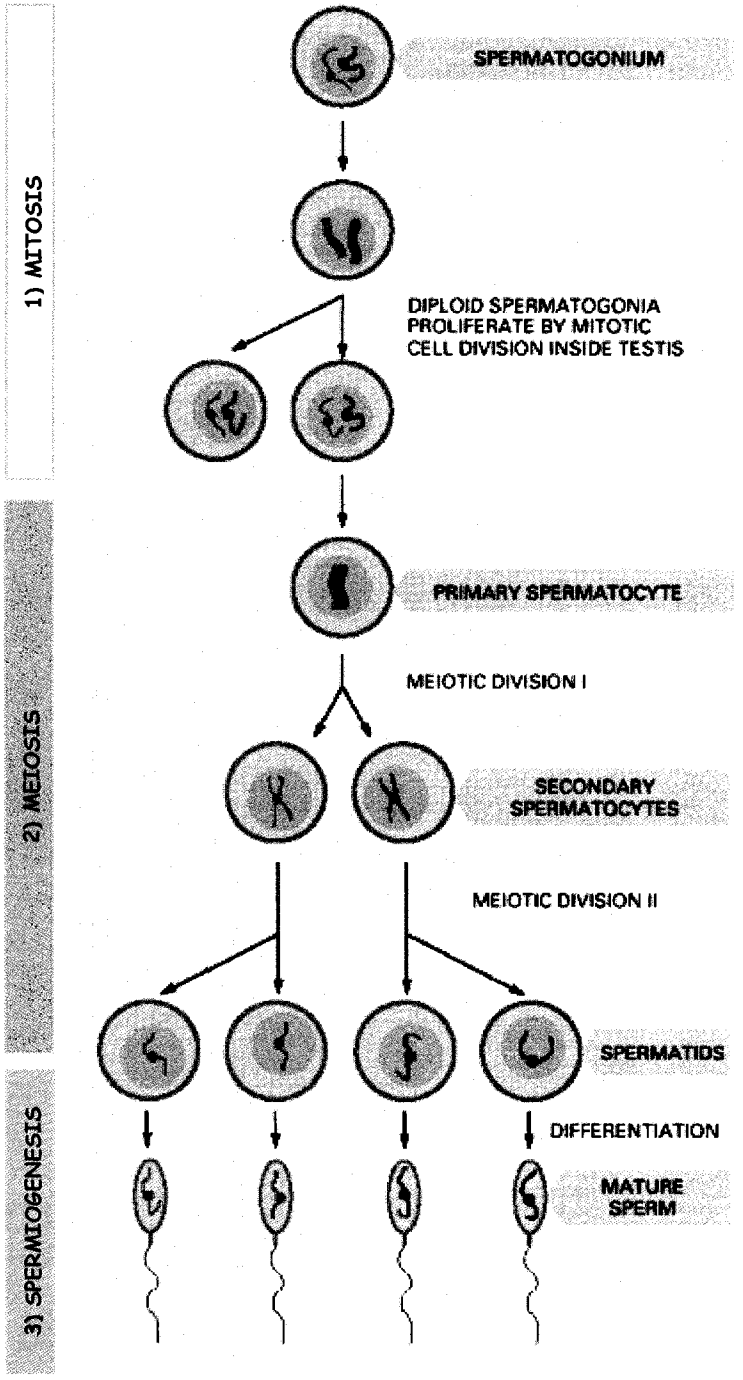
1) MITOSIS
2) MEIOSIS
3) SPERMIOGENESIS
SPERMATOGONIUM
DIPLOID SPERMATOGONIA PROLIFERATE BY MITOTIC CELL DIVISION INSIDE TESTIS
PRIMARY SPERMATOCYTE
MEIOTIC DIVISION I
SECONDARY SPERMATOCYTES
MEIOTIC DIVISION II
SPERMATIDS
DIFFERENTIATION
MATURE SPERM

haploid number of chromosomes and half the DNA content of somatic cells (1C) (Figure 1.3) (Kierszenbaum, 2002).

Since the first meiotic division is a long process (days) and the second meiotic division is very short (minutes), primary spermatocytes exist at a much higher number than secondary spermatocytes (Kierszenbaum, 2002).

3) Spermiogenesis. Each round spermatid differentiates into a structurally and biochemically unique spermatozoon. The major features of this extraordinarily complex process involve formation of the acrosome from the Golgi apparatus, condensation and elongation of the nucleus, formation of a motile flagellum, and extensive shedding of cytoplasm. The spermiogenesis process can be divided into four successive phases: Golgi, cap, acrosome, and maturation (Figure 1.4). 1) **Golgi phase**: several proacrosomic granules, rich in glycoproteins, appear in the region of the Golgi complex. These granules coalesce to form a single large granule, the acrosomic granule that becomes closely applied to the nuclear envelope. The position of the acrosomic region on the nucleus becomes the anterior pole of the spermatid. The acrosomic granule is surrounded by the less-dense acrosomic vesicle. The vesicle and granule continue to enlarge through further contributions from the surrounding Golgi substance. While the acrosomic granule and vesicle are being elaborated, the distal and proximal centrioles move from a position near the nucleus to the periphery of the cell opposite the forming acrosome. Formation of the sperm tail is initiated by the distal centriole. The proximal centriole attaches itself to the caudal pole of the nucleus (implantation fossa) while the distal centriole gives rise to the axoneme, a 9 + 2 concentric array of microtubular doublets, which constitutes the central core of the flagellum. During this phase, the mitochondria suddenly migrate toward the periphery of the cytoplasm to lie very close to the plasma membrane. 2) **Cap phase**: during this phase, the acrosomic granule

Figure 1.3 Meiotic phase of spermatogenesis. The primary spermatocyte, which contains two times the amount of DNA (4C) of a spermatogonium, undergoes first meiotic division (reductional division). During the first meiotic division, there are the pairing of homologous chromosomes (each homologous chromosome contains two sister chromatids) and genetic crossing over between non-sister chromatids. After the first meiotic division, two secondary spermatocytes which have half of DNA amount (2C) of the primary spermatocyte are formed. Each secondary spermatocyte then undergoes second meiotic division (equational division) and gives rise to two haploid (1C) spermatids, which mature into spermatozoa without further division (Kierszenbaum, 2002).

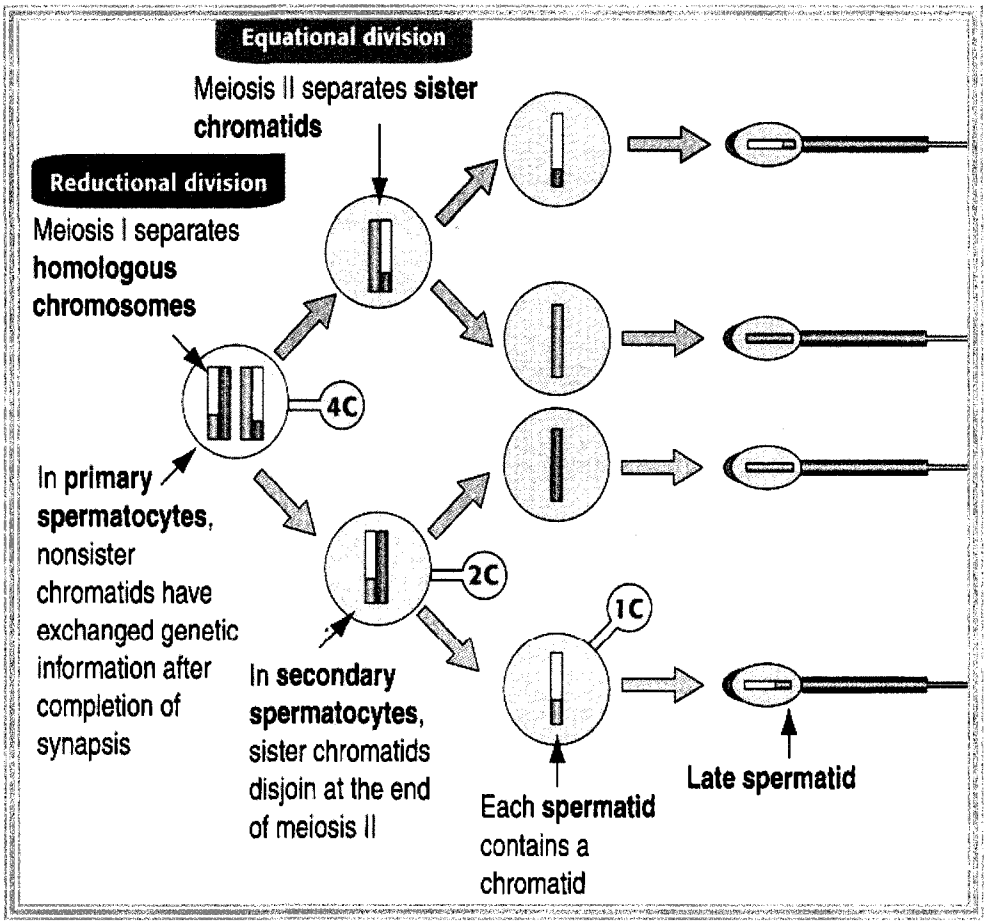
Equational division
Meiosis II separates **sister chromatids**
Reductional division
Meiosis I separates **homologous chromosomes**
4C
In **primary spermatocytes**, nonsister chromatids have exchanged genetic information after completion of synapsis
2C
In **secondary spermatocytes**, sister chromatids disjoin at the end of meiosis II
1C
Each **spermatid** contains a chromatid
Late spermatid

Figure 1.4 Spermiogenesis. A schematic drawing of spermiogenesis modified from Dym, 1977.

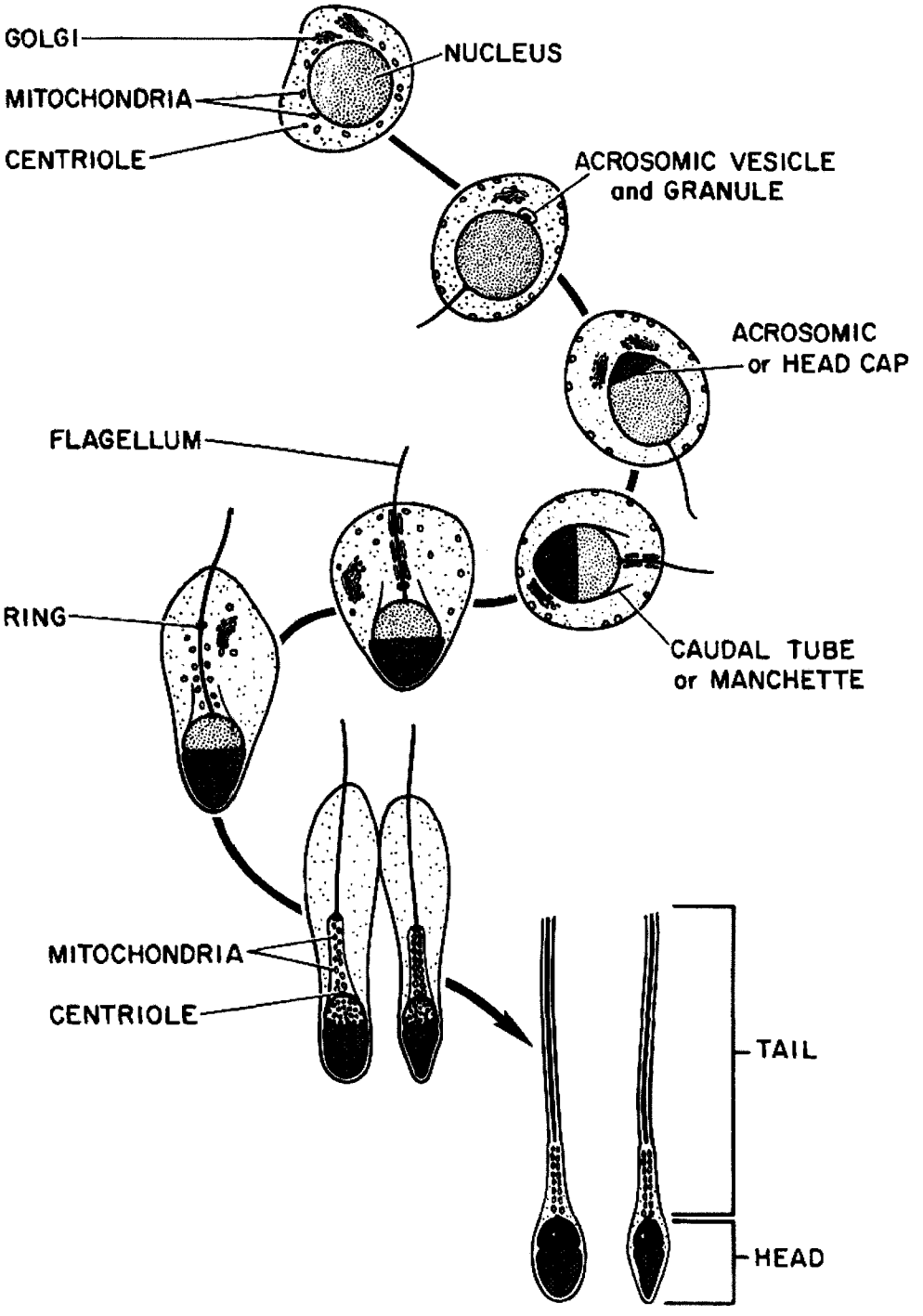
GOLGI
NUCLEUS
MITOCHONDRIA
CENTRIOLE
ACROSOMIC VESICLE
and GRANULE
ACROSOMIC
or HEAD CAP
FLAGELLUM
RING
CAUDAL TUBE
or MANCHETTE
MITOCHONDRIA
CENTRIOLE
TAIL
HEAD

forms a cap-like structure, spreading eventually to overlie the entire anterior one-half of the nucleus. The acrosomal cap consists of an outer and inner acrosomal membrane enclosing the acrosomal contents. 3) **Acrosome phase**: the main characteristics of this phase are the orientation of the anterior pole of the spermatid nucleus (acrosomic region) toward the base of seminiferous tubules and the elongation and condensation of the nucleus itself. The nucleus condensation is resulted from the replacement of the histones by the protamines, arginine-rich protein; after this replacement, there is no significant RNA synthesis in the nucleus. The spermatid cytoplasm is displaced toward the luminal region of the seminiferous tubules. In this manner, the acrosomic region of the nucleus closely approximates the plasma membrane and the cell becomes somewhat elongated. Cytoplasmic microtubules are assembled and form a cylindrical sheath that attaches itself to the caudal pole of the nucleus close to the posterior margin of the acrosome cap. This microtubular structure is called the manchette or caudal tube. There are modifications in the centriolar apparatus in the region of the implantation fossa, resulting in the formation of the neck region or connecting piece of spermatozoa. As the tail differentiates further, there is also the formation of nine longitudinally oriented coarse fibers (called outer dense fibers) along the axoneme of the flagellum. The annulus, a ringlike structure near the centrioles, migrates down the flagellum. The mitochondria line up along the outer dense fibers of the flagellum from the neck region to the annulus. This portion of the tail is called the midpiece. As the mitochondrial migration ends, the caudal tube disappears. The plasma membrane of the spermatids follows closely the contours of the developing flagellum. 4) **Maturation phase**: the major event of this phase is spermiation, the process that the spermatids shed a portion of their cytoplasm, the residual body, when they leave the seminiferous epithelium. Prior to the spermiation, spermatids (at the later stages) are deeply embedded within the cytoplasm of the Sertoli cells

in the orientation that their heads, where the acrosomal region is located, point toward the basement membrane of the seminiferous tubule. The junctional specialization occurs between late spermatids and the Sertoli cells; the cell membrane in the elongating spermatid head region projects into the surrounding cytoplasm of the Sertoli cell (Figure 1.5A). During spermiation, these Sertoli cytoplasm processes are postulated to be responsible for pulling off the residual body, resulting in release of testicular spermatozoa in the lumen of the seminiferous tubule (Figure 1.5B). Subsequently, the shed residual bodies are phagocytosed and degraded by Sertoli cells (Clermont, 1972; de Kretser and Kerr, 1994; Dym, 1977).

Highly differentiated and polarized spermatozoa are the final product of the spermatogenesis process. Each spermatozoon consists of two major parts: the head and the tail (Figure 1.6). The sperm head consists of a highly compact nucleus, containing the male genome, very little cytoplasm and the acrosome. The acrosome, located on the anterior portion of the sperm head, houses hydrolytic enzymes that will aid the spermatozoon to penetrate the zona pellucida (ZP), the extracellular glycoprotein matrix surrounding the oocyte. The sperm tail consists of the connecting piece, the midpiece, the principal piece, and the end piece. The connecting piece of the tail is a narrow segment containing the paired centrioles. The midpiece of the tail consists of the helically arranged mitochondrial sheath, the axoneme and the outer dense fibers of the flagellum. The lower limit of midpiece is marked by the termination of the mitochondrial helix at the annulus. The principal piece, the longest segment of the tail, is composed of central axoneme surrounded by the outer dense fibers and the fibrous sheath. The end piece is a very short segment of the tail in which only the axoneme is present (de Kretser and Kerr, 1994; Eddy and O'Brien, 1994; Kierszenbaum, 2002; Yanagimachi, 1994).

Figure 1.5 Spermatid and Sertoli cell interactions. A) A diagrammatic representation of the three-dimentional features of a step 19 spermatid of the rat. The concave aspect of the sperm head extends cell membrane structure termed "tubulobulbar complexes" into the surrounding Sertoli cell cytoplasm. **B)** A diagrammatic illustration of the final stage of human spermiogenesis showing the cytoplasm processes of the Sertoli cell essentially pull off the excess cytoplasm of spermatids (residual bodies) and retain them within its cytoplasm (modified from de Kretser and Kerr, 1994).

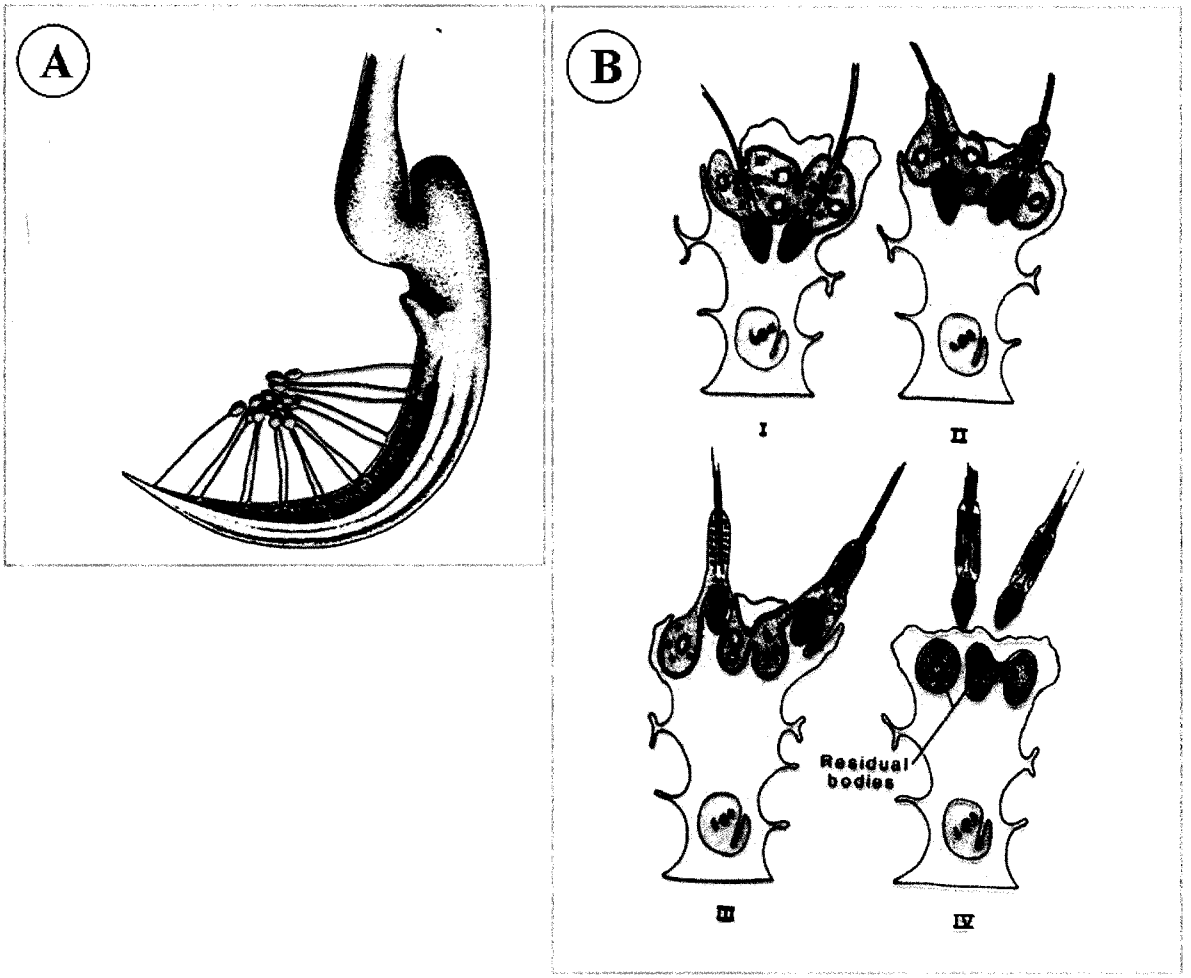
A
B
I
II
III
IV
Residual bodies

Figure 1.6 Structure of mammalian spermatozoon. A schematic drawing of the mammalian spermatozoon, as revealed by electron microscopy, showing transverse sections at different locations along its length (modified from Dym, 1977).

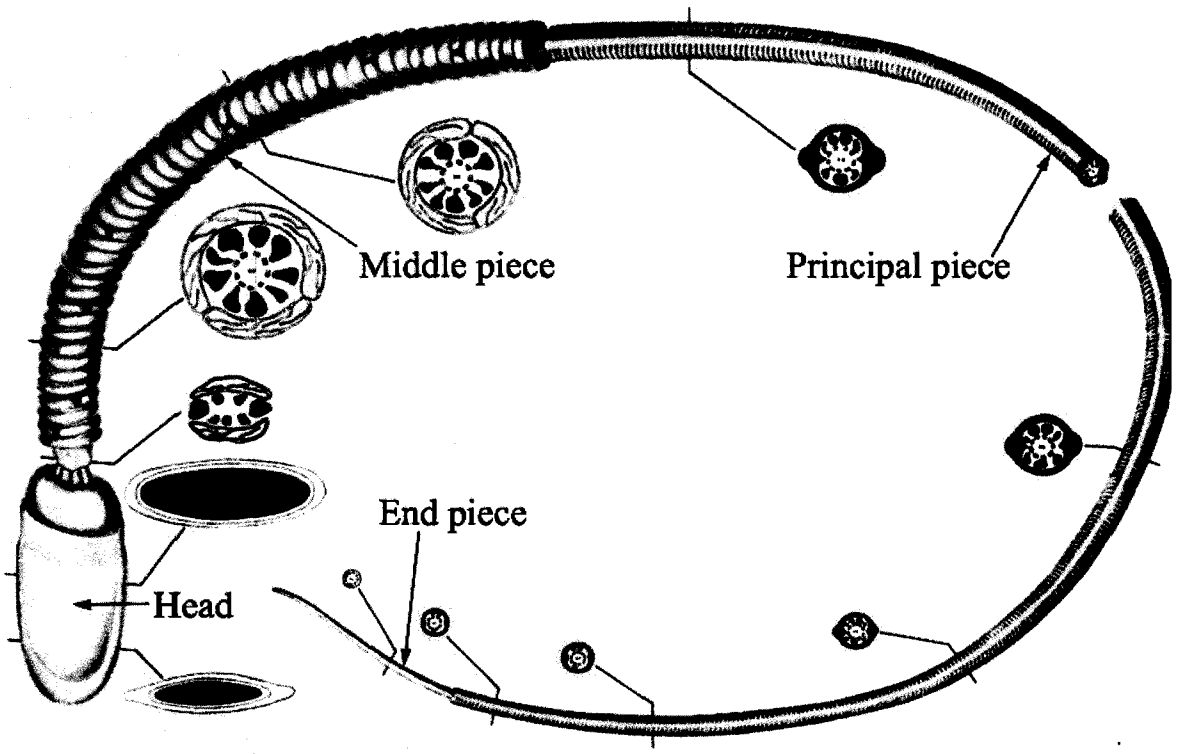
Middle piece
Principal piece
End piece
Head

During the divisions of spermatogonia, spermatocytes and spermatids, cytokinesis is not complete. The cells form a syncytium whereby each cell communicates with the others via the cytoplasmic bridges. The successive divisions produce cohorts of interconnected cells, and each cohort matures synchronously (Dym and Fawcett, 1971).

1.3 Spermatogenic stage and cycle

In all mammals, the organization of the spermatogenic cells is not random but organized into well-defined cellular associations. For instance, spermatids at a given step of spermiogenesis are always associated with the same types of spermatocytes, and spermatogonia. These organized cellular associations occur because of the following reasons: 1) along the length of the seminiferous tubule, there is more than one spermatogonium entering spermatogenesis process, although the entry of all spermatogonia into this division process is not synchronized; 2) the spermatogenic cells arrange themselves in layers (i.e., the more developed spermatogenic cells are closer to the lumen of seminiferous tubule); 3) the time period that spermatogenic cells being in each stage is constant. The typical associations of spermatogenic cells are referred to as "spermatogenic stages" and a number of criteria are used for assigning the various stages. The most useful criterion is based on the acrosomal development of the spermatids as seen in periodic acid-Schiff-hematoxylin stained sections (Clermont, 1972). With this method, 14 stages have been defined in the rat (Figure 1.7A), 12 stages in the mouse (Figure 1.7B) and 6 stages in the human. The spermatogenic stage succeeds one another and the sequence repeats itself indefinitely. The time it takes for the reappearance of the same spermatogenic stage within a given area of the seminiferous tubule is defined as "a spermatogenic cycle".

Figure 1.7 Spermatogenic cycles of rat and mouse. The diagrams show the histological relationship of spermatogenic cells in the rat (**A**) and mouse (**B**) seminiferous tubules of the testis during spermatogenesis. In each diagram, the lower row of cells is generally closer to the basement membrane and the upper row of cells is generally closer to the lumen of the seminiferous tubule. In rat, there are 14 stages (indicated by the Roman numerals) that repeat at the same location of the tubule at a 12.9-day interval. In the mouse, there are 12 stages (indicated by the Roman numerals) that repeat at an 8.6-day interval (modified from (Franca et al., 1998).

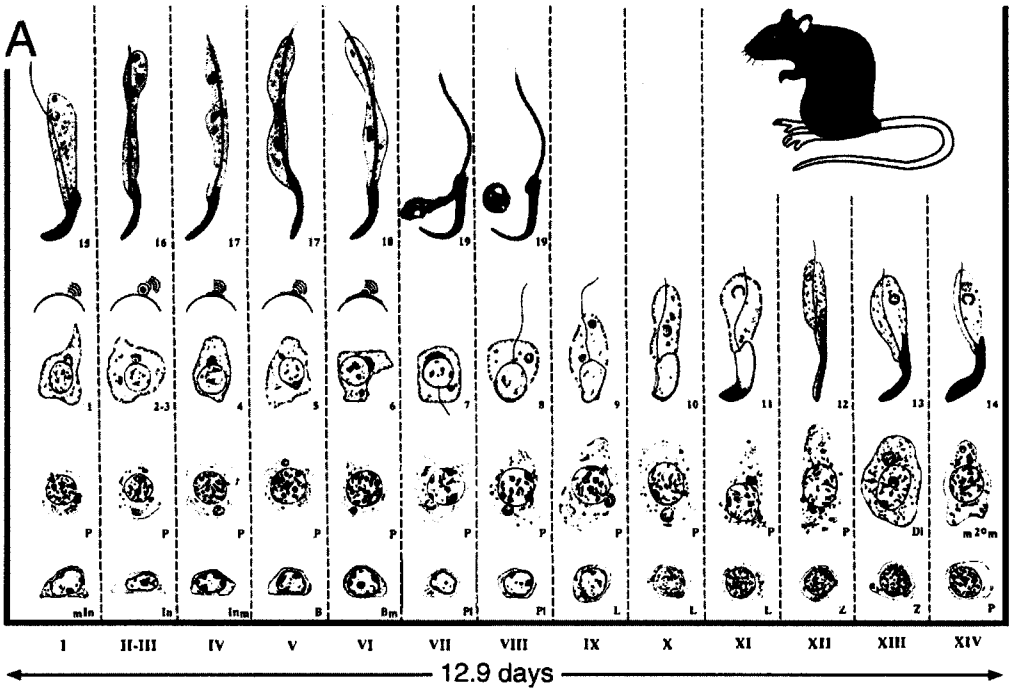

Stages of the Rat Cycle

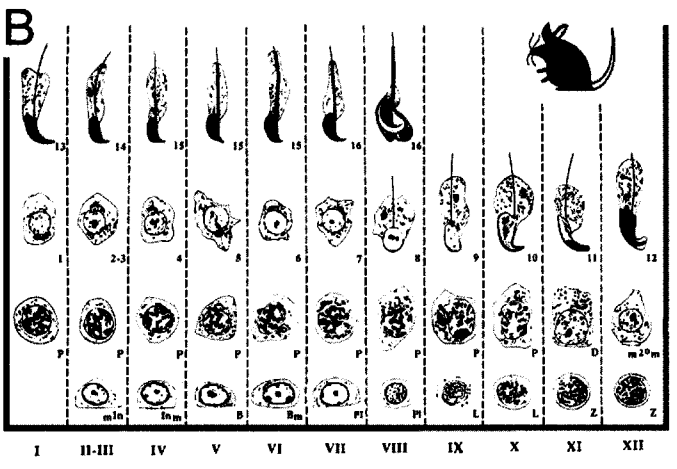

Stages of the Mouse Cycle

- In = Intermediate spermatogonium
- B = Type B spermatogonium
- PI = Preleptotene spermatocyte
- L = Leptotene spermatocyte
- Z = Zygotene spermatcyte
- P = Pachytene spermatocyte
- D/Di/2° = Dliplotene spermatocyte
- m = Cells are dividing in mitotic or meiotic processes
- 1-19 (Fig. A) = Stages 1-19 of rat spermatids
- 1-16 (Fig. B) = Stages 1-16 of mouse spermatids

1.4 Sertoli cell-germ cell interactions during spermatogenesis

Studies on reconstruction of a Sertoli cell via serial sections of rat testes revealed that one Sertoli cell contact with nearly 50 different germ cells at each stage of the spermatogenic cycle in the epithelium (Weber et al., 1983; Wong and Russell, 1983). It is known that development of germ cells largely relies on Sertoli cells for structural and nutritional support, especially during meiosis and spermiogenesis (namely beyond preleptotene spermatocytes) when germ cells are segregated from the circulation because of the blood-testis barrier, created by tight junctions between Sertoli cells near the basal lamina (Figure 1.1B). As such, germ cells and Sertoli cells develop an intimate and elaborate cellular network for cell-cell communications via direct cell-to-cell contact and also via indirect paracrine mechanisms by secreting factors (Cheng and Mruk, 2002; Jegou, 1993).

The interactions between Sertoli cell and germ cells are mediated by extracellular matrix components or cell adhesion molecules. Various cell adhesion molecules that are important for adhesion between germ cells and Sertoli cells have been shown; for example, *N*-cadherins existing on both the Sertoli cell and germ cell surface, β-1,4-galactosyltransferase on the germ cell surface that binds a carbohydrate receptor on the Sertoli cell (Jegou, 1993; Newton et al., 1993; Pratt et al., 1993).

The paracrine factors, e.g., growth factors (TGF- β, IGF-I), are secreted from Sertoli cells under control of testosterone and follicle-stimulating hormone (FSH) to regulate the germ cells. Production and secretion of testosterone by Leydig cells are regulated by luteinizing hormone (LH). LH and FSH are synthesized and secreted from the pituitary under hypothalamic control of gonadotropin releasing hormone (GnRH). The negative feedback to the pituitary also occurs via testosterone, secreted from Leydig cells and inhibin, secreted from Sertoli cells (for hormonal regulation diagram see Figure 1.8). In some rodent

Figure 1.8 Hormonal regulation of spermatogenesis via Sertoli cells (modified from Griswold, 1995).

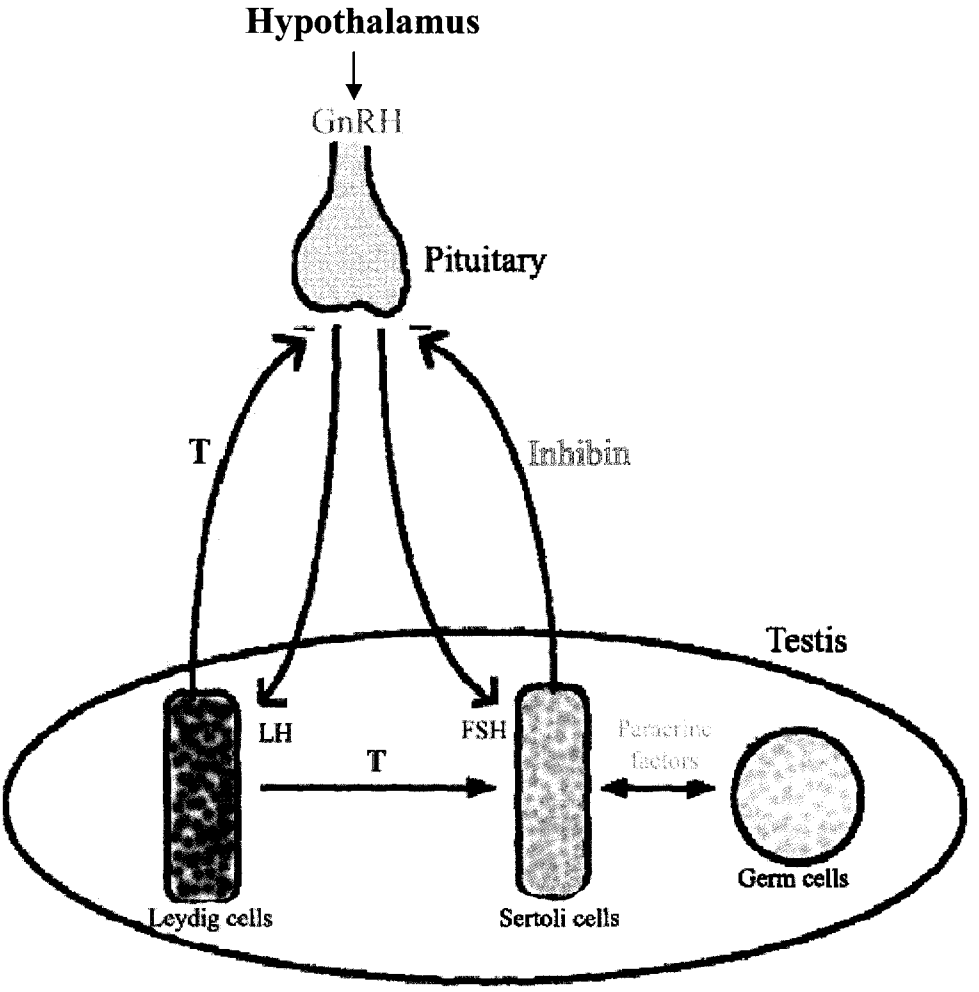
Hypothalamus
GnRH
Pituitary
T
Inhibin
Testis
LH
FSH
T
Paracrine factors
Germ cells
Leydig cells
Sertoli cells

species, the role of FSH in spermatogenesis seems to be only in the prepubertal animal; in the adult, FSH actions are replaced by testosterone (Griswold, 1995; Sharpe, 1994).

1.5 Epididymal sperm maturation

Testicular sperm, which are released into the lumen of the seminiferous tubules, do not have the ability to move and fertilize eggs. This is in contrast to sperm retrieved from the caudal epididymis, which possess fertilizing ability once they are resuspended in an appropriate medium. Therefore, sperm need to undergo the maturation process to acquire motility and fertilization capacity in the epididymis. The epididymis is composed of three major segments: caput (head), corpus (body), and cauda (tail) (Figure 1.9A). During epididymal maturation, the sperm plasma membrane undergoes intensive changes. Some of the preexisting proteins on the sperm plasma membrane, such as fertilin alpha and beta, cyritestin, alpha-D-mannosidase are cleaved by proteolytic enzymes and released into the lumen, or redistributed in different plasma membrane domains (Evans, 1999; Gatti et al., 2000). A large number of new components, present in the luminal fluid and presumably secreted from the epididymal epithelium, are also adsorbed onto the sperm surface during the epididymal maturation process (Dacheux et al., 2003). These new components include forward motility protein (FMP) involved in forward motility of sperm (Acott et al., 1983), and proteins with ZP-binding ability, such as P26h (Berube et al., 1996), β-galactosidase (Sosa et al., 1996; Tulsiani et al., 1995), and arylsulfatase A (ASA) (Weerachatyanukul et al., 2001b). In addition, sperm membrane fluidity increases due to the enrichment of polyunsaturated fatty acid (PUFA)-containing phospholipids (Cooper and Yeung, 1997; Flesch and Gadella, 2000). This increased membrane fluidity contributes to the sperm

Figure 1.9 Sperm-egg interactions. Sperm produced in testis acquire the fertilizing ability and forward motility during their transit in epididymis, which is divided into three parts (caput, corpus, and cauda) (**A**). Then, ejaculated sperm undergo further modification to attain full fertilizing ability through the process called "capacitation" in the female reproductive tract (**B**). The binding of capacitated sperm to zona pellucida, the extracellular glycoprotein matrix surrounding the egg induces acrosome reaction. The acrosome reaction results in the release of the acrosomal hydrolytic enzymes that facilitate sperm penetration through the ZP matrix. The acrosome reacted sperm enter the perivitelline space, bind nad fuse with the egg plasma membrane, and finally one sperm becomes incorporated into the egg proper, signifying that the fertilization has occurred (**C**).

A Male Reproductive Tract

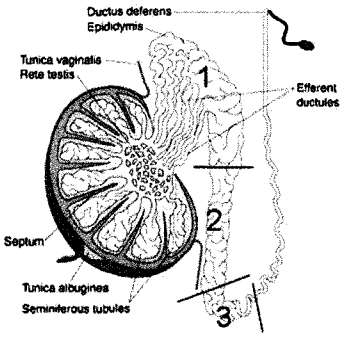

SPERM PRODUCTION IN TESTIS AND SPERM MATURATION IN EPIDIDYMIS
(1-caput, 2-corpus, 3-cauda eididymis)

B Female Reproductive Tract

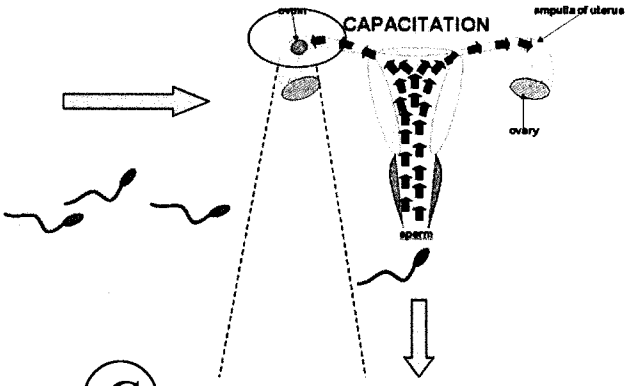

C Sperm-Zona Pellucida Binding in the female reproductive tract

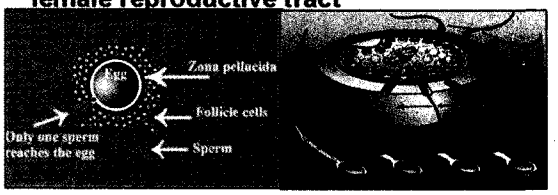

capability to move forwardly, as well as to the sperm membrane fusion ability required during fertilization (Yanagimachi, 1994). Epididymal fluid may also play an important role in sperm maturation; it contains membranous vesicles, termed epididymosomes, which interact with sperm (Fornes et al., 1995; Frenette and Sullivan, 2001; Yeung et al., 1997). Proteins and cholesterol present in epididymosomes have been shown to be transferred onto the sperm surface (Frenette et al., 2002; Saez et al., 2003; Yanagimachi et al., 1985).

1.6 Capacitation

The mature sperm are stored in the caudal epididymis until ejaculation. The ejaculated sperm then undergo further surface modification in the female reproductive tract to gain full fertilizing ability through a process known as capacitation (Figure 1.9B). Sperm capacitation can be achieved *in vitro* by incubating mature sperm in a chemically defined medium containing albumin (cholesterol releasing agent), bicarbonate, calcium and energy sources such as glucose, pyruvate or lactate (Yanagimachi, 1994).

Several processes occur during capacitation: 1) **desorption processes** during which proteins and other macromolecules from epididymal and seminal fluids that mask key sites for ZP binding on the sperm surface or suppress sperm functional activity are removed; 2) **ionic changes** in particular those involving in bicarbonate influx and Ca^{2+} influx. Such changes trigger the activation of adenylyl cyclase, and subsequent increase in intracellular cAMP. As a result, protein kinase A (PKA) is activated, which induces downstream protein tyrosine phosphorylation. 3) **plasma membrane lipid changes**. The phospholipids are distributed asymmetrically between the lipid leaflets of plasma membrane. During capacitation, a similar asymmetric distribution occurs in sperm and apparently collapses. The collapse of phospholipid asymmetry facilitates a decrease on sperm membrane

cholesterol (cholesterol efflux). The cholesterol efflux leads to a decreased ratio of cholesterol to phospholipids and an increase in fluidity of the sperm plasma membrane (Cross, 1998). The global increase in membrane fluidity in capacitated sperm is beneficial to the fusion-related events during sperm-egg interaction, i.e., acrosome reaction and the sperm-egg plasma membrane fusion (Primakoff and Myles, 2002). However, during the initial interaction between sperm and eggs, i.e., sperm-ZP binding, ordered domains on the sperm plasma membrane with clusters of ZP-binding molecules would be required for the stable interaction of gametes, withstanding the pulling force generated from ongoing sperm movement. Recently, results from our laboratory and other investigators indicate that the levels of liquid-ordered microdomains or lipid rafts, which are enriched in cholesterol, saturated phospholipids, and SGG, are increased on the sperm plasma membrane following capacitation (Bou et al., 2006; Shadan et al., 2004). In somatic cells, lipid rafts are known to function as platforms for cell adhesion and signaling molecules (Brown and London, 2000; Simons and Ehehalt, 2002). In agreement with the previous report in somatic cells, a number of ZP binding molecules have been found to exist in the sperm lipid rafts (Tanphaichitr et al., 2007). These findings suggest that lipid rafts may be involved in ZP-binding of capacitated sperm. Regarding the efflux of cholesterol, an integral component of lipid rafts, one would expect the levels of sperm lipid rafts to be decreased in capacitated sperm due to the lower cholesterol content; however, as mentioned above, the levels of lipid rafts were instead found to be increased in the capacitated sperm. A possible explanation for this controversy is that the cholesterol released during capacitation is from the non-raft fluid domains (Bou et al., 2006). This capacitation-related cholesterol efflux is accompanied by activation of lipid scramblase (Flesch et al., 2001), which catalyzes the movement of lipids. This may allow

sperm lipids to regroup themselves according to their biochemical properties, leading to the formation of liquid-ordered microdomains, or lipid rafts.

Following capacitation, sperm acquire hyperactivated motility patterns and the ZP binding sites become exposed, resulting in sperm binding to the egg ZP and subsequent penetration through the ZP matrix (Florman and Ducibella, 2006).

1.7 Acrosome reaction and sperm-ZP interaction

Once the capacitated sperm bind to the ZP, the acrosome reaction is induced. This reaction results in the release of the acrosomal contents, composed mainly of hydrolases, which facilitate sperm penetration through the ZP matrix. Acrosome reacted sperm then enter the perivitelline space, bind to and fuse with the egg plasma membrane, and finally one sperm becomes incorporated into the egg proper, signifying that fertilization has occurred (Yanagimachi, 1994) (Figure 1.9C).

The binding of sperm to ZP is the first step of gamete interaction, which leads to fertilization. The sperm-ZP binding occurs in two sequential steps, starting with the primary binding of the capacitated acrosome-intact sperm to the ZP, followed by the secondary ZP binding of the acrosome reacting/reacted sperm. The ZP consists of a few sulfoglycoproteins, and these glycoproteins are highly homologous among species (Wassarman, 2005). In the mouse, there are three ZP matrix glycoproteins: mZP3, mZP2, and mZP1. During the sperm-ZP binding, mZP3 serves as the receptor for the primary binding of sperm to ZP, whereas mZP2 is the secondary receptor and mZP1 is the cross-linker between mZP2 and mZP3.

Unlike the ZP, sperm have a number of ZP-binding molecules. Sperm molecules that are involved in the primary ZP binding are localized to the head anterior plasma membrane

of capacitated acrosome-intact sperm. Some of these primary ZP binding molecules are synthesized in spermatogenic cells and localized to the plasma membrane, such as β-1,4-galactosyltransferase (GALT), sulfogalactosylglycerolipid (SGG), mannosidase, and basigin. Other molecules, such as ASA, P26h, and β-galactosidase, are synthesized and secreted from the epididymal epithelium into the lumen, and adsorbed onto the sperm plasma membrane during the sperm transit trough the epididymis (as mentioned in the section of epididymal maturation). In contrast to sperm molecules involved in primary ZP binding, secondary ZP binding molecules, such as proacrosin, Sp38, zonadhesin, Sp17 and sp56 are mostly synthesized in spermatogenic cells and they are directly targeted to the acrosome (Tanphaichitr et al., 2007).

The reasons for having many ZP-binding molecules on the sperm surface are unknown. One possibility that many scientists agree upon is that these molecules may act simultaneously/sequentially or serve as a backup for one another during sperm-ZP binding, an initial step that crucially leads to the complete fertilization (Tanphaichitr et al., 2007).

1.8 Sulfogalactosylglycerolipid (SGG)

Sulfogalactosylglycerolipid (SGG), also known as seminolipid, is a sulfoglycolipid substantially present in male germ cells (10 mole% of total lipids) across all the mammalian species studied (Ishizuka et al., 1973; Kornblatt et al., 1974; Suzuki et al., 1973; Tanphaichitr et al., 2003). SGG consists of a glycerol backbone with 3-*O*-sulfated galactose at the *sn*-3 position and an akyl and acyl chain (both mainly 16:0) at the *sn*-1 and *sn*-2 positions, respectively (Figure 1.10A) (Ishizuka et al., 1973). Sulfogalactosylceramide (i.e., SGC or sulfatide), an analog of SGG, is a major lipid component of the myelin sheath; it is also found in epithelial cells of the kidney and digestive tract as well as in male germ cells of

Figure 1.10 Chemical structures of SGG (A) and SGC (B).

A

Sulfogalactosylglycerolipid (SGG)

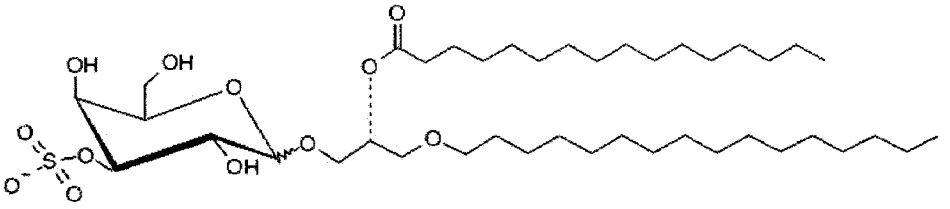

The acyl and alkyl chains are mainly 16:0.

B

Sulfogalactosylceramide (SGC)

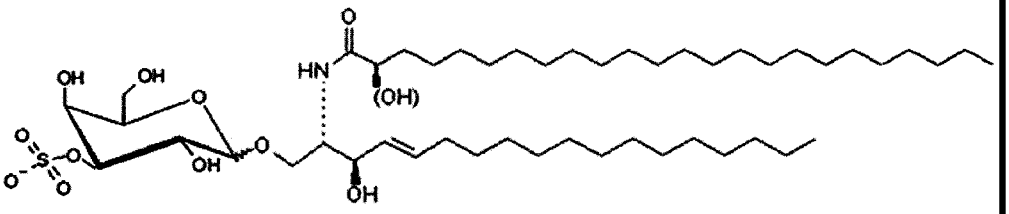

SGC can exist as hydroxylated and non-hydroxylated forms. The acyl chain is mainly 24:0 for OH form, and mainly 24:1 for non-OH form.

lower vertebrates and invertebrates. SGC has the same carbohydrate moiety as SGG but it has ceramide as a lipid backbone, unlike SGG (Figure 1.10B).

1.8.1 Biosynthesis of SGG and SGC

SGG and SGC have identical polar head groups but different lipid backbones (i.e., 1-*O*-hexadecyl 2-*O*-hexadecanoyl glycerol and ceramide, respectively). The biosynthesis of SGC, occurring mainly in the brain, involves two enzymes: UDP-galactose: ceramide galactosyltransferase (**CGT**; EC 2.4.1.62) and cerebroside sulfotransferase (**CST**; EC 2.8.2.11) (Figure 1.11). CGT catalyzes the formation of galactosylceramide (GC) also known as cerebroside from ceramide with UDP-galactose as the galactose donor. CST catalyzes the synthesis of GC to SGC using 3'-phosphoadenosine -5'-phosphosulfate (PAPS) as sulfate donor. Accumulated evidence suggests that the biosynthetic pathway of SGG in the testis is similar to that of SGC described in the brain. Following the intratesticular injection of [^{14}C]palmitate, [^{14}C]galactose and [^{14}C]cetyl alcohol, both galactosylglycerol (GG) and SGG were radiolabeled, but the radioactivity peak of GG preceded that of SGG (Hsu et al., 1983). This suggested that SGG was synthesized from GG via sulfation. In fact, sulfotransferase, localized in the Golgi complexes of primary spermatocytes, has been described to catalyze this reaction using PAPS as a sulfate donor (Knapp et al., 1973), and the purification of testicular sulfotransferase has been reported (Sakac et al., 1992). The enzyme has a molecular mass of 56 kDa and is activated by phosphorylation (Sakac et al., 1992). The apparent sulfotransferase activity is sharply reduced in the mid-pachytene stage due to the appearance of a small molecular weight inhibitor (Lingwood, 1985), identified as a glycosyl phosphoinositide (Lingwood et al., 1994). Recently, Honke et al. (Honke et al., 2002) have shown that the testicular sulfotransferase is encoded by the same gene as that of

Figure 1.11 Biosynthetic pathway of SGG/SGC. The first step in the pathway involves ceramide galactosyltransferase (CGT), the enzyme that transfers galactoses onto the lipid precursors yielding the formation of galactosylglycerolipid (GG) and galactosylceramide (GC). Then, cerebroside sulfotransferase (CST) delivers the sulfate groups to GG and GC, yielding SGG and SGC.

PAPS = 3'-Phosphoadenosine -5'-phosphosulfate; UDP-Gal = Uridine diphosphogalactose;
PAP = 3'-Phosphoadenosine-5'-phosphate; UDP= Uridine diphosphate

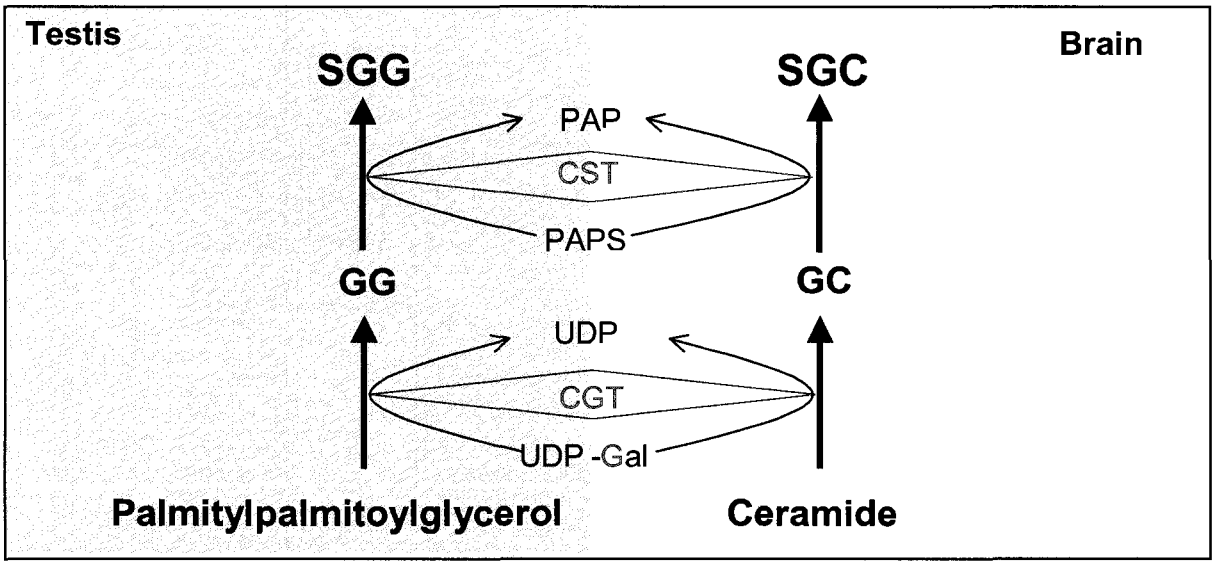
Testis
Brain
SGG
SGC
PAP
CST
PAPS
GG
GC
UDP
CGT
UDP -Gal
Palmitylpalmitoylglycerol
Ceramide

cerebroside sulfotransferase (CST) present in the brain and kidney. *Cst*$^{-/-}$ mice genetically depleted of CST lacks SGC in brain, kidney and testis. A buildup of GG in testes of these mice also confirms that GG is the precursor of SGG (Honke et al., 2002).

In the metabolic radiolabeling studies of Hsu et al. (Hsu et al., 1983), a small amount of alkylacylglycerol (AAG) was detected and therefore AAG was postulated to be galactosylated to form GG. Lately, *Cgt*$^{-/-}$ mice have been generated (Coetzee et al., 1996a), and in these mice, GG and GC are not found in the testis and the brain, respectively (Coetzee et al., 1996a; Fujimoto et al., 2000). Thus, these findings indicate that formation of GG from AAG is via the same enzyme responsible for GC formation. UDP-galactose, a galactose donor for GC formation in the brain, is also likely to be the galactose donor for GG formation in the testis. Unlike CST, testicular CGT has not yet been characterized. However, CGT from the myelinating rat brain has been isolated and characterized as a 61-kDa high-mannose glycoprotein (Schulte and Stoffel, 1993). Localization of CGT using antibody made against N-terminus of CGT revealed that CGT is localized in the endoplasmic reticulum (ER) of CGT-transfected CHO cells (Sprong et al., 1998). This result agrees with the presence of the ER retrieval signal sequence KKXX at the C-terminal end of the enzyme (Nilsson and Warren, 1994). All these results suggest that the synthesis of GG by testicular CGT should also occur in this organelle.

1.8.2 Synthetic sites and cellular localization of SGG

Lines of evidence indicate that SGG is actively synthesized in early stages of primary spermatocytes during spermatogenesis (Kornblatt et al., 1974; Letts et al., 1978). Thin layer chromatography of isolated testicular glycolipids from 15-20-day-old rats, which just have primary spermatocytes appearing in their testes, showed the first appearance of SGG; this

indicates that SGG is synthesized in primary spermatocytes (Kornblatt et al., 1974). To investigate SGG synthesis sites during spermatogenesis, Lett et al. (1978) also performed intratesticular injection of [^{35}S] sulfate into adult rats followed by isolation of spermatogenic cells using albumin gradient. The results revealed that early primary spermatocytes had a high degree of ^{35}S incorporation into SGG whereas late primary spermatocytes and spermatids showed minimal corporation of the radiolabel.

Once synthesized in early primary spermatocytes, SGG is transported from its site of synthesis via Golgi-derived vesicles towards the plasma membrane, and remains on plasma membrane throughout all the subsequent stages of germ cells (Klugerman and Kornblatt, 1980; Lingwood et al., 1981; Shirley and Schachter, 1980; Tanphaichitr et al., 2003). Indirect immunofluorescence (IIF) of frozen rat testis sections, using non-affinity purified rabbit anti-SGG IgG, revealed patchy staining patterns of SGG in fixed pachytene spermatocytes, and spermatids, but not in spermatogonia and Sertoli cells (Lingwood, 1981). Similar results were also described with loose spermatogenic cells released from minced rat testis (Lingwood et al., 1981). Subsequently, Lingwood reported SGG immunofluorescent staining in the rat epididymal sperm head (Lingwood, 1986). Using affinity purified rabbit polyclonal anti-SGG IgG antibody, patchy fluorescent staining patterns of SGG have also been described in live mouse primary spermatocytes, round and elongated spermatids, as well as in testicular and epididymal sperm (Tanphaichitr et al., 2003; Weerachatyanukul et al., 2003). In addition, SGG was shown to exist exclusively on the sperm head anterior plasma membrane overlying the acrosomal ridge and postacrosome of mature mouse sperm (White et al., 2000), pig sperm (Bou et al., 2006), and human sperm (Weerachatyanukul et al., 2001a). Biochemical studies demonstrated that SGG is present in isolated head anterior plasma membranes of pig, bull, stallion, and rooster sperm at appreciable amounts (i.e., < 10

mole% of total lipids (Parks and Lynch, 1992)). Since the anterior head plasma membrane is the ZP binding site of the acrosome-intact sperm (Chen and Cardullo, 1994; Kerr et al., 2002; Yanagimachi, 1994), the results from both immunolocalization and biochemical studies implicate the function of SGG in the primary ZP binding.

1.8.3 Degradation of SGG during spermatogenesis

SGG and SGC are postulated to share similarity not only for their synthetic pathway, but also for the degradative pathway. The enzyme responsible for SGC desulfation is arylsulfatase A (ASA) (EC 3.1.6.8), a lysosomal enzyme with a molecular mass of 65-68 kDa. To desulfate sulfoglycolipids, ASA requires a sphingolipid activator protein, saposin B, which extract the target sulfoglycolipid from the membrane. The soluble sulfoglycolipid-saposin B complex can be recognized by ASA (Kolter and Sandhoff, 2005; von Figura et al., 2001). Saposin B is derived from its precursor protein, prosaposin (O'Brien and Kishimoto, 1991). The fact that ASA and saposin B are responsible for physiological degradation of SGC is obtained from phenotypes observed in metachromic leukodystrophy (MLD) patients, genetically deficient in either ASA or, more rarely, saposin B. These patients have abnormal accumulation of SGC in the brain (the most affected organ) and other visceral organs. Similar but much milder phenotypes are also found in ASA deficient ($ASA^{-/-}$) mice (Molander-Melin et al., 2004; Schott et al., 2001).

Desulfation of SGG to GG by arylsulfatse A (ASA) has been shown *in vitro* by the enzymatic assay using purified human ASA (Fluharty et al., 1974) and isolated boar testis ASA (Yamato et al., 1974). Moreover, accumulation of SGG has been observed in testes of $ASA^{-/-}$ mice (Schott et al., 2001). Therefore, these findings suggest that SGG can be desulfated by ASA *in vivo*. In addition, accumulation of SGG was observed in testes of

mice deficient in prosaposin, the precursor protein of saposin B (Tadano-Aritomi et al., 2003). These results suggest the role of saposin B in facilitating ASA action in SGG desulfation in the testis. Although where/how exactly testicular ASA functions in SGG degradation has yet to be determined, there is evidence suggesting that this action may occur in Sertoli cells. Immunolocalization studies on the testis sections revealed that ASA resides not only in the acrosomal process of spermatids but also in the lysosomes of Sertoli cells (Moviglia et al., 1982; Weerachatyanukul et al., 2003). Moreover, prosaposin has been found in lysosomes containing residual bodies in Sertoli cells (Morales et al., 1998). This co-presence of ASA and prosaposin implies that ASA and saposin B (derived from prosaposin) may act together in the degradation of membrane SGG from residual bodies, which are shed from differentiating spermatids and phagocytosed by Sertoli cells.

1.8.4 Roles of SGG in male reproduction

SGG and SGC have affinity to a number of cell adhesion proteins, extracellular matrix glycoproteins, growth factor, and microorganisms (see the details in Table 1). All these findings suggest that SGG may serve as an adhesion molecule in cell-cell/extracellular protein interactions during male germ cell development and fertilization process.

In fact, our lab has shown that SGG is involved in the binding between acrosome intact sperm and the ZP and between acrosome-reacted sperm and the egg plasma membrane (Ahnonkitpanit et al., 1999; White et al., 2000). Moreover, during the sperm transit in epididymis, SGG also serves as a ligand for adsorption of arylsulfatase A, a ZP binding molecule, onto the sperm surface (Weerachatyanukul et al., 2003). These results altogether implicate SGG as an adhesion molecule in sperm maturation and sperm-egg interaction.

Besides affinity to a number of adhesion molecules, SGG also has unique biophysical properties. Our accumulated infrared spectroscopy studies of SGG liposomes indicate that SGG is an ordered lipid with a T_m of 45°C for the transition from the ordered lamellar crystalline phase to the disordered stage (Attar et al., 2000). It interacts well with saturated phospholipids and cholesterol (Attar et al., 2000), but not with a phospholipid containing polyunsaturated fatty acids (PUFA), such as docosahexaenoic acid (Tanphaichitr et al., 2003). Supporting these properties of SGG, we found that when SGG is mixed with other cholesterol and saturated fatty acid-and PUFA containing phospholipids, SGG exists in the liquid-ordered domains with cholesterol and saturated phospholipids, but not in the surrounding fluid phase of PUFA containing phospholipids (Weerachatyanukul et al., 2007). Moreover, we have shown that 70% of SGG in capacitated sperm exists in lipid rafts isolated as Triton X-100 resistant membranes, along with cholesterol and saturated phospholipids (Bou et al., 2006). Therefore, all these results suggest the roles of SGG as a structural lipid contributing to the formation of mammalian sperm lipid rafts, which possess ZP-binding molecules needed for the gamete interaction. Isolated sperm lipid rafts, in fact, have direct ZP binding ability (Bou et al., 2006).

Furthermore, *Cgt* and *Cst* knockout mice whose testes are depleted of SGG are infertile due to the spermatogenesis disruption at the primary spermatocyte stage (Fujimoto et al., 2000; Honke et al., 2002). These findings indicate that SGG is vital for the spermatogenesis process. Nonetheless, the molecular basis of SGG involvement in spermatogenesis is still unknown. The spermatogenesis process mostly relies on cell-cell interactions; and SGG is known as an adhesion molecule, expressed on the surface of spermatogenic cells and spermatozoa. Therefore, it is possible that SGG is responsible for germ cell-germ cell and/or germ cell-Sertoli cell interactions during spermatogenesis.

Table 1 SGG/SGC binding molecules

Type	SGG/SGC-binding molecules	Note	Reference
Microorganisms and surface proteins of microorganisms	*Escherichia coli* Enterotoxin b	A protein in a specific *E. coli* strain that causes diarrhea in animals and humans	(Rousset et al., 1998)
	Mycoplasma hominis	A human pathogen that is transmitted sexually and causes infertility	(Olson and Gilbert, 1993)
	Circumsporozoite proteins*	A coat protein of malaria (plasmodia) sporozoites	(Pancake et al., 1992)
	gp120	A surface glycoprotein of the human immunodeficiency virus (HIV-1)	(Brogi et al., 1995; Brogi et al., 1996)
	Mycoplasma pulmonis	Infertility-related mycoplasmas in rodents	(Lingwood et al., 1990)
Adhesive proteins	Properdin*	A globulin protein found in blood serum	(Holt et al., 1990)
	Antistatin*	A saliva protein from the leech that inhibits blood coagulation	(Holt et al., 1989)
	Thrombospondin*	A major component of platelet α granules	(Roberts, 1988)
	Von Willebrand factor*	A large plasma glycoprotein which binds to platelet and promotes platelet adhesion	(Roberts et al., 1986)
	L-selectin	A protein in the selectin family found on leukocytes	(Needham and Schnaar, 1993; Suzuki et al., 1993)
	P-selectin (CD62)	A protein in the selectin family found in granules in endothelial cells	(Bajorath et al., 1994; Needham and Schnaar, 1993)
	Cycotactin	A glial glycoprotein that plays roles in neural development of animals	(Crossin and Edelman, 1992)
	Amphoterin (p30)	A 30 kDa protein found in the rat cerebellum	(Mohan et al., 1992)
Extracellular matrix (ECM) glycoprotein	Laminin	A major noncollagenous glycoprotein of the basement membranes	(Roberts et al., 1985)
	Perlecan (C-terminal domain V)	An abundant proteoglycan component of the basement membranes	(Friedrich et al., 1999)
Components of myelin lipid rafts	Myelin and lymphocyte protein (MAL)	A myelin membrane protein expressed in central and peripheral nerve, and found in rafts of the myelin; A T-cell differentiation protein	(Frank, 2000)
	GC and SGC	Major glycolipids of the myelin	(Boggs et al., 2000)
Intracellular chaperone	Heat shock proteins of the 70-kDa family (hsp70)	Molecular chaperones found on the surface of bacteria, male germ cells, and carcinoma cell lines	(Mamelak and Lingwood, 2001)
Growth factor	Midkine	A basic heparin-binding growth factor in the nervous system	(Kurosawa et al., 2000)
Anticoagulant	Annexin V	A calcium-dependent phospholipid-binding protein	(Ida et al., 2004)

* Contain the amino acid sequence homology , C-S/T-V-S/T-C-G-X-G-X-X-X-R/K-X-R/K (X = any amino acid) (Holt et al., 1989)

1.9 Statements of problems

Due to the unique properties and significance in male germ cell functions, SGG can serve as a potential biomarker for sperm fertilizing ability as well as a target for development of a non-hormonal contraceptive. However, prior to any applications, roles of SGG in sperm functions have to be confirmed *in vivo*. For this purpose, the animal models are still required. Unfortunately, the *Cgt* and *Cst* knockout mice cannot produce sperm which can be used for studying SGG functions in sperm-egg interaction. Nevertheless, the heterozygous male mice can still produce sperm and sire offspring. Therefore, the main objective of this thesis was to determine whether *Cgt* heterozygous male mice, expected to have reduced testis and sperm SGG amounts, can be used as animal models for the SGG study.

1.9 Hypothesis

$Cgt^{+/-}$ male mice should produce only 50% SGG amounts relative to the wild type and they should be able to serve as an *in vivo* model for studying the roles of SGG in fertilization and spermatogenesis.

1.10 Specific Aims

1. To examine the fertility and spermatogenesis status in $Cgt^{+/-}$ mice

2. To determine the SGG amounts as well as the lipid profiles of $Cgt^{+/-}$ mouse sperm and testes.

CHAPTER TWO

MATERIALS AND METHODS

2.1 Animals

One wild type male and two *Cgt* heterozygous ($Cgt^{+/-}$) female (C57BL/6J) mice were generously given to us by Dr. Brian Popko (who was then at the University of North Carolina at Chapel Hill, Chapel Hill, North Carolina) to start the colony. These mice were bred to keep the line and to produce heterozygous males and females. $Cgt^{+/-}$ males and females were bred to generate *Cgt* knockout ($Cgt^{-/-}$) mice. The colony was maintained in a temperature-controlled room (22°C) with a 12:12 dark/light cycle. Genotypes were determined using tail tissues. Briefly, the mice were anesthetized using isoflurance and their tail tissues (about 2 mm) were collected. To lyse the cells, the tail tissues were incubated with a homogenization buffer (50 mM KCl, 10 mM Tris-HCl pH 8.3, 2 mM $MgCl_2$, 0.1 mg/ml gelatin, 0.45% Nonidet P-40, 0.45% Tween 20) containing Proteinase K (120 ug/ml) at 55-60°C overnight. The tail lysate was then heated to 95°C for 10 min to stop the enzyme action and was centrifuged (12,000 x g, 1 min, 4°C) to pellet the particulates. The supernatant, containing DNA from tail tissues, was used for PCR of the *Cgt* nucleotide wild type sequence and the *Cgt* sequence with a Neo gene insert. Two sets of primers were used for amplifying the DNA samples: ***Cgt (forward)***, 5'-CTC TCA GAA GGC AGA GAC ATT GCC-3' and ***Cgt (reverse)***, 5'-CAT CCA TAG GCT GGA CCC ATG AAC-3' (this set gave a wild type gene product of 500 bp); ***Neo (forward)***, 5' – GGA GAG GCA ATT CGG CTA TGA C -3' and ***Neo (reverse)***, 5' – CGC ATT GCA TCA GCC ATG ATG G -3' (This *Neo* primer set gave a 300 bp product of the inserted neomycin gene in the exon 2 of *Cgt* in $Cgt^{-/-}$ mice) (see diagram of PCR with the expected products in Figure 3.1A).

2.2 Mating study

To determine whether the *Cgt*$^{+/-}$ males had the same fecundity as the wild type males, a systematic mating study was conducted. Five pairs of *Cgt*$^{+/-}$ males and their wild type male littermates from five different litters (2 pairs of 3-month-old and 3 pairs of 9-month-old males) were used for this study. Each of these males was individually caged with an eight-week-old wild type female (C57BL/6J) in the evening. The females were checked for vaginal plugs on the following morning. Caging and plug checking were continued for two weeks if a plug was not observed for the first day. However, in this study, the plugs were observed in all the females within the first week of the experiment. The first day that vaginal plugs were detected was counted as Day1 of gestation. Since the females of this strain usually eat their new born pups, the pregnant females were killed on Day14-18 of gestation before the pups were born. This allowed us to obtain actual litter sizes by counting the number of fetuses or implantation sites in the uteri.

2.3 *In Vitro* Fertilization (IVF)

To compare fertilizing ability of *Cgt*$^{+/-}$ sperm with that of the wild type, IVF was carried out as previously described (Tantibhedhyangkul et al., 2002; Wu et al., 2007). CF-1 females were superovulated by sequential intraperitoneal injection of PMSG (5 IU) and hCG (5 IU) (Sigma Chemical Co., St. Louis, MO) with a 48 h interval. Ovulated cumulus masses containing mature eggs were retrieved from the females 14 h after hCG injection and placed in Krebs Ringer bicarbonate medium buffered with Hepes (KRB-Hepes) containing 0.3% BSA. The KRB-Hepes contained 119.4 mM NaCl, 4.8 mM KCl, 1.7 mM $CaCl_2$, 1.2 mM KH_2PO_4, 1.2 mM Mg_2SO_4, 4 mM $NaHCO_3$, 1 mM sodium pyruvate, 25 mM sodium lactate,

5.6 mM glucose, 1 U/ml of penicillin G, 1 μg/ml of streptomycin sulfate, 21 mM Hepes, and 28 μM phenol red at pH 7.4. Cumulus layers were dissociated by treating the cumulus masses with 0.1% hyaluronidase in KRB-0.3% BSA for 1-2 min (Hogan et al., 1994); this freed up the eggs which were then washed with KRB-0.3% BSA and stored at 37°C under 5% CO_2 until insemination. KRB was composed of the same ingredients as KRB-Hepes, except that 25.1 mM $NaHCO_3$ was used as a buffering component instead of 4 mM $NaHCO_3$ and 21 mM Hepes.

Cgt$^{+/-}$ and wild type male mice with ages around 3-5 months from 5 different litters were used for this study. Caudal epididymal and vas deferens sperm of each mouse were collected into 1 ml of KRB-Hepes. Motile sperm were prepared by two-step Percoll gradient centrifugation (PGC) as described previously (Tanphaichitr et al., 1990). PGC sperm were capacitated in KSOM containing 0.3%BSA for 1 hour at 37°C, in an incubator equilibrated with 5% CO_2, 5% O_2, 90% N_2. The KSOM medium consisted of 95 mM NaCl, 2.5 mM KCl, 1.7 mM $CaCl_2$, 0.35 mM KH_2PO_4, 0.2 mM Mg_2SO_4, 25 mM $NaHCO_3$, 0.2 mM sodium pyruvate, 10 mM sodium lactate, 0.01 mM sodium EDTA, 1 mM L-glutamine, 1 U/ml of penicillin G, 1 μg/ml of streptomycin sulfate, and 28 μM phenol red at pH 7.4. Capacitated sperm (0.5 million in 0.5 ml of KSOM-0.3%BSA) were then co-incubated with approximately 20 cumulus free eggs under mineral oil. Six hours afterwards, the eggs were scored under an inverted microscope for evidence of two-pronuclei formation. Fertilization rate was defined as percentage of total eggs fertilized in each sample. This *in vitro* fertilization experiment was performed in collaboration with Hongbin Xu, a Ph.D. student in our laboratory.

2.4 Collection of sperm and testes for biochemical and histological work

Sperm were collected from the caudal epididymis and vas deferens of both *Cgt*$^{+/-}$ males and wild type control littermates into 1 ml of KRB-Hepes. A small aliquot of the sperm suspension (10 µl) was used to determine the sperm number in a hemocytometer. The remaining sperm suspension was centrifuged (430 x *g*, 10 min, 25°C) to pellet the sperm. The sperm pellet was then washed twice with phosphate buffered saline (PBS: 155.17 mM NaCl, 1.06 mM KH_2PO_4, and 2.97 mM Na_2HPO_4, pH 7.4) and subjected to lipid extraction. Testes were collected from *Cgt*$^{+/-}$ and wild type mice. One side of the testes was either fixed for histological analyses or kept frozen for protein/RNA analyses (see more details in the following sections). The other side of the testes was used for lipid analyses; the testes were weighed before and after decapsulation. The decapsulated testes were then homogenized in 1 ml of PBS and the testis homogenates were subjected to lipid extraction.

2.5 Lipid extraction

Lipids were extracted from washed sperm and testis homogenates of *Cgt*$^{+/-}$ and wild type males, using the modified Bligh-Dyer method (Bligh and Dyer, 1959; Kates, 1986). This method involved two major steps. First, the water was added to the sperm suspension or the testis homogenates to bring a total volume to 1 ml, then 1.25 ml of chloroform and 2 ml of methanol were added subsequently to make one-phased chloroform/methanol/water mixture with a final ratio of 1:2:0.8 (v/v/v). This one-phased mixture was left at room temperature (25°C) for 1 hour to allow the chloroform to extract lipids from the tissue samples. Second, the volume ratio of chloroform/ methanol/water was adjusted to 1:1:0.9 to allow two-phased separation to take place. At this two-phased step, the total lipids were extracted in the chloroform phase (bottom), whereas aqueous-soluble compounds were

maintained in the methanol/water phase (top). In between the two phases, a plaque of proteins was formed. The chloroform phase containing lipids was collected into a glass tube and dried at room temperature under a nitrogen stream. The dried lipids were re-dissolved in chloroform-methanol 1:1 (v/v) and kept at -20°C for further characterization.

2.6 SGG quantification by Azure A assay

Quantification of SGG by the Azure A assay was based on the reaction of the Azure A dye with the sulfate group of sulfolipids in the total lipid extracts. The blue lipid-Azure A complex was separated from the free Azure A dye in the solution by the Bligh-Dyer lipid extraction and was quantified spectrometrically at 635 nm. Briefly, an aliquot of the total sperm and testis lipids of *Cgt*$^{+/-}$ and wild type samples was transferred to a screw capped glass tube and dried under N_2. To each tube, 1.5 ml of $CHCl_3$:MeOH (1:1, v/v), 1.5 ml of 0.05 M H_2SO_4 and 0.3 ml of Azure A blue dye solution (4 mg of Azure A in 0.5 ml of 0.05 M H_2SO_4 adjusted to 10 ml with Milli Q water) were added. Each tube was vortexed for 30 seconds and centrifuged (300 x g, 10 min, 4°C). The chloroform phase, which contained the blue complex of Azure A-lipid complex, was then carefully removed from the bottom phase and transferred to a new glass tube. The collected chloroform phase was placed in a 0.5 ml glass cuvette and the absorbance was read at 635 nm using an Ultraspec 2000 UV/Visible Spectrophotometer (Pharmacia Biotech, Piscataway, NJ).

For each assay point, the lipid extract corresponding to 7 million sperm or 1 milligram wet weight of testes was used. All sperm lipid samples were assayed in duplicate, whereas all testis lipid samples were assayed in triplicate. A standard curve was constructed using 0-10 μg of SGC (an analog of SGG which is commercially available).

2.7 Electrospray ionization mass spectrometry (ESI-MS)

Since the Azure A assay is based on the reaction of Azure A dye with the sulfate group of solfolipids, this assay is valid for SGG quantification only when SGG is the major sulfolipid in sperm and testes. In order to confirm this, ESI-MS was performed in collaboration of Dr. Kym Faull (University of California, Los Angeles, CA). Firstly, the m/z signature of purified pig testis SGG was obtained by negative ion scanning. The purified pig testis SGG was dissolved in methanol/chloroform (4:1, v/v, 20 pmol/μl) and injected (20 μl/injection) into a stream of the same solvent flowing (20 μl/min) into an ESI (Ionspray™) source connected to a triple quadrupole mass spectrometer (API III+, Perkin-Elmer Sciex, Thornhill, ON, Canada). Negative ion mass spectra were recorded by scanning from m/z 100-1000 (orifice 70 volts, 0.3 Da step size, 5 sec/scan). Total lipids extracted from sperm of CD-1 male mice were then prepared and scanned for negatively charged lipids in the same m/z range as that described for the purified pig testis SGG. To further scan for sulfolipids in the total sperm lipids, fragment ion spectra were obtained for Q_1 pre-selected parent ions by scanning Q_3 (m/z 50-1000, orifice varied between 70-200 volts, collision gas thickness instrumental setting between 200-330, 5-6 seconds/scan). The parent ions (in Q_1) that gave the signals of daughter ions (in Q_3) at m/z 97 (HSO_4^-) were identified as ions of sulfolipids. Instrument supplied software was used to average all the spectra from each sample injected.

2.8 High Performance Thin Layer Chromatography (HPTLC)

HPTLC was peformed using an HPK silica gel 60 Å plate (200 μm thickness, 10 x 10 cm dimension, Whatman, Kent, U.K.). HPTLC plates were pre-washed in chloroform-methanol 1:1 (v/v), dried and heat-activated at 100°C for 1 h.

Two sets of total lipids extracted from sperm (7 million sperm/sample) and testes (5 mg of testis weight/sample) of *Cgt*$^{+/-}$ and wild type mice were used for HPTLC (one set for each plate). Total lipids from each set were resuspended in 20 µl of chloroform/methanol (1:1, v/v) and loaded as a 0.8-cm band onto each HPTLC plate. A 25-µl glass syringe with a 22-gauge needle was used for sample loading (Hamilton, Reno, NV). Both plates were developed in parallel in chloroform/methanol/water (65:25:4, v/v/v). One plate was sprayed with 0.2% orcinol in 50% H_2SO_4 and heated at 120°C for 2-3 min. After charring, glycolipid bands became purple, whereas phospholipid bands and cholesterol band became yellow-brown and red, respectively (Kates, 1986). To obtain the total lipid profiles, the charred orcinol-stained plate was further stained with 0.03% Coomassie Brillliant Blue G-250 in 30% methanol/100 mM NaCl and destained with the destaining solution (30% methanol in 100 mM NaCl) ((Furimsky et al., 2005; Iida et al., 1989). The other HPTLC plate was sprayed with 0.016% Azure A in 1 mM H_2SO_4 to specifically reveal sulfolipid bands. The excess Azure A dye was washed off the plate with 0.05 M H_2SO_4: methanol (3:1, v/v). Lipid standards, including SGG, galactosylglycerol (GG), phosphatidylethanolamine (PE), phosphatidylcholine (PC), cholesterol (Chol) and sphingomyelin (SM) were co-chromatographed with the lipid samples. SGG and GG standards were prepared from ram testis as described previously (Tupper et al., 1994). PE, PC, and SM were purchased from Doosan Serdary Research Laboratories (Eaglewood Cliffs, NJ). Chol was obtained from Sigma Chemical Co (St. Louis, MO).

2.9 Histological analyses of testes

Testes collected from *Cgt*$^{-/-}$, *Cgt*$^{+/-}$ and wild type mice were fixed in Bouin's solution (Sigma Chemical Co, St. Louis, MO) at room temperature overnight and then transferred to

70% ethanol. The fixed testes were sent to the Centre for Bone and Periodontal Research (Mcgill University, Montreal) for further processing (sectioning and staining). Briefly, the testes were serially dehydrated in increasing concentrations of ethanol and embedded in paraffin. The testis paraffin blocks were cut into 6-μm-thick sections and the sections were placed on glass slides. The sections were deparaffinized, rehydrated with decreasing concentrations of ethanol (100%, 95%, 80%) and water, respectively, and stained with hematoxylin (nuclear staining) and counterstained with eosin (cytoplasmic staining). The sections topped with Permount (Fisher scientific company, Ottawa, Ontario, Canada) and a coverslip were viewed under a Zeiss IM35 epifluorescent microscope and the images were captured at 100x and 400x magnification. Testes collected from three animals of each genotype were used for sectioning and fifty seminiferous tubules were viewed for each animal sample.

2.10 RNA extraction and reverse transcription

Total RNA was extracted from *Cgt*$^{+/-}$ and wild type testes using an RNeasy kit (Qiagen, Mississauga, ON, Canada) following the manufacturer's instructions. Total RNA from *Cgt*$^{-/-}$ mouse testis was also prepared to be used as a negative control. The concentrations of total extracted RNA were assessed by their absorbance values at 260 nm. (i.e., 1 unit of A_{260} of the RNA = 40 μg/ml). The purity of the RNA extracts was revealed by the ratio of the absorbance values at 260 nm and 280 nm. The ratio of 1.8-2.1 is indicative of highly purified RNA according to the recommendation by Qiagen. All of my extracted RNA samples had the A_{260}/A_{280} ratio of this suggested range. The RNA sample was then reverse-transcribed into cDNA using a Retroscript Kit (Ambion, Foster City, CA). An aliquot (~2

μg) of each RNA sample (*Cgt*$^{-/-}$ *Cgt*$^{+/-}$ and wild type) was used in each reaction mixture which also contains random decamers, RT buffer, dNTPmix, RNase inhibitor and reverse transcriptase provided in the kit. The cDNA products from reverse transcription were then purified from the other components in the reactions using a QIAquick PCR Purification Kit (Qiagen) following to the manufacturer's protocol. The concentrations of the cDNA samples were determined by their absorbance values at 260 nm (i.e., 1 unit of A_{260} of the double stranded DNA = 50 μg/ml), and the cDNA samples were stored at -20°C prior to analysis by real-time PCR.

2.11 Quantitative real-time PCR

The quantitative real-time PCR was used to compare the amounts of *Cgt* mRNA transcribed in *Cgt*$^{+/-}$ testes versus those in the wild type. Various concentrations of *Cgt* and *β-actin* cDNAs (The *β-actin* served as an internal control for RNA analysis.) were used to derive the standard curves for each set of *Cgt*$^{+/-}$ and wild type samples that were assayed. To prepare *Cgt* and *β-actin* cDNAs for the standard curve construction, an aliquot of the cDNA products from reverse transcription of the wild type sample was further subjected to PCR using the specific primer sets for *Cgt* or *β-actin* amplification: *Cgt (forward)*, 5'-CTC TCA GAA GGC AGA GAC ATT GCC-3' and *Cgt (reverse),* 5'-CAT CCA TAG GCT GGA CCC ATG AAC-3'; *β-actin (forward)*, 5' –GTG GGC CGC TCT AGG CAC CA-3' and *β-actin (reverse)*, 5' –TGG CCT TAG GGT TCA GGG GG-3'. The amplified *Cgt* or *β-actin* products were then purified from the other components in the PCR reactions using a QIAquick PCR Purification Kit (Qiagen) following the manufacturer's protocol. To quantify the purified *Cgt* and *β-actin* cDNA products, an aliquot of each cDNA product and DNA molecular weight marker (Qiagen) were then subjected to 2% agarose gel electrophoresis

(120 V, 45 min) (Sambrook and Russell, 2001). The gel was stained with ethidium bromide (10 μg/ml) and scanned with a Typhoon 8600 scanner (Molecular Dynamics, Sunnyvale, CA) using the 532 nm excitation filter and the 610 BP emission filter. To determine the cDNA amounts, the intensity of the purified *Cgt* and *β-actin* cDNA bands was compared with that of the DNA markers by densitometric analyses using ImageQuant software (Molecular Dynamics). Different dilutions of the purified *Cgt* and *β-actin* cDNA (0.0001, 0.001, 0.01, 0.1, and 1 pg/μl) products were made and further used to construct a standard curve for the real-time PCR.

The cDNA samples of each genotype ($Cgt^{+/+}$, $Cgt^{+/-}$, $Cgt^{-/-}$) and different dilutions of purified *Cgt* and *β-actin* cDNAs were used as templates in 20-μl fluorometric quantitative PCR reactions. Each reaction mixture includes 1x Quantitect SYBR Green PCR master mix (Qiagen, Mississauga, ON, Canada), and 0.5 μM of each primer (*Cgt* and *β-actin* primers). The PCR was performed in a Roche LightCycler version 2.0 (Roche Diagnostics, Laval, Quebec). The PCR was started with 15-min initial activation of Tag polymerase at 95°C, followed by 40 cycles of denaturation at 95°C for 20 sec, annealing at 54°C for 30 sec and extension at 72°C for 40 sec. Fluorescent data were collected at the end of the extension step in each cycle. SYBR Green binds and intercalates into double-stranded DNA during the extension step of the amplification cycle. The fluorescent data were plotted against the number of cycles and the threshold cycle (C_T), the PCR cycle at which the statistically increase of fluorescent signal is first detected, was used as a tool for calculation the starting template amount in each sample. The software for Roche LightCycler version 2.0 was used to construct a standard curve of cycle threshold (C_T) values from all dilutions of standard cDNAs and calculate the concentrations of mRNA products in each sample based on their C_T

values. The concentrations of the *Cgt* mRNA in each sample were expressed as relative values to that of the *β-actin* mRNA content in the same sample.

2.12 Production of anti-CGT antibody

To generate an antibody against CGT, an antigenic peptide within the CGT peptide sequence was determined using MacVector Software Program version 7.0 (Macvector, Inc., Cary, NC). Peptides were scored for their antigenicity (Parker antigenicity, Protrusion Index antigenicity, Welling antigenicity), hydrophilicity (Kyte/Doolittle hydrophilicity, Hopp/Woods hydrophilicity, Argos transmembrane, von Heijne transmembrane), and structure (protein flexibility, amphiphilic helix, amphiphilic sheet) (see Appendix I for these analysis profiles). Based on this analysis, a C-terminal peptide sequence, RNGKYKGNGRVKHEKKVR, which is corresponding to amino acids 524-541 of mouse CGT, was chosen for immunization and antibody production.

The peptide synthesis and antibody production were performed by AnaSpec Company (San Jose, CA). Polyclonal anti-CGT antisera were produced against the purified synthetic peptide in New Zealand White rabbits. Two rabbits were initially immunized with the peptide (0.5 mg) conjugated to keyhole limpet haemocyanin (KLH) in complete Freund's adjuvant. Following the first immunization, three booster injections in Freud's incomplete adjuvant were given to animals at weeks 3, 6 and 10. The animals were bled at week 7 and 11 to yield first and second samples of the anti-CGT antiserum, respectively. Preimmune serum was collected before any injections.

Specific binding of immune serum to the antigenic peptide was demonstrated by enzyme-linked immunosorbent assay (ELISA). The ELISA test was also performed by AnaSpec Company. Peptide conjugated to BSA, diluted in coating buffer (0.05 M $NaHCO_3$,

pH 9.5) at a concentration of 20 μg/ml, was plated in a 96-well plate (100 μl per well). After incubation at 4°C overnight on an orbital shaker, the unbound peptide-BSA conjugate was removed by washing the wells twice with 200 μl of washing buffer (0.01 M PBS -0.05% Tween 20, pH 7.0-7.2). Each well was then blocked with 200 μl of blocking buffer (0.1 M PBS – 0.1% BSA, pH 7.5) for 2 h at room temperature, followed by washing three times. Serum samples prepared in the blocking buffer at different dilutions (1:100, 1:1,000, 1:5,000, 1:25,000, 1:125,000 and 1:625,000) were added to wells (100 μl per well). After 2 h incubation at room temperature, the wells were washed three times and incubated with secondary antibody (goat anti-rabbit IgG conjugated with HRP prepared in the blocking buffer at a 1:2,000 dilution) for 1 h at room temperature. The unbound secondary antibody solution was removed from the wells and the wells were washed five times with the washing buffer, then twice with distilled water. K-Blue substrate (Neogen Corporation, Lexington, KY) was added into each well (100 μl per well) and the blue color was allowed to develop at room temperature for 10-30 min before reading the absorbance at 630 nm to obtain the reference absorbance values. To stop the color development, 50 μl of 1 N HCl was added to each well and the absorbance was read at 450 nm (yellow color). The antiserum titer value was estimated to be the dilution where the $O.D._{450/630}$ (The absorbance values after substracting the reference values) was about 0.1, except when the $O.D_{450/630}$ of the "prebleed" (preimmune) serum was equal to 0.2. In such the case, $O.D._{450/630}$ value of 0.2 was used to determine the titer.

2.13 Immunoblotting and densitometric analysis

Testes collected from $Cgt^{+/-}$ and wild type littermates as well as $Cgt^{-/-}$ testis (used as a negative control) were decapsulated, weighed and homogenized in 250 mM sucrose, 1 mM

EDTA, 10 mM Hepes,pH 7.2 (homogenization buffer) by a glass homogenizer. Post nuclear supernatants (PNS) were prepared from the testis homogenates by centrifugation at 375 x *g* for 15 min (Sprong et al., 1998). Protein concentrations in all the PNS samples were determined using a Bio-Rad Protein Assay Solution (Bio-Rad Laboratories, Hercules, CA). Proteins (20 μg) from each PNS sample were subjected to SDS-PAGE (10% polyacrylamide, 1.0 mm thick) (Laemmli, 1970), followed by electroblotting onto a nitrocellulose membrane (Towbin and Gordon, 1984). The nitrocellulose was blocked for 1 hour with 5% fat free milk in Tris-buffered saline (TBS: 137 mM NaCl in 20 mM Tris-HCl, pH 7.6) containing 0.05% Tween 20. Immunoblotting was performed using either anti-CGT antiserum (1:5,000 dilution) or anti-ASA antiserum (1:1,000 dilution) as primary antibody, and goat anti-rabbit immunoglobin conjugated with horseradish peroxidase (Bio-Rad Laboratories) (1:5,000 dilution) as secondary antibody. The primary and secondary antibodies were prepared in the blocking medium. The reactivity of antibody-antigen was detected by enhanced chemiluminescence (ECL) using an ECL kit (Pierce, Rockford, IL). Relative CGT expression levels in the $Cgt^{+/-}$ samples compared with those in the wild type samples were analyzed by densitometric analysis using AlphaImager Software (AlphaEase version 5.5, Alpha Innotech Co., San Leandro, CA).

2.14 CGT enzymatic activity assay

The post nuclear supernatants (prepared as described above) of the $Cgt^{+/-}$, wild type and knockout mouse testes were used for the CGT activity assay. This assay was based on the reaction of CGT (in the supernatant) with a fluorescently labeled lipid substrate, C_6-NBD-ceramide: *N*-[6-[(7-nitro-2-1,3-benzoxadiazol-4-yl)amino] hexanoyl]-D-*erythro*-sphingosine (Avanti Polar Lipids, Inc., Alabaster, AL) to yield a fluorescent lipid product,

NBD galactosylceramide (NBD-GC). The post nuclear supernatant (20 μg of proteins) of each sample was incubated for 25 minutes at 37°C in a 200 μl-reaction mixture containing homogenization buffer, 1% BSA, 2 mM UDP-galactose, 2 mM $MgCl_2$, 2 mM $MnCl_2$, and 50 μM C_6-NBD-ceramide. After the incubation, the reaction mixture was subjected to lipid extraction (see the section above). Lipids extracted in the chloroform phase was dried under a stream of nitrogen, solubilized in 20 μl of chloroform and applied to a HPTLC plate. The C_6-NBD-GC (Avanti Polar Lipids) was also included as a standard lipid in the HPTLC plate. The plate was developed using the same solvent system as described in the HPTLC section and the chromatographed fluorescent lipids were detected by a Typhoon 8600 Scanner (Molecular Dynamics, Sunnyvale, CA) using an excitation wavelength of 470 nm and emission wavelength of 530 nm. Densitometric analysis of NBD-GC in the samples was done using AlphaImager software (AlphaEase version 5.5, Alpha Innotech Co., San Leandro, CA).

2.15 ASA enzymatic activity assay

p-nitrocatechol sulfate (NCS) was used as an artificial substrate for assaying ASA activity in wild type and $Cgt^{+/-}$ testis postnuclear supernatant samples (prepared as described previously). The reaction mixture, consisting of 5 mM NCS, 0.25 mM $Na_4P_2O_7$, 0.85 M NaCl, 1 mg/ml of BSA, 0.25 M sodium acetate, pH 5 and the sample homogenate containing 0.1-0.3 mg of total proteins in a total volume of 200 μl, was incubated at 37°C for 1 h. At the end of the incubation time, 800 μl of 1 M NaOH was added and the nitrocatechol produced was measured at 515 nm and quantified using its molar extinction coefficient (i.e., 1 M of nitrocatechol has A_{515} of 12400). One unit of ASA activity was defined as 1 μmole of nitrocatechol released in 1 h.

2.16 Statistical analyses

The Student *t*-test was used to analyze significant differences between two sets of data from the $Cgt^{+/-}$ and wild type samples in this study. A *P* value of less than 0.05 was considered to be statistically significant.

CHAPTER THREE

RESULTS

3.1 Genotyping of *Cgt* transgenic mice

Mice heterozygous for the *Cgt* mutation were intercrossed to generate *Cgt*-deficient mice. The genotypes of the offspring were determined by PCR of tail DNA using specific primers for the *Cgt* and neomycin resistance (*Neo*) genes. The *Neo* gene was inserted into a Kpnl site within exon 2 of the *Cgt* gene for disruption of this gene in the knockout mice (Coetzee et al., 1996a). The specific primers for the *Cgt* gene (*Cgt* primers) and the *Neo* gene (*Neo* primers) gave an amplified product of 557 bp and 320 bp, respectively (Figure 3.1A). Therefore, DNA samples from wild type mice, which possess only *Cgt* gene, had only one size of amplified product (557 bp), whereas those of the knockout mice showed a 320 bp product of amplified *Neo* inserted gene. DNA samples from heterozygous mice, which have both *Cgt* and *Neo* genes, showed both 557 bp and 320 bp amplified products (Figure 3.1B). The genotyping result from 26 litters of 4 generations of heterozygous parents demonstrated that the offspring (n = 186) was 26% $Cgt^{+/+}$, 52% $Cgt^{+/-}$, and 22% $Cgt^{-/-}$ mice in numbers consistent with normal Mendelian segregation of the targeted *Cgt* allele. The $Cgt^{-/-}$ mice were not embryonic lethal; however, they were born smaller than their heterozygous and wild type littermates. With age, the $Cgt^{-/-}$ mice exhibited a progressive loss of function in the hind limbs, tooth protrusion, and died around three to four weeks of age (Figure 3.1C).

3.2 Fecundity of $Cgt^{+/-}$ mice

To determine whether $Cgt^{+/-}$ sperm had compromised fertilizing ability, *in vitro* fertilization (IVF) experiments and a mating study were performed. The IVF experiments were conducted using 5 pairs of $Cgt^{+/-}$ and wild type male littermates from 5 different litters.

Figure 3.1 Genotyping of *Cgt* transgenic mice. The genotypes of *Cgt* transgenic mice were examined by PCR analysis. The *Cgt* and *Neo* primers were used to amplify 557 bp and 320 bp fragments of wild type and knockout alleles, respectively (**A**). PCR products were subjected to agarose gel electrophoresis. The gel was stained by ethidium bromide and viewed under UV light. The DNA marker (M) was included in the same gel to determine the size of PCR products. The expected DNA products from PCR amplification of wild type, $Cgt^{+/-}$, and knockout samples were shown in lane 1, 2 and 3, respectively (**B**). The *Cgt* knockout mice also exhibited overt phenotypes, such as paralysis of hind limbs and protrusion of front teeth (**C**).

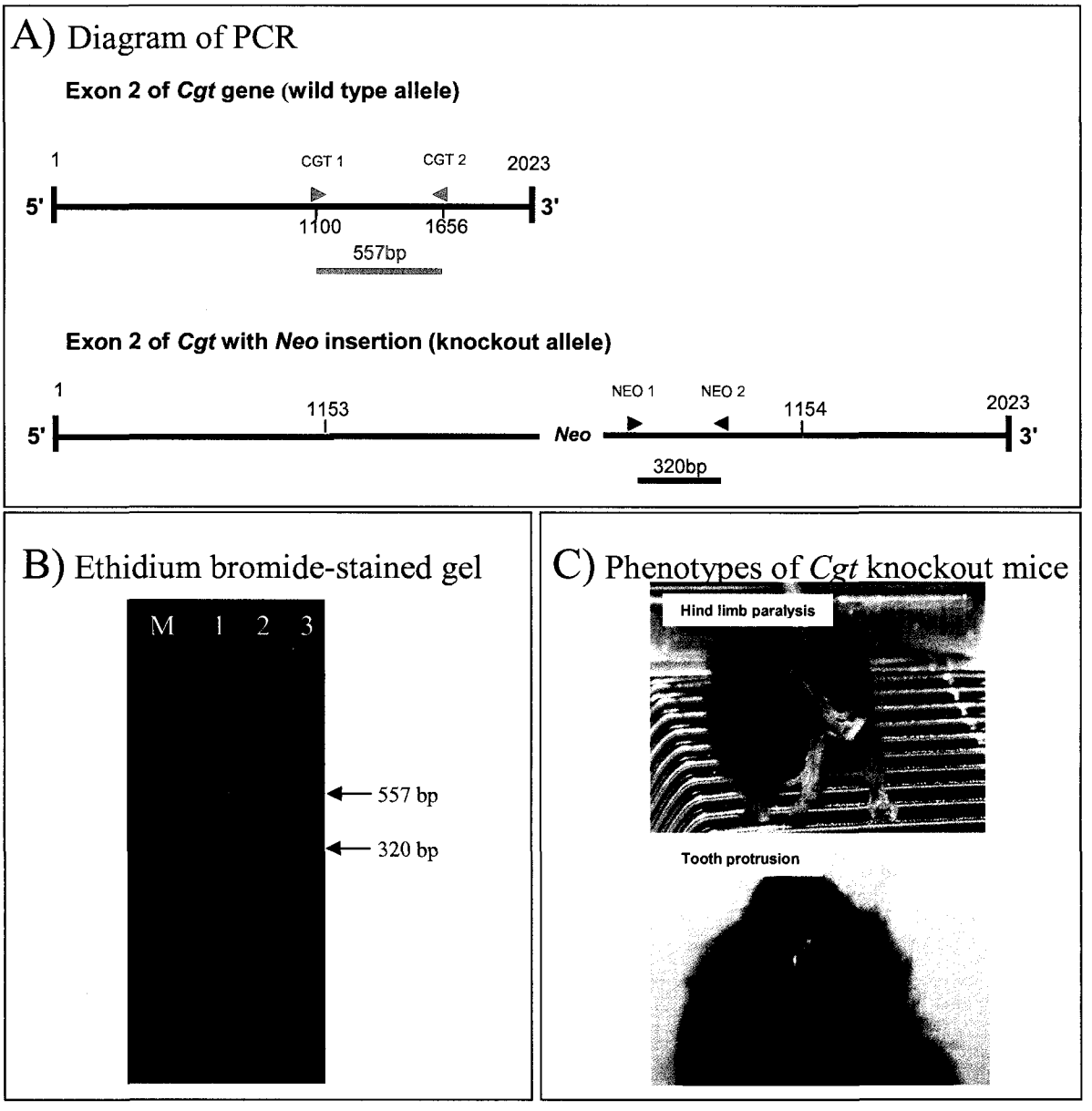
A) Diagram of PCR
Exon 2 of Cgt gene (wild type allele)
1
CGT 1
CGT 2
2023
5'
3'
1100
1656
557bp
Exon 2 of Cgt with Neo insertion (knockout allele)
1
1153
NEO 1
NEO 2
1154
2023
5'
Neo
3'
320bp
B) Ethidium bromide-stained gel
M 1 2 3
557 bp
320 bp
C) Phenotypes of Cgt knockout mice
Hind limb paralysis
Tooth protrusion

The results of these experiments revealed no significant difference in the *in vitro* fertilizing ability of $Cgt^{+/-}$ sperm and the wild type sperm (50.4 ± 9.2 vs 55.9 ± 9.1 % eggs fertilized; P = 0.20) (Figure 3.2A). The total number of eggs assessed was 66 for both $Cgt^{+/-}$ and wild type samples. The average percentage of eggs fertilized by $Cgt^{+/-}$ sperm was 90.1 ± 16.5 % of the wild type control (Figure 3.2B). Corroborating the IVF result was the result from the mating study, using $Cgt^{+/-}$ or wild type males to mate with wild type females. The average litter size obtained from the wild type females mated with $Cgt^{+/-}$ males was similar to that obtained from the females mated with the wild type males (8.4 ± 0.9 vs 7.4 ± 0.9 pups/litter; n = 5; P = 0.12) (Figure 3.3). These results indicated that the $Cgt^{+/-}$ mouse sperm had normal fertilizing ability both *in vitro* and *in vivo*.

3.3 Spermatogenesis status of $Cgt^{+/-}$ mice

To determine the spermatogenesis status of $Cgt^{+/-}$ mice, histology of the testis sections was examined. Overall, the morphology of the seminiferous tubules of $Cgt^{+/-}$ mice was not different from that of the wild type (Figure 3.4). All the major spermatogenic cell stages including spermatogonia, primary spermatocytes, and spermatids (round and elongated) were observed in both $Cgt^{+/-}$ and wild type testis sections. When compared at the same spermatogenic stages, the organization of germ cell layers (i.e., starting from the spermatogonia cell layer at the basal membrane, then the layer of primary spermatocytes, and the layer of spermatids closest to the lumen) in the seminiferous tubules of $Cgt^{+/-}$ testes was similar to that of the wild type. The presence of sperm in the lumen of the $Cgt^{+/-}$ seminiferous tubules suggested that the spermatogenesis process was complete in these mice. To further verify that spermatogenesis in $Cgt^{+/-}$ mice occurred at the same rate as in the wild type mice, the total numbers of sperm collected from both sides of the caudal epididymis and

Figure 3.2 *In vitro* fertilizing ability of wild type and *Cgt*$^{+/-}$ sperm. Percoll gradient centrifuged (PGC) sperm were prepared from *Cgt*$^{+/-}$ and wild type littermates from 5 different litters. Cumulus-free zona-intact mouse eggs were incubated with sperm from wild type or *Cgt*$^{+/-}$ male mice. Six hours afterwards, eggs were scored for evidence of fertilization (two pronuclei formation) under the microscope. Percentages of total eggs fertilized in each gamete co-incubate were recorded. n = total number of eggs assessed. The data are expressed as mean ± S.D. of percent eggs fertilized (**A**) and the percentage of the wild type (control) values (**B**). Differences in fertilization rates between the *Cgt*$^{+/-}$ and wild type samples were analyzed using Student's *t*-test. There was no significant difference between *Cgt*$^{+/-}$ and wild type samples ($P = 0.20$).

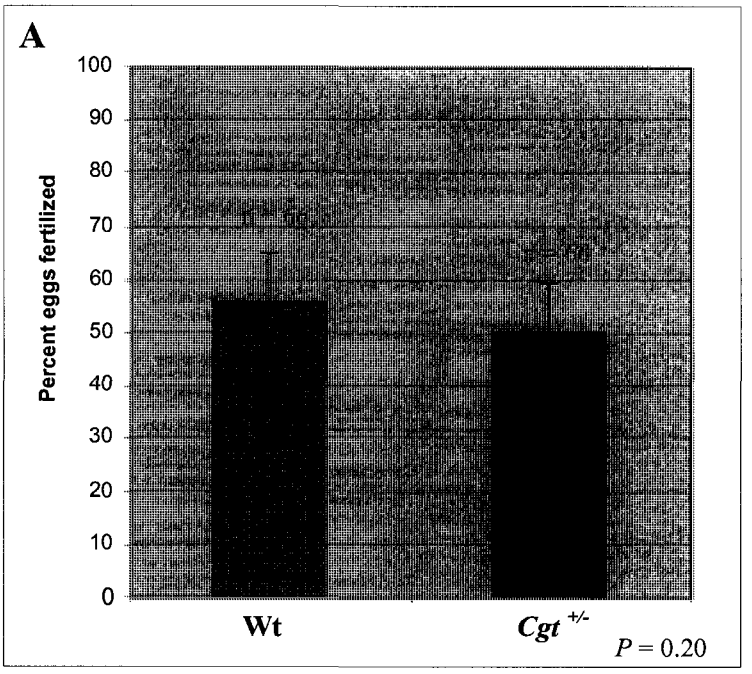
A
Percent eggs fertilized
100
90
80
70
60
50
40
30
20
10
0
Wt
Cgt +/-
P = 0.20

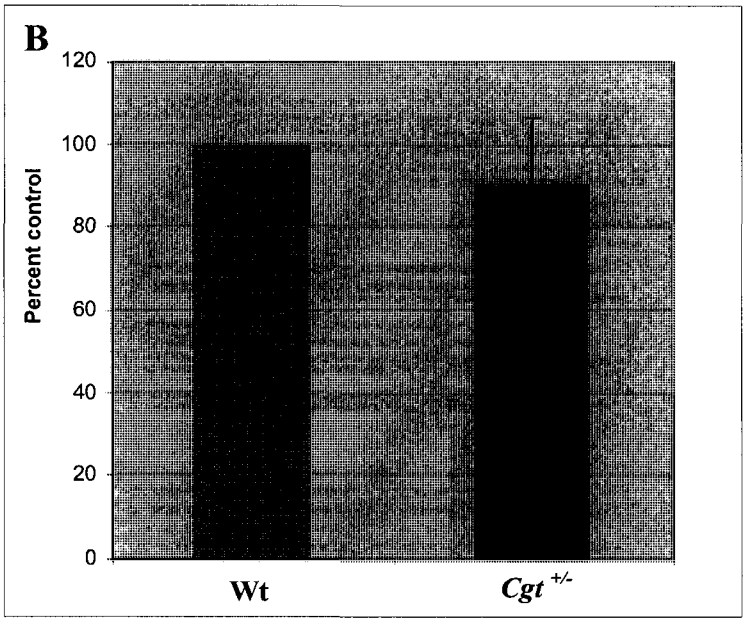
B
Percent control
120
100
80
60
40
20
0
Wt
Cgt +/-

Figure 3.3 Average litter size obtained from females mated with *Cgt*$^{+/-}$ and wild type male littermates. *Cgt*$^{+/-}$ males and wild type male littermates from 5 different litters were individually mated with wild type females (1 male with 1 female per cage). During Day 14-18 of gestation, the females were killed to determine the number of fetuses (litter size) in the uteri. The average litter size obtained from females mated with *Cgt*$^{+/-}$ males and wild type littermates was 8.4 ± 0.9 and 7.4 ± 0.9 pups/litter, respectively. For comparison, data obtained from each pair of *Cgt*$^{+/-}$ and wild type male littermates were indicated by dashed lines. The Student's *t*-test analysis revealed no significant difference between the two sets of data ($P = 0.12$).

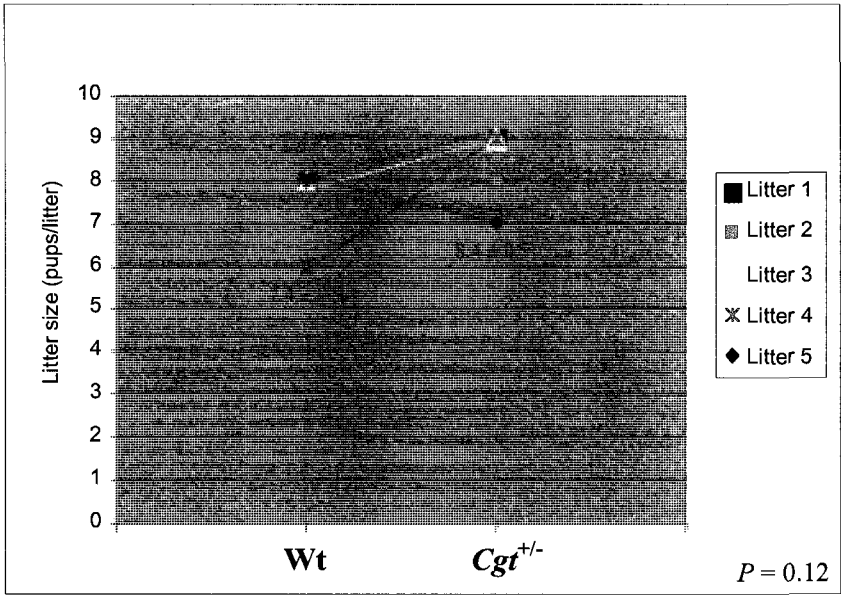
10
9
8
7
6
5
4
3
2
1
0
Litter size (pups/litter)
Litter 1
Litter 2
Litter 3
Litter 4
Litter 5
Wt
Cgt+/-
P = 0.12

Figure 3.4 Light microscopy of testis sections from adult *Cgt*$^{+/-}$ (A, C, E, G) and wild type (B, D, F, H) littermates. The paraffin sections of wild type and *Cgt*$^{+/-}$ testes were stained with hematoxylin and eosin. The overall morphology of seminiferous tubules was shown by low (100x) magnification images (**A and B**), and different spermatogenic stages (indicated by Roman numerals) were shown by high (400x) magnification images (**C-H**). The scale bars represent 50 μm. Each type of spermatogenic cells was also indicated in the inset of D: spermatogonium (black arrow), primary spermatocyte (blue arrow), round spermatid (green arrow) and elongated spermatid (red arrow).

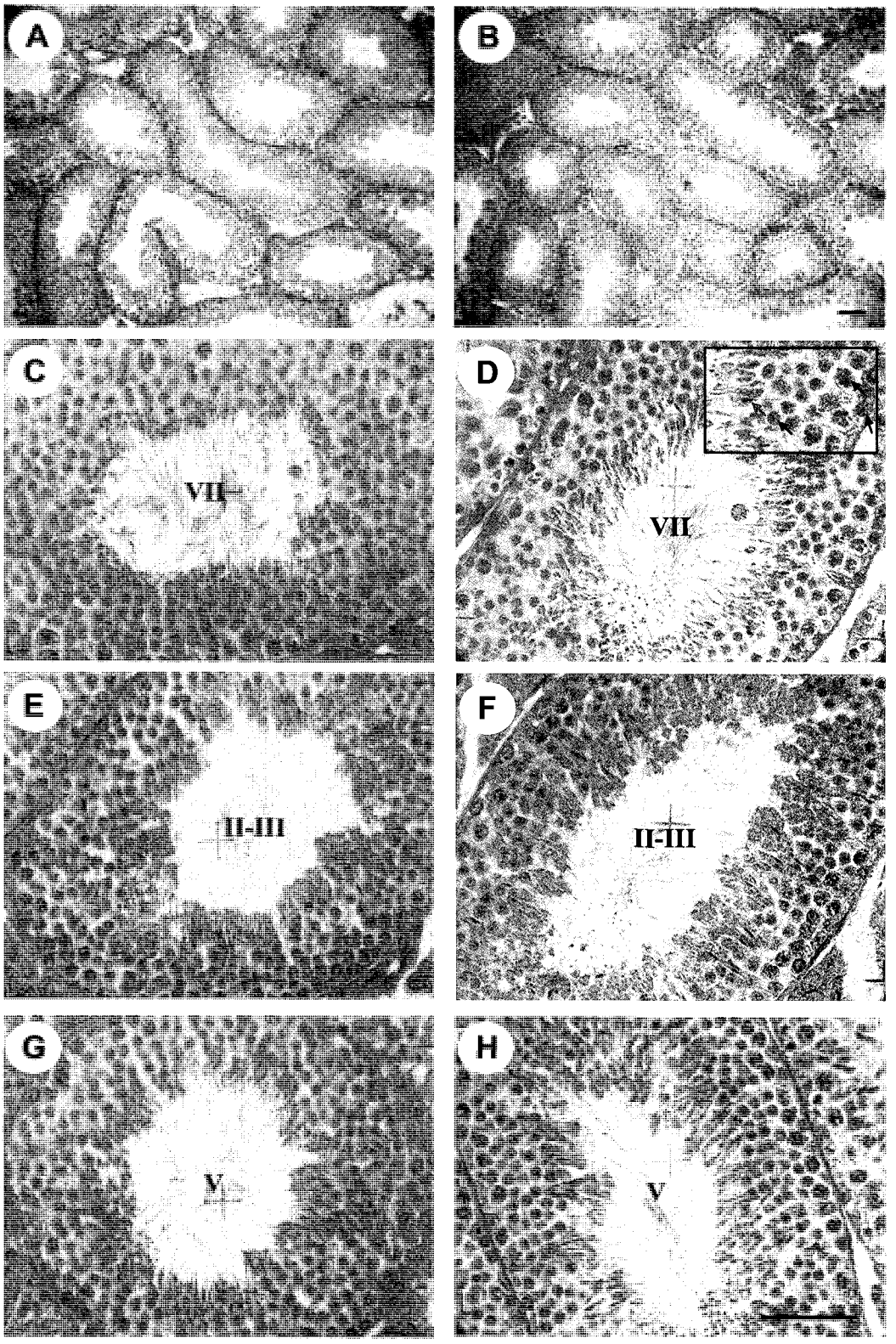
Cgt+/-
Wild type
A
B
C
VII
D
VII
E
II-III
F
II-III
G
V
H
V

vas deferens of these mice were assessed. The results showed no significant difference between these values in the *Cgt*$^{+/-}$ mice and the wild type littermates (21.1 ± 6.9 vs 18.5 ± 4.3; n = 7; $P = 0.42$) (Figure 3.5). In addition, the average testis weight of *Cgt*$^{+/-}$ mice was similar to that of the wild type littermates (103.7 ± 6.3 vs 110.1 ± 2.6; n = 5; $P = 0.07$). All these results showed that *Cgt*$^{+/-}$ mice had a normal spermatogenesis status.

3.4 Lipid profiles of testis and sperm of *Cgt*$^{+/-}$ and wild type mice

To examine whether there were any changes in *Cgt*$^{+/-}$ testis and sperm lipid profiles, isolated testis/sperm lipids were subjected to HPTLC. Figure 3.6 showed that SGG and other major testis and sperm lipids, including cholesterol (Chol), phosphatidylethanolamine (PE), phosphatidylcholine (PC) and sphingomyelin (SM), were present in both *Cgt*$^{+/-}$ and wild type lipid extracts. The orcinol staining showed glycolipid profiles of *Cgt*$^{+/-}$ sperm and testes similar to those of the wild type (Figure 3.6A). Namely, SGG was the only major glycolipid in the testis and sperm lipids of *Cgt*$^{+/-}$ mice and the wild type. Following the orcinol staining, Coomassie blue staining also showed no difference in the total lipid profiles of *Cgt*$^{+/-}$ and wild type samples (Figure 3.6B). Moreover, the sulfolipid profiles of *Cgt*$^{+/-}$ and wild type lipids were similar. Only SGG was present in the testis and sperm lipids of *Cgt*$^{+/-}$ and wild type mice after the Azure A staining (Figure 3.6C). Taken together, these results indicated no major changes in the sperm and testis lipid profiles of *Cgt*$^{+/-}$ mice as compared with those of the wild type littermates. Also, based on the intensity of SGG bands on HPTLC, the amounts of SGG in testes and sperm of *Cgt*$^{+/-}$ mice did not appear to be different from those of the wild type.

Figure 3.5 Total numbers of sperm from *Cgt*$^{+/-}$ mice and their wild type littermates. Sperm from both sides of caudal epididymis and vas deferens of a *Cgt*$^{+/-}$ mouse or a wild type mose were collected into 1 ml of KRB-Hepes. A small aliquot of the sperm suspension was used for counting. The data were presented as mean ± S.D. of the total number of sperm. n = number of mice from each genotype used for assessment of total sperm number. Data were analyzed for significant differences using Student's *t*-test and no significant difference was found between two sets of data ($P = 0.42$).

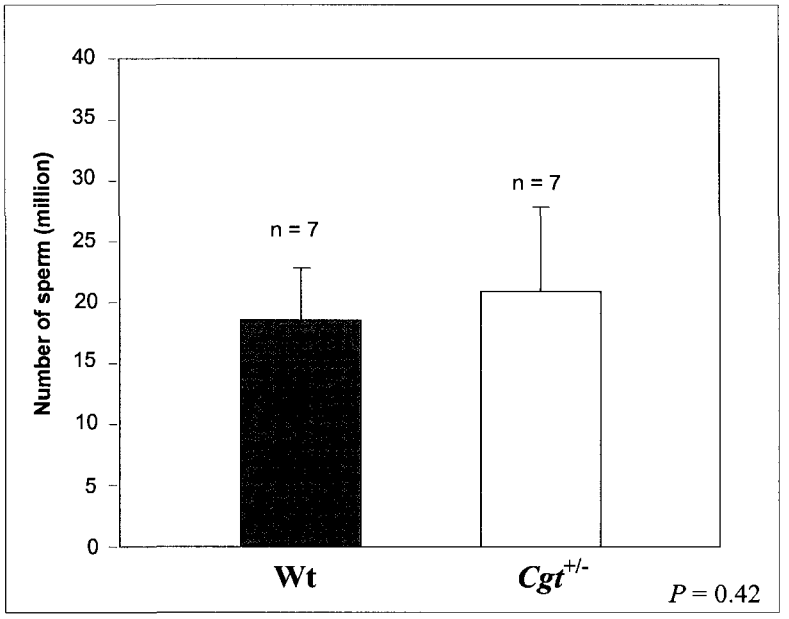
40
35
30
25
20
15
10
5
0
Number of sperm (million)
n = 7
n = 7
Wt
Cgt+/-
P = 0.42

Figure 3.6 HPTLC of sperm and testis lipids from *Cgt*$^{+/-}$ and wild type mice. Lipids extracted from 5 mg of testes (lanes 1&2) and from 7 million sperm (lanes 3&4) were used for loading. Standard lipids were also co-chromatographed. Samples and standard lipids were loaded onto two parallel HPTLC plates. One HPTLC plate was sprayed with orcinol solution, which stained glycolipids purple and stained other lipids different colors (e.g., phospholipids brown, cholesterol red) (Panel **A**). After orcinol charring, the same HPTLC plate was furthered immersed in Coomassie blue solution, which stained all lipids blue (Panel **B**). The other HPTLC plate was sprayed with Azure A solution, which specifically stained the sulfolipids blue (Panel **C**).

Abbreviation: Chol – Cholesterol, PE – Phosphatidylethanolamine, SGG – Sulfogalactosylglycerolipid, PC – Phosphatidylcholine, SM – Sphingomyelin, Wt – Wild type.

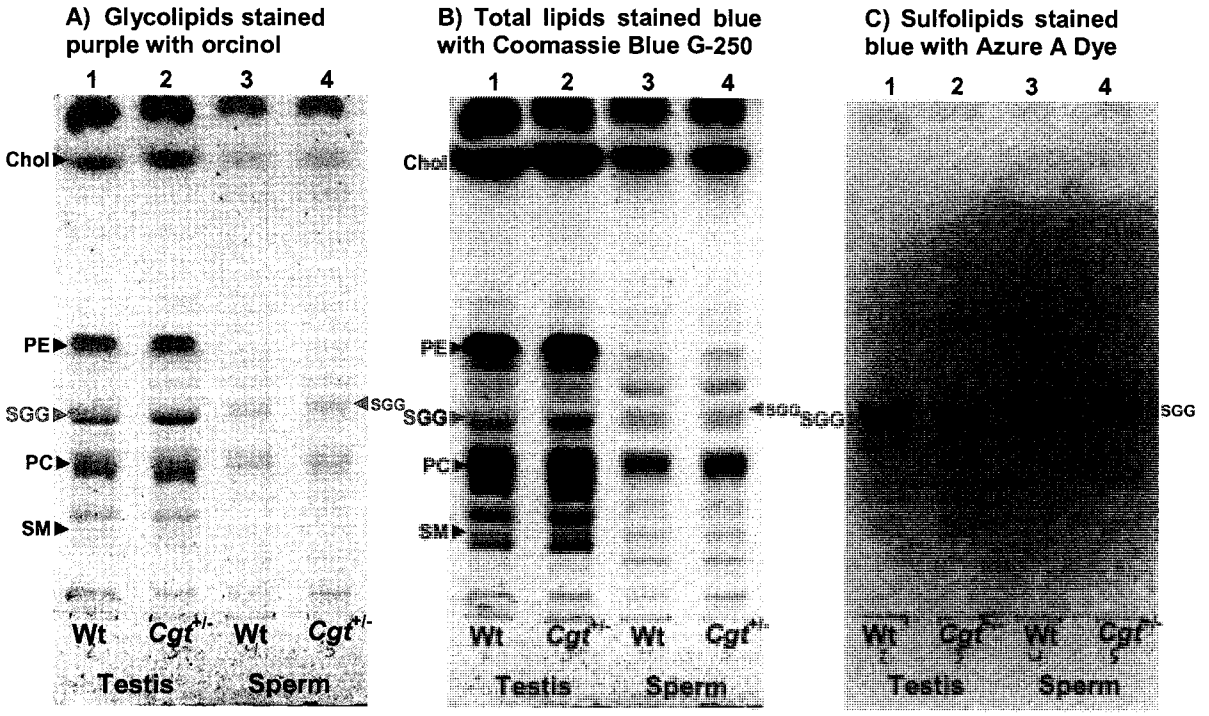
A) Glycolipids stained purple with orcinol
B) Total lipids stained blue with Coomassie Blue G-250
C) Sulfolipids stained blue with Azure A Dye
1 2 3 4
Chol
PE
SGG
PC
SM
Wt
Cgt+/-
Testis
Sperm

3.5 Quantification of SGG in sperm and testes of *Cgt*$^{+/-}$ and wild type mice

To determine the amounts of SGG in *Cgt*$^{+/-}$ sperm and testes in comparison with those of the wild type littermates, SGG in the total lipids extracted from testes and sperm of these mice was quantified by Azure A assay. Since this Azure A assay is based on the reaction of Azure A dye with the sulfate groups of lipids, this assay would be valid when SGG is the only major sulfolipid in the total lipid extracts (Figure 3.7A). From the Azure A stained-HPTLC plate (Figure 3.6C), it was evident that SGG was the only sulfolipid in the total sperm and testis lipids of *Cgt*$^{+/-}$ and wild type mice. To further confirm this, electrospray ionization mass spectrometry (ESI-MS), a very sensitive and accurate technique, was also used. First, the purified SGG standard (isolated from pig testis by the described method (Tupper et al., 1994) was scanned in the negative ion mode to reveal the signature of SGG at 795 m/z (Figure 3.7B). The ESI-MS in the negative ion mode was then performed on total lipids extracted from mouse caudal epididymal and vas deferens sperm. The 795 m/z peak was found as the major negatively charged lipid (Figure 3.7C). The parent ion scanning of the sulfate group (HSO_4^-) by MS-MS of the total mouse sperm lipids also revealed that the 795 m/z peak was the major lipid that possessed the sulfate group (Figure 3.7D). Therefore, it was valid to use the Azure A assay for quantifying SGG in the total lipids extracted from sperm.

The quantification of SGG by the Azure A assay revealed that the levels of SGG in sperm of *Cgt*$^{+/-}$ and wild type littermates were not significantly different from each other (0.760 ± 0.180 vs 0.917 ± 0.258 nmol/million sperm; n = 5; P = 0.16) (Figure 3.8). Moreover, the SGG levels in the testes of *Cgt*$^{+/-}$ and wild type mice were similar (3,213.973 ± 392.654 vs 3,220.555 ± 387.177 nmol/g of tissue; n = 6; P = 0.45) (Figure 3.9). These results suggested that the compensatory mechanisms occurred in *Cgt*$^{+/-}$ mice, adjusting SGG

Figure 3.7 Azure A assay and electrospray ionization mass spectrometry (ESI-MS) of SGG. The diagram showed steps involved in Azure A assay **(A)**. ESI-MS in the negative ion mode of purified pig testis SGG showed the 795 m/z signature of SGG **(B)**. The negative ion ESI/MS of total mouse sperm lipids in the range of 600 to 1200 m/z revealed that 795 peak was the major negatively charged lipid **(C)**. The identity of this 795 peak as SGG was confirmed by the sulfate precursor scanning **(D)**.

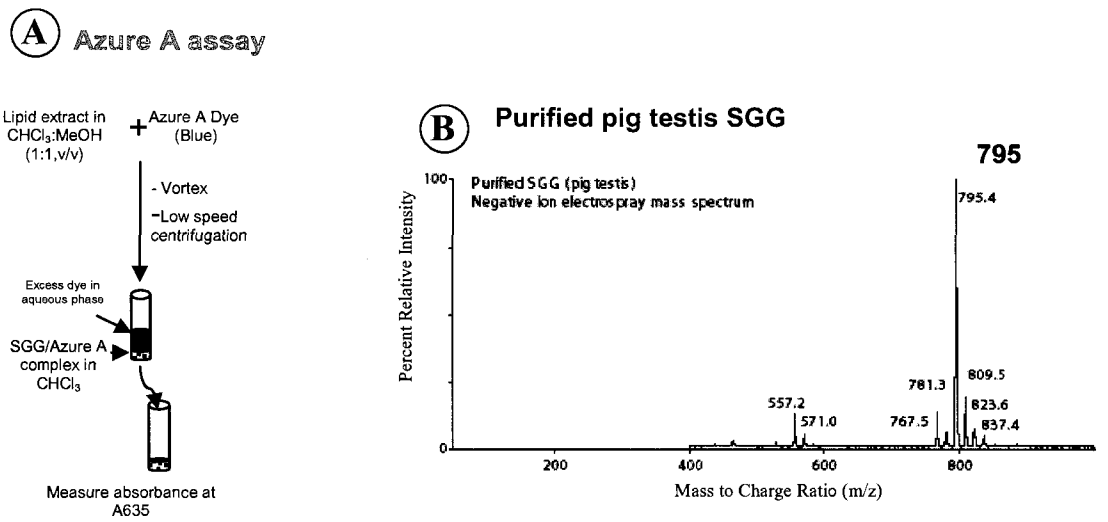
A Azure A assay
Lipid extract in CHCl3:MeOH (1:1,v/v)
+ Azure A Dye (Blue)
- Vortex
-Low speed centrifugation
Excess dye in aqueous phase
SGG/Azure A complex in CHCl3
Measure absorbance at A635
B Purified pig testis SGG
795
Purified SGG (pig testis)
Negative ion electrospray mass spectrum
795.4
809.5
781.3
823.6
557.2
571.0
767.5
837.4
Percent Relative Intensity
Mass to Charge Ratio (m/z)
Total mouse sperm lipids
C Negative ion ESI-MS
795
Percent Relative Intensity
Mass to Charge Ratio (m/z)
D Precursor Scan for sulfate
795
Percent Relative Intensity
Mass to Charge Ratio (m/z)

Figure 3.8 Quantification of SGG in *Cgt*$^{+/-}$ and wild type sperm. Sperm were collected from the caudal epididymis and vas deferens of *Cgt*$^{+/-}$ males and wild type littermates from 5 different litters. One pair of mice was used for this experiment in all litters except litter 2 in which 3 pairs of wild type and *Cgt*$^{+/-}$ mice were used. Total lipids were extracted from the sperm by the Bligh/Dyer method and quantified by the Azure A assay. A standard curve was constructed using SGC (SGG analog). Each sperm lipid sample was assayed in duplicate. For comparison, data obtained from each pair of *Cgt*$^{+/-}$ and wild type littermates were indicated by dashed lines. Data were analyzed by Student's *t*-test. The significant difference was determined at a confidence level of $P \leq 0.05$. No significant difference was found between the two sets of samples ($P = 0.16$). The average amounts of sperm SGG in *Cgt*$^{+/-}$ mice and wild type littermates were shown in the figure.

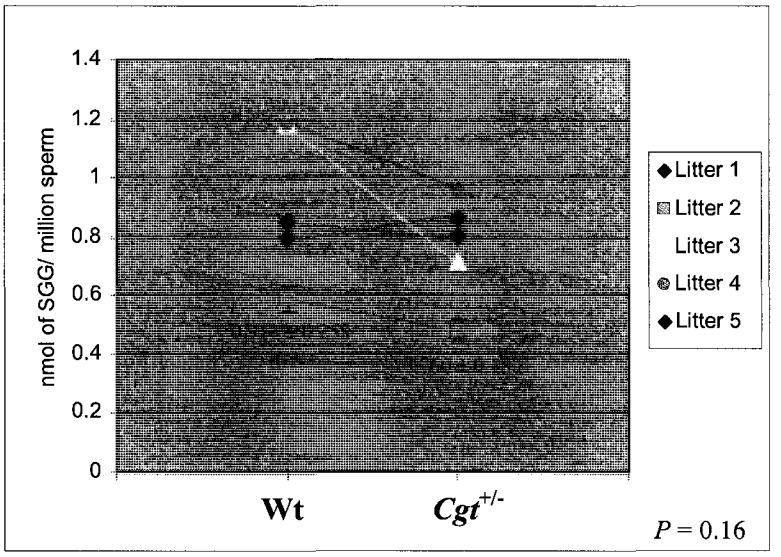
1.4
1.2
1
0.8
0.6
0.4
0.2
0
nmol of SGG/ million sperm
Litter 1
Litter 2
Litter 3
Litter 4
Litter 5
Wt
Cgt+/-
P = 0.16

Figure 3.9 Quantification of SGG in *Cgt*$^{+/-}$ and wild type testes. Testes were collected from *Cgt*$^{+/-}$ males and their wild type littermates from 6 different litters. Lipid extraction and SGG quantification were the same as that described for the sperm samples. Each testis lipid sample was assayed in triplicates. For comparison, data obtained from each pair of *Cgt*$^{+/-}$ and wild type littermates were indicated by dashed lines. Data were analyzed by Student's *t*-test and the significant difference was determined at a confidence level of $P \leq 0.05$. No significant difference was found between the two sets of samples ($P = 0.98$). The average amounts of testis SGG in *Cgt*$^{+/-}$ mice and wild type littermates were shown in the figure.

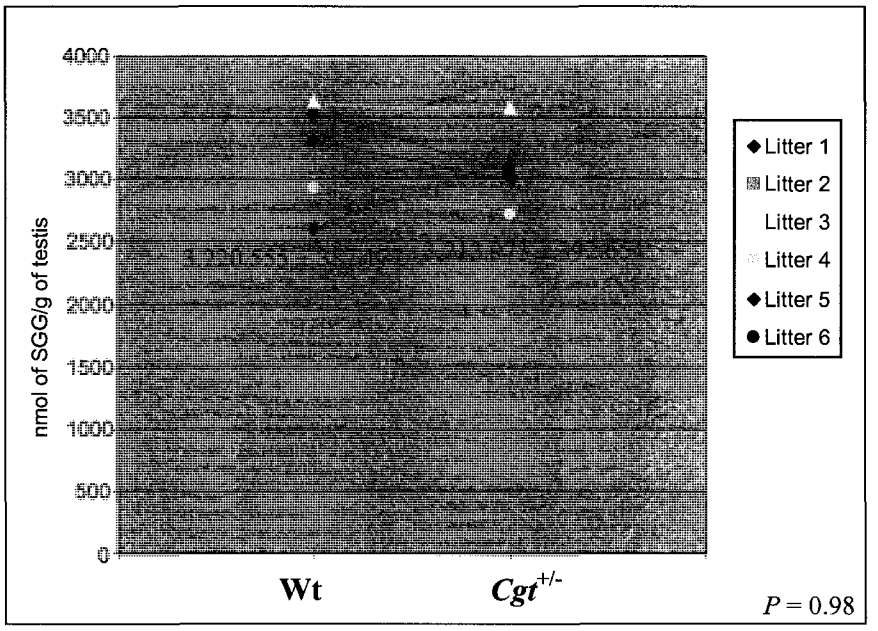
4000
3500
3000
2500
2000
1500
1000
500
0
nmol of SGG/g of testis
Litter 1
Litter 2
Litter 3
Litter 4
Litter 5
Litter 6
Wt
Cgt+/-
P = 0.98

levels to be the same as those of the wild types. These normal levels of SGG might be essential for maintaining the normal status of spermatogenesis and fertility of the $Cgt^{+/-}$ mice.

3.6 *Cgt* mRNA expression levels in $Cgt^{+/-}$ mice

One possible compensatory mechanism to adjust SGG in $Cgt^{+/-}$ mice to the wild type levels could be an increased level of *Cgt* mRNA expression in the testes of $Cgt^{+/-}$ mice. To further investigate this possibility, real time RT-PCR was performed to quantify *Cgt* mRNA in wild type and $Cgt^{+/-}$ testes. The levels of β-actin mRNA expression were also measured to be used as an internal standard for normalizing *Cgt* mRNA. The results showed that β-actin mRNA levels were similar in both $Cgt^{+/-}$ and wild type testis samples (average amounts of β-actin mRNA in $Cgt^{+/-}$ and wild type testes were 0.02610 ± 0.00039 and 0.02761 ± 0.00505 pg, respectively). As expected, the $Cgt^{+/-}$ testes expressed about half the *Cgt* mRNA levels of the wild type testes. The average amounts of *Cgt* mRNA in wild type and $Cgt^{+/-}$ samples were 0.01519 ± 0.00283 and 0.00610 ± 0.00054 pg per pg of β-actin mRNA, respectively ($n = 3$; $P = 0.005$) (Figure 3.10A). In other words, the amount of *Cgt* mRNA in the $Cgt^{+/-}$ testis samples was $40.9 \pm 6.6\%$ of the wild type control (Figure 3.10B). This indicated that the compensatory mechanisms for SGG biosynthesis in $Cgt^{+/-}$ mice did not happen at the transcriptional step of *Cgt*.

3.7 CGT polypeptide levels in $Cgt^{+/-}$ mice

The compensatory mechanisms for SGG might occur through other steps involved in SGG metabolism e.g., CGT polypeptide expression, CGT activity or ASA-regulating degradation steps of SGG. Firstly, to determine the CGT polypeptide levels in $Cgt^{+/-}$ testes, the anti-CGT antibody was produced as described in the Materials and Methods. Anti-CGT

Figure 3.10 *Cgt* mRNA expression levels in $Cgt^{+/-}$ versus wild type testes. Total RNA extracted from $Cgt^{+/-}$ and wild type testes were reverse transcribed into cDNA, which was used as a template for real time RT-PCR. The amounts of *Cgt* mRNA expressed in each sample were normalized by the amounts of β-actin mRNA expressed in the same sample (**A**). The *Cgt* mRNA expression levels in $Cgt^{+/-}$ testes were expressed as percentage of the wild type samples (control) (**B**). The statistical analysis result showed that *Cgt* expression levels in $Cgt^{+/-}$ testes were significantly different from those in the wild type testes ($P = 0.005$).

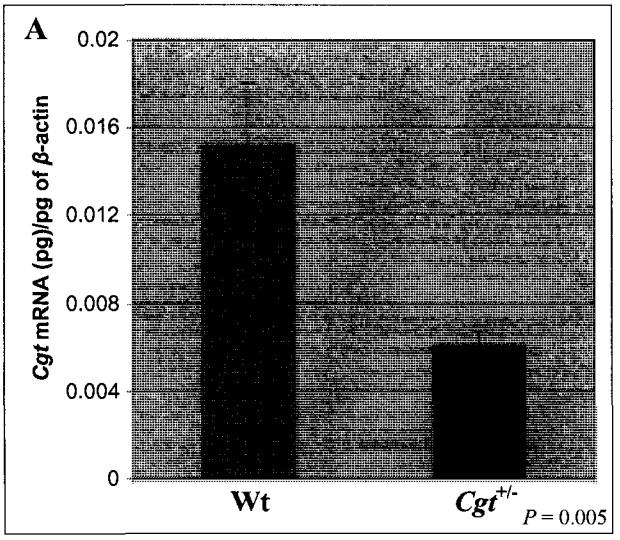
A
0.02
0.016
0.012
0.008
0.004
0
Cgt mRNA (pg)/pg of β-actin
Wt
Cgt+/-
P = 0.005

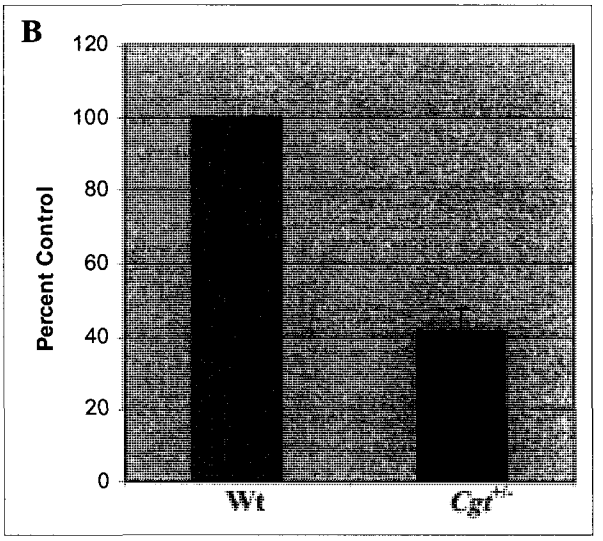
B
120
100
80
60
40
20
0
Percent Control
Wt
Cgt+/-

antiserum was used for immunoblotting of postnuclear supernatant samples prepared from *Cgt*$^{+/-}$ and wild type testes. The immunoblotting result revealed the presence of a testis protein with a molecular mass of 72 kDa in wild type and *Cgt*$^{+/-}$ samples, but not in the knockout sample (Figure 3.11A). The absence of this 72 kDa band in the knockout sample validated the identity of this band as CGT. The amounts of the 72 kDa bands in wild type and *Cgt*$^{+/-}$ samples were assessed by densitometry. The results revealed similar intensities of this band in the wild type and *Cgt*$^{+/-}$ testis samples (average integrated density values after subtracting background values were 150.7 ± 24.5 and 138.3 ± 21.0 arbitrary units, respectively, n = 3; $P = 0.54$) (Figure 3.11B). In other words, the expression of CGT in *Cgt*$^{+/-}$ samples was 96.6 ± 18.5% of that of the wild type (Figure 3.11C). Therefore, the compensatory mechanisms of SGG occurred through the increased levels of CGT translation.

3.8 Enzymatic activity of CGT in *Cgt*$^{+/-}$ mice

A similar activity of the CGT enzyme in *Cgt*$^{+/-}$ and wild type testes was further confirmed. In this CGT activity assay, a fluorescent substrate, NBD-Cer, was used to measure the CGT activity in the postnuclear supernatant (containing endoplasmic reticula, expected locales of CGT) prepared from *Cgt*$^{+/-}$ and wild type testes. In order to precisely compare the enzymatic activity of CGT in *Cgt*$^{+/-}$ and wild type samples, a proper incubation time must be first defined. This incubation time should be when the enzyme activity is still in the linear range and doest not reach saturation. Postnuclear supernatants prepared from wild type testis homogenate were incubated with NBD-Cer in a neutral pH buffer containing a galactose donor, UDP-Gal, for different periods of time (0, 15, 30, 45, 60, 90, and 120 min). Lipids extracted from each reaction were subjected to HPTLC, which separated NBD-Cer from the NBD-GC product (Figure 3.12A). Being fluorescent, the intensity of NBD-GC

Figure 3.11 Expression levels of CGT polypeptides in *Cgt*$^{+/-}$ and wild type testes. The post nuclear supernatants (20 μg of total proteins) prepared from two sets of *Cgt*$^{+/-}$ and wild type testes were used for immunoblotting with anti-CGT antibody (**A**). The supernatant from a *Cgt* null testis was used as a negative control to confirm the specificity of the antibody. The levels of CGT polypeptide expressed in *Cgt*$^{+/-}$ testes were analyzed by densitometry and present as mean ± S.D. of CGT band intensity (**B**) or the percentage of the control values (obtained from the wild type littermate samples, defined as 100%) (**C**). Statistical analysis of the CGT band intensity values revealed no significant difference between the *Cgt*$^{+/-}$ and wild type data ($P = 0.54$).

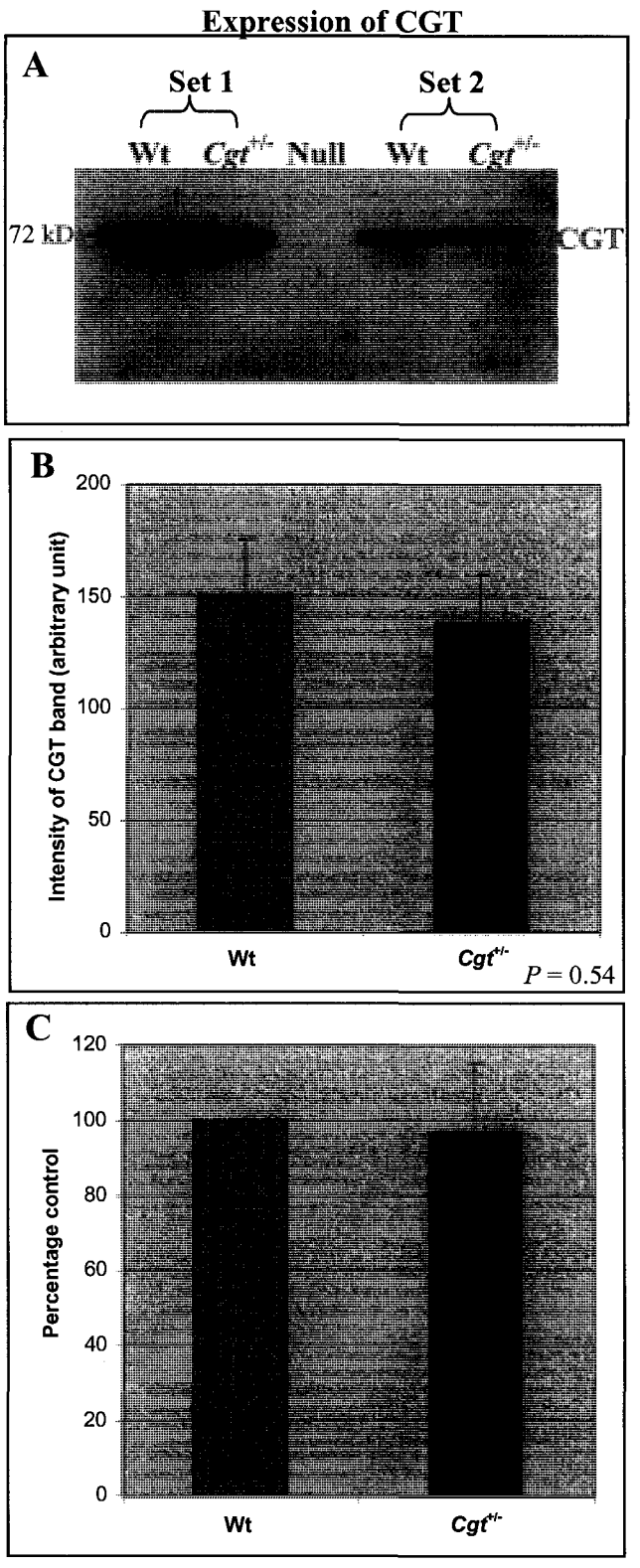
Expression of CGT
A
Set 1
Set 2
Wt
Cgt+/-
Null
Wt
Cgt+/-
72 kD
CGT
B
Intensity of CGT band (arbitrary unit)
200
150
100
50
0
Wt
Cgt+/-
P = 0.54
C
Percentage control
120
100
80
60
40
20
0
Wt
Cgt+/-

Figure 3.12 CGT enzymatic activities at various incubation periods. Postnuclear supernatants of wild type testis sample (20 μg of total protein/reaction) were incubated in a reaction mixture containing NBD-Cer for different periods of time (0, 15, 30, 45, 60, 90 and 120 min). The lipids were extracted from the reaction mixtures and subjected to HPTLC (**A**). The intensity of NBD-GC bands, products of CGT enzymatic activity, was determined by densitometric analysis and plotted as a function of time. The red dashed arrow indicated the incubation time (25 min) when NBD-GC intensity was in the middle of the linear range (**B**).

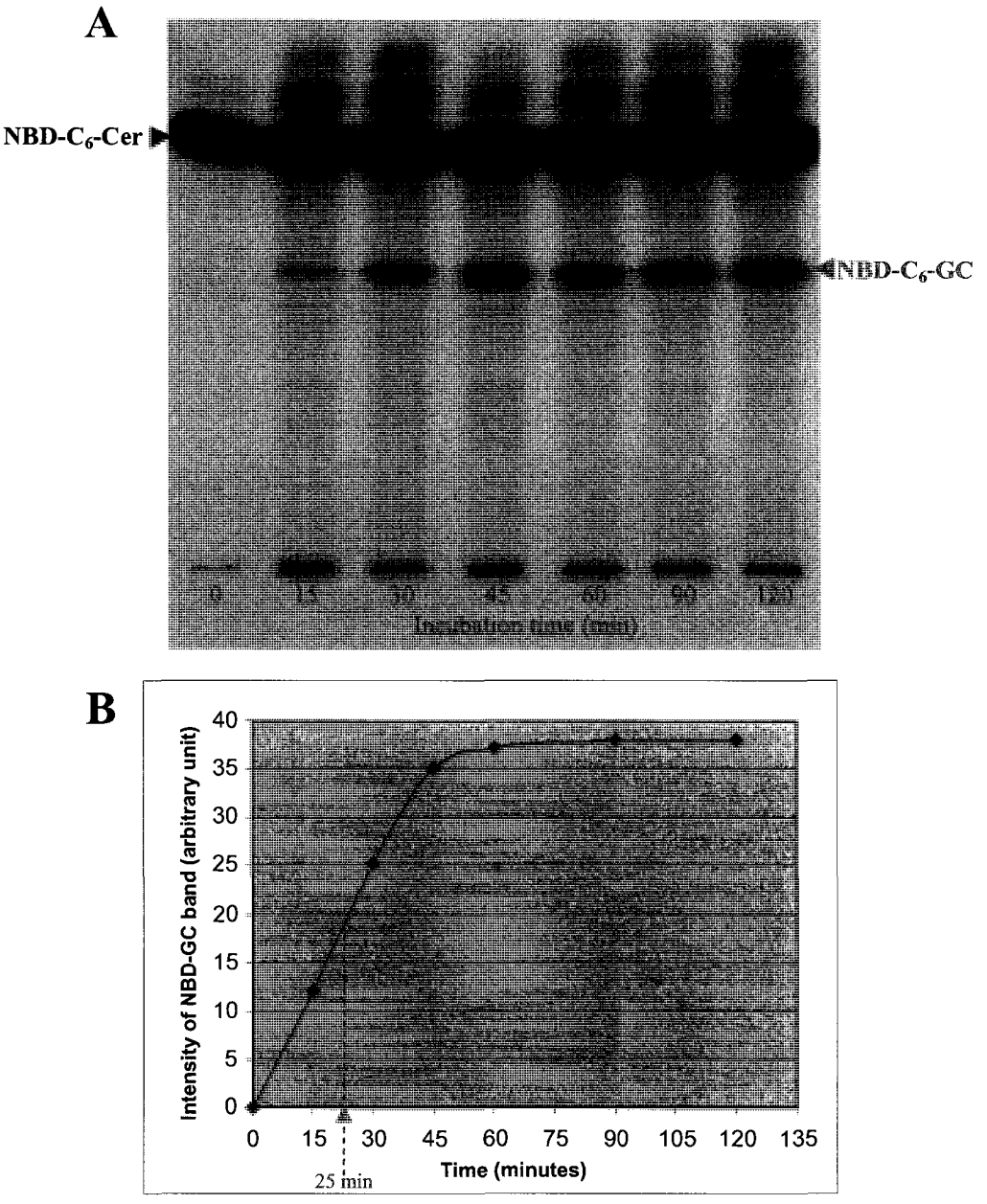
A
NBD-C6-Cer
NBD-C6-GC
0
15
30
45
60
90
120
Incubation time (min)
B
Intensity of NBD-GC band (arbitrary unit)
40
35
30
25
20
15
10
5
0
0
15
30
45
60
75
90
105
120
135
Time (minutes)
25 min

could be determined by a Typhoon phosphoimager, and densitometry of this intensity was plotted as a function of time. The intensity of NBD-GC product was increased in a linear fashion from 0 min up to 45 min of the incubation, but beyond 45 min of incubation, the intensity of the NBD-GC product reached a plateau (Figure 3.12B). The NBD-GC intensity was in the middle of the linear range when the reaction was incubated for 25 min; therefore, this incubation time was selected and used for the assay to compare activity of CGT in $Cgt^{+/-}$ and wild type samples (Figure 3.12B). As shown in Figure 3.13A, the NBD-GC products of CGT activity were observed in both wild type and $Cgt^{+/-}$ samples. In contrast, there was no NBD-GC product found in the knockout sample, as expected. The densitometric analyses revealed similar intensity of NBD-GC in the wild type and $Cgt^{+/-}$ samples. Average integrated density values of the wild type and $Cgt^{+/-}$ samples (3 animals used for each genotype) after subtracting the background values were 16.7 ± 4.7 and 15.7 ± 5.5 arbitrary units, respectively ($P = 0.82$) (Figure 3.13B). The intensity of NBD-GC in $Cgt^{+/-}$ samples from 3 experiments was 93.0 ± 15.0% of the wild type samples (Figure 3.13C). Therefore, these results indicated that the enzymatic activity of CGT in $Cgt^{+/-}$ testes was comparable to that in the wild type testes.

3.9 Levels of SGG degradation mediated by arylsulfatase A (ASA) in $Cgt^{+/-}$ mice

From the immunoblotting and CGT activity assay, it was likely that the SGG levels in $Cgt^{+/-}$ testes were adjusted through the SGG biosynthetic pathway. However, SGG levels in testes may also be regulated through its degradation by arylsulfatase A (ASA), an enzyme which has been shown to have SGG desulfation activity *in vitro* and found in lysosomes of the Sertoli cells. The levels of testis ASA expression or activity may be increased in $Cgt^{+/-}$ mice. To determine this possibility, the expression of ASA at the mRNA and polypeptide

Figure 3.13 Enzymatic activity of CGT in *Cgt*$^{+/-}$ and wild type testes. Twenty micrograms of *Cgt*$^{+/-}$ and wild type postnuclear supernatants in homogenization buffer were incubated in a reaction mixture containing NBD-Cer for 25 min at 37°C. The sample from a null testis was used as a negative control. The lipids extracted from the reaction mixtures were subjected to HPTLC (**A**). The NBD-GC bands, representing the product of CGT enzymatic reaction, were subjected to densitometric analysis. The intensity of NBD-GC bands obtained from the densitometric analysis was expressed as mean ± S.D. (**B**) and the percentage of the wild type (control) value (**C**). Differences in intensity of NBD-GC bands between the *Cgt*$^{+/-}$ and wild type samples were analyzed using Student's *t*-test and no significant difference was found between two sets of samples ($P = 0.82$).

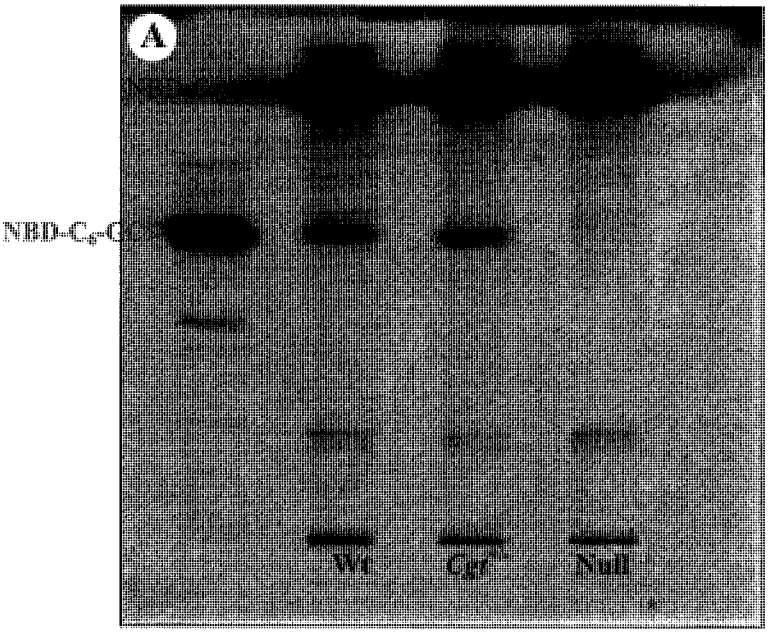
A
NBD-C6-GC
Wt
Cgt+/-
Null

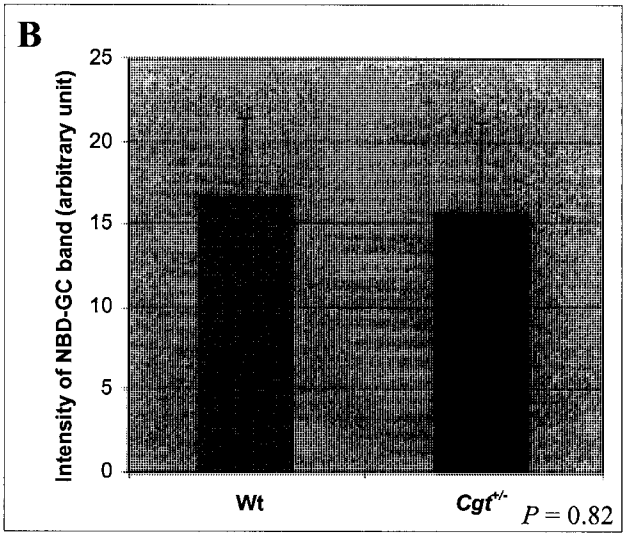
B
Intensity of NBD-GC band (arbitrary unit)
25
20
15
10
5
0
Wt
Cgt+/-
P = 0.82

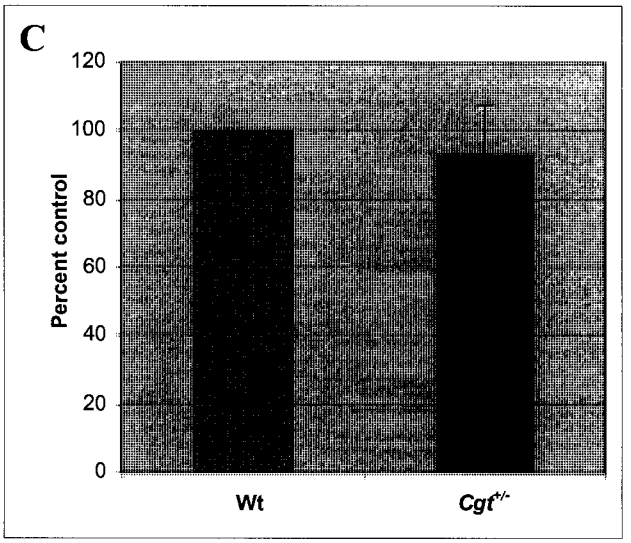
C
Percent control
120
100
80
60
40
20
0
Wt
Cgt+/-

levels were determined using the real time RT-PCR and immunoblotting approach, respectively. Real time RT-PCR results revealed that the *ASA* mRNA levels in $Cgt^{+/-}$ testes were similar to those of the wild type testes (The average amounts of *ASA* mRNA in wild type and $Cgt^{+/-}$ samples were 0.02292 ± 0.00285 and 0.02279 ± 0.00171 pg per pg of β-actin mRNA, respectively; n = 3; $P = 0.95$) (Figure 3.14A). The *ASA* mRNA level in $Cgt^{+/-}$ testes was 100.6 ± 16.3% of that of the wild type (Figure 3.14B). Immunoblotting results also showed that there was no change in ASA polypeptide levels in the $Cgt^{+/-}$ testes compared to those in the wild type testes (Figure 3.15A).

To test whether the enzymatic activity of ASA in $Cgt^{+/-}$ testes was increased, the ASA desulfation assay was performed using NCS as the artificial substrate. The average of ASA specific activity from $Cgt^{+/-}$ and wild type samples were 0.057 ± 0.021 and 0.056 ± 0.021 U/mg of protein, respectively (Figure 3.15B). The statistical analysis revealed no significant difference between the two samples ($P = 0.96$). Therefore, all these results indicated that the compensatory mechanisms of SGG in $Cgt^{+/-}$ testes did not occur at the degradation step.

Figure 3.14 Expression levels of *ASA* mRNA in *Cgt*$^{+/-}$ and wild type testes. Expression levels of *ASA* mRNA in *Cgt*$^{+/-}$ and wild type testes were quantified by real time RT-PCR and normalized by amounts of β-actin mRNA (**A**). The *ASA* mRNA level of *Cgt*$^{+/-}$ testis was presented as percentage of the wild type value (**B**). *ASA* mRNA expression levels in *Cgt*$^{+/-}$ and wild type testis samples were analyzed by Student's *t*-test and no significant difference was found between the two samples ($P = 0.95$).

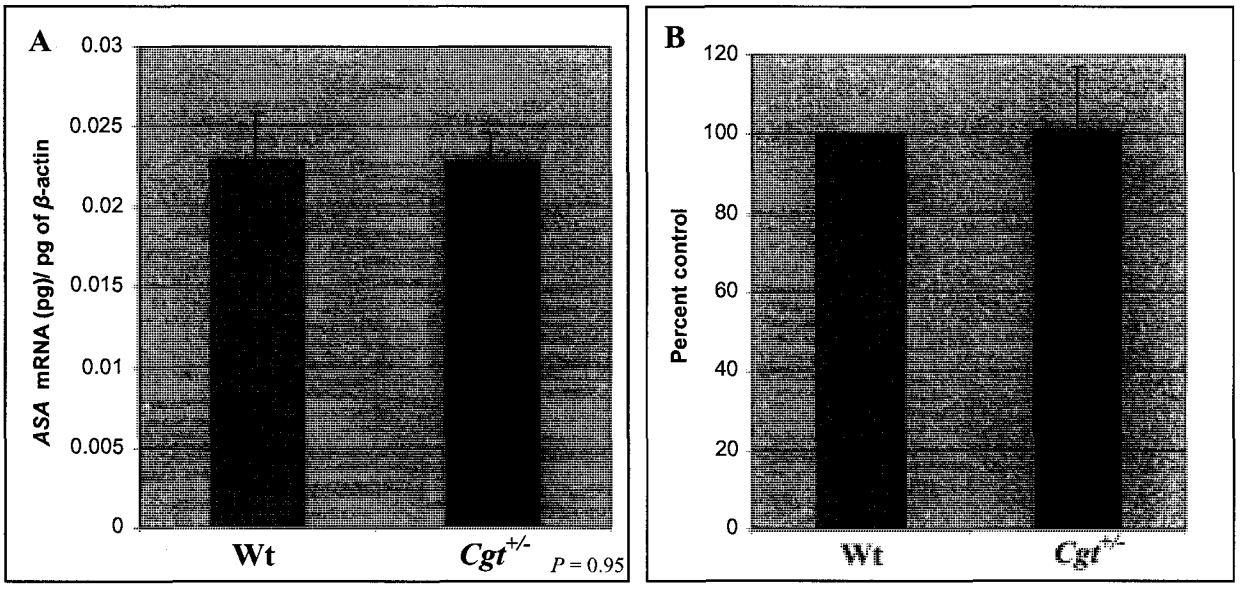
A
0.03
0.025
0.02
0.015
0.01
0.005
0
ASA mRNA (pg)/ pg of β-actin
Wt
Cgt+/-
P = 0.95
B
120
100
80
60
40
20
0
Percent control
Wt
Cgt+/-

Figure 3.15 Immunoblotting and desulfation activity of ASA in *Cgt*$^{+/-}$ and wild type testes. The ASA polypeptide levels in *Cgt*$^{+/-}$ and wild type testes were shown by immunoblotting using anti-ASA antibody (**A**). The average specific activity of ASA (U/mg protein) obtained from three pairs of *Cgt*$^{+/-}$ and wild type samples were expressed as mean ± S.D. (**B**). Data were analyzed by Student's *t*-test. No significant difference was found between two sets of samples (P =0.96).

A) Immunoblotting of ASA

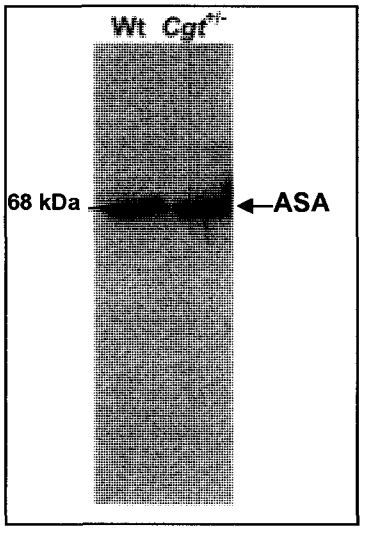

B) Specific activity of ASA

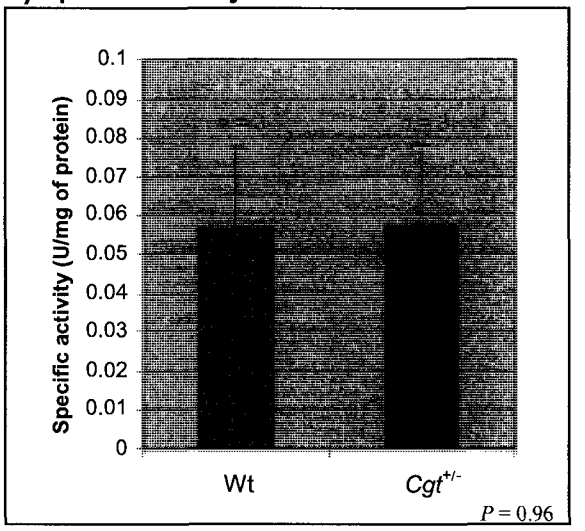

CHAPTER FOUR

DISCUSSION

4.1 Fertility status and sperm SGG levels of *Cgt*$^{+/-}$ mice

SGG has been shown to be important for sperm-egg interaction *in vitro* (Ahnonkitpanit et al., 1999; White et al., 2000). It was therefore reasonable to hypothesize that *Cgt*$^{+/-}$ mouse sperm, expected to have about 50% the SGG level of the wild type, would have compromised fertilizing ability. Surprisingly, the results from IVF experiments and mating studies revealed that *Cgt*$^{+/-}$ mouse sperm had no defects in their fertilizing ability *in vitro* and *in vivo* (Figure 3.2 and 3.3, respectively). To find an explanation for these unexpected results, the SGG levels in the sperm of *Cgt*$^{+/-}$ mice were determined in comparison to those of the wild type. Interestingly, the SGG levels of *Cgt*$^{+/-}$ sperm were not significantly different from those of the wild type sperm (Figure 3.8). Moreover, the lipid profiles of *Cgt*$^{+/-}$ and wild type sperm were also similar (Figure 3.6). These results explain why there was no difference in fertilizing ability of the *Cgt*$^{+/-}$ and the wild type sperm. Therefore, the *Cgt*$^{+/-}$ mice cannot be used as the *in vivo* models for studying the roles of SGG in sperm fertilizing ability due to the normal levels of SGG in sperm as well as the normal fecundity of these mice. However, these results indicate that a normal level of sperm SGG is important for maintaining the sperm fertilizing ability.

4.2 Spermatogenesis status and testis SGG levels of *Cgt*$^{+/-}$ mice

In accordance to the normal fertilizing ability of *Cgt*$^{+/-}$ sperm, the spermatogenesis process in the *Cgt*$^{+/-}$ mice also appeared to be normal. This was revealed by two lines of evidence. First, there was no difference in the organization of germ cells and Sertoli cells in the seminiferous tubules as observed in *Cgt*$^{+/-}$ and wild type testis sections and various stages

of seminiferous epithelium cycle were observed in testes of both genotypes (Figure 3.4). Second, the total numbers of sperm obtained from caudal epididymal sperm and vas deferens of $Cgt^{+/-}$ mice were similar to those of the wild type littermates (Figure 3.5); this similarity confirmed that spermatogenesis process in $Cgt^{+/-}$ testes was completed and had resulted in normal production of sperm. In addition, sperm morphology of $Cgt^{+/-}$ mice appeared to be the same as that of the wild type.

In agreement with the unimpaired spermatogenesis, total lipid profiles and SGG levels of $Cgt^{+/-}$ testes were not different from those of the wild type testes (Figure 3.6 and Figure 3.9). The similar SGG level of $Cgt^{+/-}$ and wild type testes revealed in this study is in contrast to the previous result of Fujimoto et al. (2000), which revealed that the SGG level in $Cgt^{+/-}$ testes of the adult mice was reduced to 68% of the wild type level. However, reliability of the result from Fujimoto's group was doubtful because the SGG level data obtained were not statistically analyzed for significant difference between the heterozygous and wild type animals. Also, it was unclear whether pairs of $Cgt^{+/-}$ and wild type males, used for the comparison of the testis SGG levels were from the same litters.

Recently, the new accurate quantitative method for quantifying SGG has been established under our collaborative work with Dr. Luigi Panza (University of Milan, Italy) and Dr. Kym Faull (University of California Los Angeles, USA) (manuscript in preparation). This new method combines the use of ESI-MS, a very sensitive method, with the suitable internal standard, deuterium-labelled SGG, with almost an identical structure to SGG. Therefore, this new, highly reliable approach is being used to quantify SGG in $Cgt^{+/-}$ and wild type testes, in order to confirm the SGG quantification results obtained from the Azure A assay. Preliminary data from this approach revealed that SGG levels in $Cgt^{+/-}$ and the wild type testes to be 421.50 ± 14.54 and 503.11 ± 62.45 nmol/g of wet tissue, respectively (see

more details in the Appendix II). However, we are now in the process of investigating why the SGG amounts obtained from this new method were 6-7 times lower than those of the Azure A assay ($Cgt^{+/-}$ vs wild type testes; 3213.97 ± 392.65 vs 3220.55 ± 387.18 nmol/g of tissue). The lower values obtained from ESI-MS analyses may be explained as follows. First, in the ESI-MS analysis, SGG recovered from the SGG band of the total testis lipid sample chromatographed on the HPTLC plate was used. Therefore, the analyses were specific for SGG. In contrast, the total testis lipids were used in the Azure A assay for SGG quantification; the Azure A could also react with other sulfated lipids, which were not well detected by our HPTLC system. The scraping of the SGG band and the subsequent recovery of SGG from this band by Bligh/Dyer extraction may also have led to some loss of SGG. Regardless of the dissimilarity in these SGG values, both ESI-MS and Azure A method showed no significant difference of SGG levels between $Cgt^{+/-}$ and the wild type testes.

Altogether, these findings suggested that normal levels of SGG in testes and sperm were needed for maintaining normal fertility status of the $Cgt^{+/-}$ mice, thus emphasizing the significance of SGG in male fertility. To adjust their SGG amounts to be at the wild type levels, it was likely that compensatory mechanisms have been occurred in these heterozygous mice.

4.3 Compensatory mechanisms to adjust SGG levels in $Cgt^{+/-}$ mice to the levels of the wild type

Testis SGG levels can be regulated through biosynthetic and/or degradative pathways. Therefore, to maintain SGG levels in the $Cgt^{+/-}$ mice, it was possible that the enzymes involved in SGG biosynthesis were up-regulated and/or the enzymes involved in SGG degradation were down-regulated. The levels of these enzymes could be manipulated

through the transcriptional and translational steps or though changes of their enzymatic activities.

To examine where the compensatory mechanisms occur, the mRNA and polypeptide levels as well as enzymatic activity of CGT, the SGG-synthesizing enzyme, were determined in the $Cgt^{+/-}$ and wild type testes. The *Cgt* mRNA level in $Cgt^{+/-}$ testes was previously reported to be half that of the wild type level (Fujimoto et al., 2000). In agreement with this previous finding, our real time RT-PCR also revealed that approximately 50% of *Cgt* mRNA was transcribed in the $Cgt^{+/-}$ testis (Figure 3.10). Unlike the *Cgt* mRNA, the CGT polypeptide expression and the CGT enzymatic activity in the testis have never been studied. Therefore, my thesis described for the first time the combined results of the polypeptide expression and enzymatic activity of CGT in the mouse testis (Figure 3.11 and Figure 3.13, respectively). I first tried to detect CGT polypeptide expression in the wild type testis sample using the anti-CGT antibody obtained from Dr. Sprong's group, which previously showed the CGT localization in the CHO-transfected cells (Sprong et al., 1998). However, this anti-CGT antibody, recognizing the specific sequence at the N-terminus of CGT, gave a number of non-specific bands in the testis sample. Therefore, the new anti-CGT antibody was produced against the C-terminal sequence of CGT polypeptide and used for this thesis study (see the details described in the materials and methods). Using this new antibody, I demonstrated that testis CGT had a molecular mass of 72 kDa by immunoblotting. This polypeptide was absent in *Cgt* null testes, indicating the specific reactivity of the antibody produced. According to the amino acid sequence (541 amino acid residues), the molecular weight of CGT in the brain was predicted to be around 61 kDa (Coetzee et al., 1996b). Therefore, the 72 kDa band observed was likely to be a glycosylated form of CGT in the testes. When the CGT polypeptide expression and enzymatic activity were determined in the

testes of the heterozygous animals, surprisingly, the $Cgt^{+/-}$ testes showed similar expression (also with the molecular mass of 72 kDa) and enzymatic levels to those of the wild type despite the fact that the heterozygous testes had only half *Cgt* mRNA of the wild type level. This suggested that the compensatory expression of the CGT polypeptide was one of the mechanisms to adjust SGG levels in the $Cgt^{+/-}$ mice. Nonetheless, the possible compensatory mechanism through the degradative pathway of SGG could not yet be excluded. Arylsulfatase A (ASA) is believed to be the enzyme responsible for SGG degradation in the testis. In mice, the *ASA* mRNA level in the testis was shown to be about 20 times higher than that in other tissues, including brain, liver, and kidney (Kreysing et al., 1994). However, the polypeptide level and the enzymatic activity of ASA in the testis were not different from those in other tissues; this translation repression was ascribed to the association of *ASA* mRNA with nonpolysomal ribonucleoproteins (Kreysing et al., 1994). This highly regulated *ASA* translation in the mouse testis may be another possible step through which SGG levels in the $Cgt^{+/-}$ testes were adjusted, i.e., by a decreased level of ASA expression. However, no difference was found in *ASA* mRNA levels, ASA polypeptide levels and activities between the $Cgt^{+/-}$ and the wild type testes (Figures 3.14 and 3.15). Overall, these results indicated that SGG levels of $Cgt^{+/-}$ mice were adjusted through the SGG biosynthetic pathway by the increased level of CGT polypeptide expression but not through the degradation step. It is still not known why the CGT polypeptide can be adjusted to the normal level despite only 50% of *Cgt* mRNA transcribed in the $Cgt^{+/-}$ testes. It is possible that only half of the mRNA level might be sufficient for the full translation of CGT.

Interestingly, when SGC, an analog of SGG, was absent in the brain and kidney of $Cgt^{-/-}$ mice, other compensatory processes also occurred. This compensation was via de novo syntheses of other ceramide-based glycolipids and may be a partial salvage event for the

functions and morphology of these tissues. For example, in the brain of *Cgt* knockout mice, glucosylceramide (GlcCer), another ceramide-based lipid not previously defined in the myelin, was synthesized and used for the formation of myelin instead of GC and SGC. This compensation resulted in normal appearance of the myelin ultrastructure in the $Cgt^{-/-}$ brain, although the function of the myelin could not be restored (Coetzee et al., 1996a). In the $Cgt^{-/-}$ kidney, two polar sulfoglycolipids (i.e., lactosylceramide II^3-sulfate (SM3) and gangliotetraosylceramide II^3, IV^3-*bis*-sulfate (SB1a)) were expressed at 2 to 3 times higher than the normal levels, indicating that the biosynthetic pathway of SB1a from GlcCer via lactosylceramice and SM3 was up-regulated (see the pathway in Figure 4.1). As a result, $Cgt^{-/-}$ mice showed no differences in the kidney morphology and functions, as compared with their wild type and heterozygous littermates (Tadano-Aritomi et al., 2000). All these findings suggested that a balance in membrane glycolipids and sulfoglycolipids is essential for the normal cell morphology and functions.

Supporting the idea that the balanced levels of structural lipids are important for cell function is the evidence from mice deficient in phosphatidylethanolamine methyltransferase (PEMT), an enzyme responsible for the synthesis of phosphatidylcholine (PC). PC, known to be one of the major lipid components of the cell membrane, can be synthesized in the liver via two distinctive pathways: 1) the cytidine diphosphate (CDP) choline pathway, utilizing cytidine triphosphate (CTP)-choline cytidylyltransferase as the key enzyme, and 2) the methylation of phosphatidylethanolamine by action of PEMT. Surprisingly, in the liver of the PEMT knockout mice, the level of PC is unchanged due to the compensatory increase in activity of CTP-choline cytidylyltransferase, the key enzyme in the other pathway (Walkey et al., 1997).

Figure 4.1 The diagrammatic pathway shows that when CGT is absent in the *Cgt* knockout mice, other ceramide-based glycolipids (indicated with green labels) utilizing ceramide as their precursor are increased (modified from Tadano-Aritomi et al., 2000).

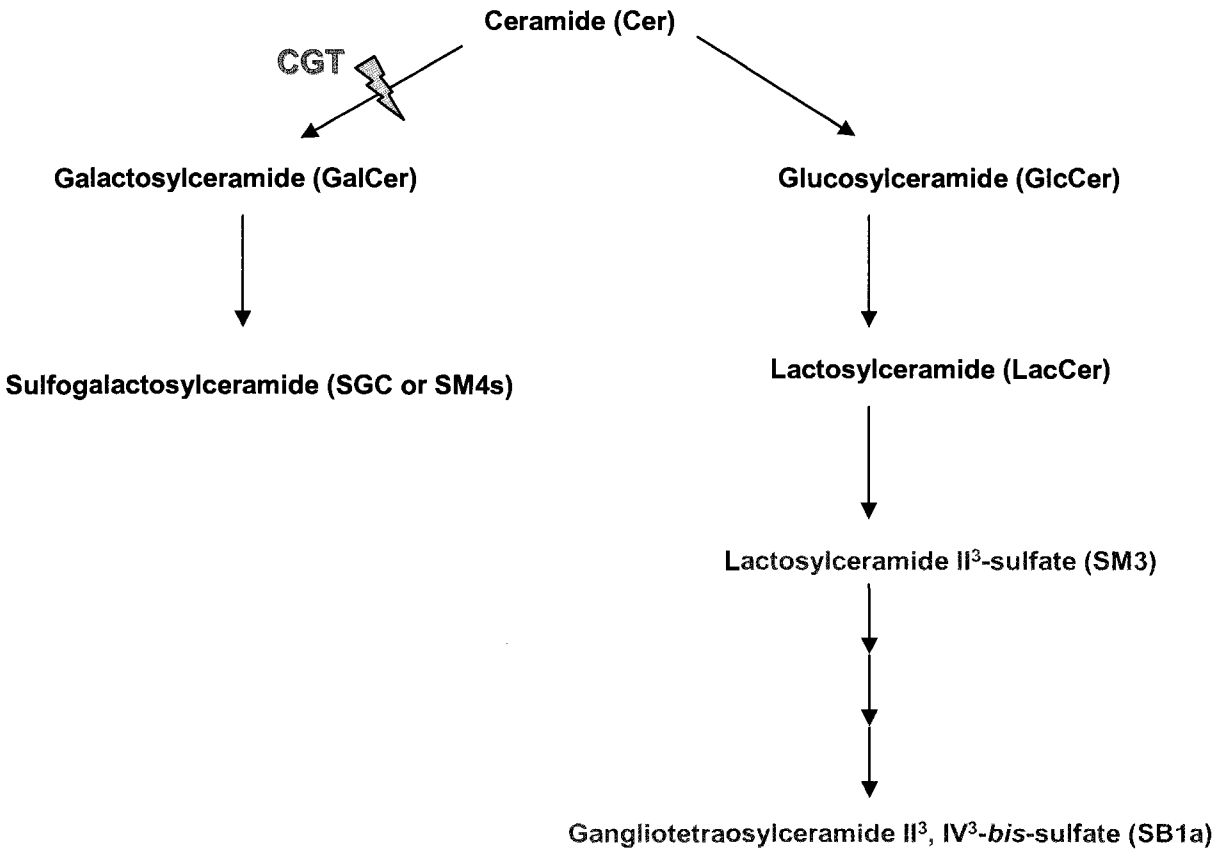
Ceramide (Cer)
CGT
Galactosylceramide (GalCer)
Glucosylceramide (GlcCer)
Sulfogalactosylceramide (SGC or SM4s)
Lactosylceramide (LacCer)
Lactosylceramide II3-sulfate (SM3)
Gangliotetraosylceramide II3, IV3-bis-sulfate (SB1a)

4.4 Future directions

It is interesting that the CGT polypeptide expression of the $Cgt^{+/-}$ testis is compensated, resulting in the wild type levels of SGG. Moreover, the normal level of testicular SGG seems to be needed for maintaining normal spermatogenesis. This might be because SGG, which is present at a substantial amount in the male germ cell plasma membrane, plays critical roles in this physiological process. The next question to be addressed is at which stage of spermatogenic cells that the CGT compensation occurs in $Cgt^{+/-}$ testis in order to produce SGG to be at the wild type level. To answer this question, the information on expression levels of CGT and SGG in each spermatogenic cell stage of the wild type and $Cgt^{+/-}$ mice is needed.

Ideally, to determine expression levels of CGT and SGG, the *de novo* synthesis of these molecules should be studied by including the radioactive precursors in the germ cell culture medium, followed by isolation of these molecules and quantification of the radioactivity incorporated. This approach has already been used for studying *de novo* synthesis of acrosomal proteins in isolated round spermatids of the guinea pig (Joshi et al., 1990) and the rat (Abou-Haila and Tulsiani, 2001). However, the viability of spermatogenic cell populations decline with increasing time in culture and so far, there is no effective long-term culture system that mimics the whole *in vivo* process of spermatogenesis available. Therefore, total CGT and SGG levels in each type of spermatogenic cells will be measured instead. Both immuno-related and biochemical approaches can be used for these measurements. To first obtain global information on the type of spermatogenic cells in which CGT and SGG are expressed, immunofluorescence of testis sections will be performed. The intensity of the fluorescence signals in wild type and $Cgt^{+/-}$ sections will then be compared to roughly indicate at which spermatogenic cell type(s) the compensation

of CGT and SGG expression occurs. Comparison of the expression levels of CGT and SGG in wild type and $Cgt^{+/-}$ spermatogenic cells can further be done in a more quantitative manner via flow cytometry of loose testicular germ cells that are immunostained with antiCGT and antiSGG antibodies. A mixed population of loose germ cells will be prepared by trypsin digestion of seminiferous tubules (isolated from the testis removed from the connective tissue by collagenase treatment). Significantly, preparation of pure populations of spermatogenic cells for the flow cytometry is not required as different types of spermatogenic cells can be sorted via the gating function based on cell size and shape, as well as various DNA amounts (stained by a DNA fluorochrome such as propidium iodide) in different germ cell types (see spermatogenesis part in the introduction). Biochemical quantifications of CGT and SGG can also be performed using purified populations of different germ cell types. This purification can be achieved via sedimentation of spermatogenic cells through a BSA density gradient (the so-called STA-PUT technique) (Bellve, 1979). CGT expression can be detected by immunoblotting and the levels of expression in wild type and $Cgt^{+/-}$ spermatogenic cells can be compared by densitometric analyses. For SGG, its absolute amounts can be obtained via Azure A assay and/or quantitative ESI-MS (see the materials and methods and the results for more details).

Hopefully, the combined results from these approaches will provide the definite answer to which stage that CGT level is compensated in $Cgt^{+/-}$ testes, resulting in wild type levels of SGG. We anticipated that the answer to this question may lead to the better understanding of which stages of the germ cells that CGT and SGG are needed for the germ cell development.

4.5 Alternative approaches to study *in vivo* functions of SGG

From the knockout mice, it is known that the complete absence of SGG in the testis causes disruption of spermatogenesis, resulting in no sperm production (Fujimoto et al., 2000; Honke et al., 2002). Therefore, to obtain sperm for studying SGG functions, testis SGG cannot be completely depleted. The ideal model to study physiological roles of SGG would be the animals having reduced SGG levels in the testes that can still produce sperm also with lower SGG levels. However, from the results in this thesis, it seems that the SGG level in the testes is well maintained, and reduction of the *Cgt* gene expression to 50% of the wild type level is not enough to alter the testis SGG levels. Thus, a new approach to study the functions of SGG in vivo is needed. Ideally, the *Cgt* gene expression should be <50% of the wild type value, but still at the level that sufficient SGG is produced to maintain spermatogenesis.

To date, RNA interference (RNAi) has emerged as a powerful tool to silence gene expression and has rapidly transformed gene function studies in many organisms. In mammals, the introduction of chemically synthesized siRNA or a vector-based system expressing short hairpin type of siRNA (shRNA) transcribed from RNA polymerase III promoter induces sequence-specific gene silencing in various cell types and tissues (Dorsett and Tuschl, 2004; Shi, 2003). This method has already been used to study the in vivo functions of a sperm factor important for egg activation (Knott et al., 2005).

A transient elevation in intracellular Ca^{2+} concentration is a unique feature of fertilization in eggs of all species studied to date. In mammals, sperm evoke a series of repetitive Ca^{2+} oscillations that persist for several hours and terminate with pronucleus formation (Marangos et al., 2003). The increase intracellular Ca^{2+} concentration is triggered via phospholipase C (PLC)-catalyzed production of inositol 1, 4, 5-triphosphate (IP_3) in the

egg (Runft et al., 2002). Lately, a novel, sperm-specific PLC, termed PLC-ζ, has been shown to be a sperm soluble factor that triggers Ca^{2+} oscillations in the mouse eggs *in vitro* (Saunders et al., 2002). To confirm the physiological role of sperm PLC-ζ during egg activation *in vivo*, the RNAi system has been used (Knott et al., 2005). Knott et al (2005) used a short hairpin transgene driven by the RNA polymerase III-specific U6 promoter to target the PLC-ζ in mice and found 40% reduction of PLC-ζ in the mouse sperm. The IVF and Ca^{2+} imaging results revealed that in contrast to eggs fertilized by non-transgenic mouse sperm, a number of eggs fertilized by sperm from transgenic mice exhibited only a few Ca^{2+} rises and failed to establish persistent oscillations. The results from the RNAi approach provide direct evidence that PLC-ζ is critical for triggering Ca^{2+} oscillations following fertilization.

According to these results, it seems promising that the RNAi system might be used to regulate the expression of *Cgt* or *Cst* during spermatogenesis, which will result in reduction of SGG in the germ cells. Hopefully, SGG-reduced sperm derived from this method can be used for studying *in vivo* functions of sperm SGG. However, there are still some obstacles in generating transgenic mice following the RNAi implementation. One of the problems is attributed to mosaicism of the germ-line (Knott et al., 2005; Williams and Schultz, 2006). Specifically, the efficiency and specificity of RNAi targeting *Cgt* or *Cst* genes still need to be determined.

4.6 Potential translation of CGT and SGG in male contraceptives

Regardless of the unknown mechanisms, accumulative evidence including the results from this thesis study has strongly suggested the crucial functions of CGT and SGG during spermatogenesis. From the study in *Cgt* and *Cst* knockout mice, it is known that disruption

of SGG synthesis leads to male infertility. Therefore, an agent, such as an inhibitor for CGT, that alters the biosynthesis of SGG would be expected to affect the spermatogenesis process and may serve as a potential male contraceptive.

Supporting this idea, an inhibitor of ceramide-specific glucosyltransferase, the alkylated imino sugar *N*-butyldeoxynojirimycin (NB-DNJ), has been shown to result in a reversible suppression of fertility in mice (van der Spoel et al., 2002). The ceramide-specific glucosyltransferase is the first enzyme in the biosynthetic pathway of glycosphingolipids, the other class of glycolipids present in the testis with the lesser extent than SGG (see the synthetic pathway in Figure 4.2). The inhibition of this enzyme by oral administration of NB-DNJ to mice causes abnormalities in nucleus, mitochondrial sheath and acrosome of sperm. However, at doses that resulted in complete inhibition of fertility, there were no detectable effects on body weight, hormonal parameters (e.g., serum LH, FSH, and testosterone), testicular and epididymal weights, or epididymal sperm counts.

The result from this NB-DNJ study suggested that a drug that interferes with glycolipid biosyntheses may be promising and safe in regulating male fertility in a reversible manner. Besides safety and reversibility, an ideal contraceptive must be specific and effective. For these aspects, the biosynthetic pathway and the exertion mode of physiological functions of SGG, the glycolipid present specifically and substantially in the mammalian male germ cells, may be suitable targets in non-hormonal contraceptive development.

Figure 4.2 The ceramide-specific glucosyltransferase is the first enzyme in the biosynthetic pathway of glycosphingolipids, other class of glycolipids present in the testis.

Abbreviations: Cer, ceramide; Glc, glucose; Gal, galactose; GalNAc, *N*-acetylgalactosamine; SA, sialic acid (neuraminic acid); Gg3Cer, gangliotriosyl ceramide; Gg4Cer, gangliotetraosyl ceramide.

For GM3, GM2, GM1a, GM1b, GD1a, GD1b, GD2, GD3, GT1a, GT1b, GT3, and GQ1b, their abbreviations are designated according to Svennerholm's nomenclature (1994). The first letter, G, is for ganglio-series ganglioside. The second letter, M, D, T or Q, represents the number of sialic acid residues (M = mono; D = di; T = tri; and Q = quatro-sialosyl groups, respectively). The numbers, 1, 2 or 3 indicates the terminal/pre-terminal sugar residues of gangliosides (1 = having terminal galactose; 2 = lacking terminal galactose; and 3 = lacking pre-terminal galactosyl-N-acetylgaslactosamine). Isomeric configurations of sialic acids are distinguished by a and b (a = one sialic acid attached to the internal galactose; b = two sialic acids attached to the internal galactose).

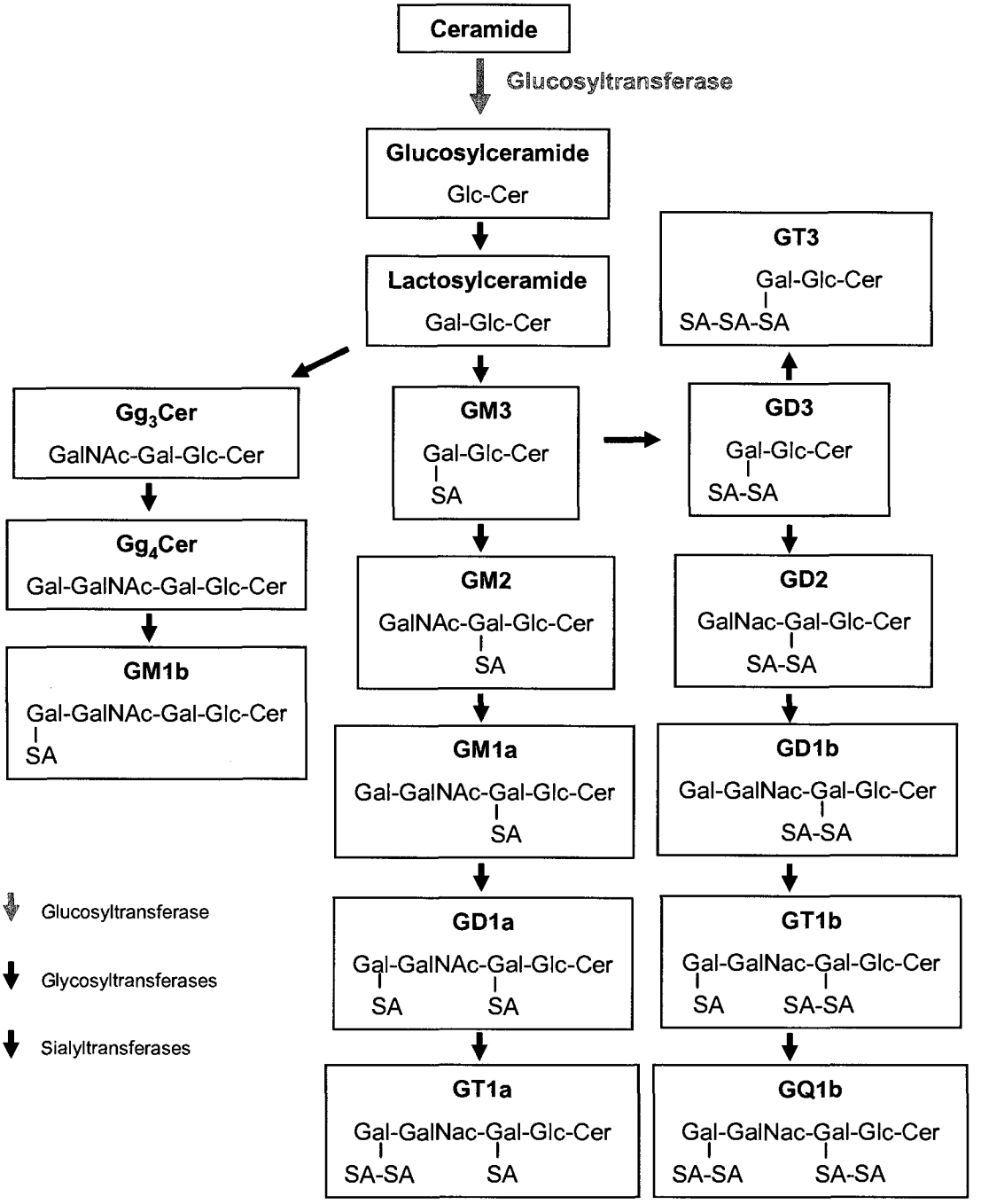
Ceramide
Glucosyltransferase
Glucosylceramide
Glc-Cer
Lactosylceramide
Gal-Glc-Cer
GT3
Gal-Glc-Cer
SA-SA-SA
Gg3Cer
GalNAc-Gal-Glc-Cer
GM3
Gal-Glc-Cer
SA
GD3
Gal-Glc-Cer
SA-SA
Gg4Cer
Gal-GalNAc-Gal-Glc-Cer
GM2
GalNAc-Gal-Glc-Cer
SA
GD2
GalNac-Gal-Glc-Cer
SA-SA
GM1b
Gal-GalNAc-Gal-Glc-Cer
SA
GM1a
Gal-GalNAc-Gal-Glc-Cer
SA
GD1b
Gal-GalNac-Gal-Glc-Cer
SA-SA
GD1a
Gal-GalNAc-Gal-Glc-Cer
SA SA
GT1b
Gal-GalNac-Gal-Glc-Cer
SA SA-SA
GT1a
Gal-GalNac-Gal-Glc-Cer
SA-SA SA
GQ1b
Gal-GalNac-Gal-Glc-Cer
SA-SA SA-SA
Glucosyltransferase
Glycosyltransferases
Sialyltransferases

Reference List

Abou-Haila,A. and Tulsiani,D.R. (2001). Acid Glycohydrolases in Rat Spermatocytes, Spermatids and Spermatozoa: Enzyme Activities, Biosynthesis and Immunolocalization. Biol. Proced. Online. *3*, 35-42.

Acott,T.S., Katz,D.F., and Hoskins,D.D. (1983). Movement characteristics of bovine epididymal spermatozoa: effects of forward motility protein and epididymal maturation. Biol. Reprod. *29*, 389-399.

Ahnonkitpanit,V., White,D., Suwajanakorn,S., Kan,F., Namking,M., Wells,G., and Tanphaichitr,N. (1999). Role of egg sulfolipidimmobilizing protein 1 (SLIP1) on sperm-egg plasma membrane binding. Biology of Reproduction *61*, 749-756.

Alberts,B., Johnson,A., Lewis,J., Raff,M., Roberts,K., and Walter,P. (2002). Molecular Biology of the Cell. (New York: Garland).

Attar,M., Kates,M., Bou Khalil,M., Carrier,D., Wong,P.T.T., and Tanphaichitr,N. (2000). A Fourier-transform infrared study of the interaction between germ-cell specific sulfogalactosylglycerolipid and dimyristoylglycerophosphocholine. Chemistry and Physics of Lipids *106*, 101-114.

Bajorath,J., Hollenbaugh,D., King,G., Harte,W., Jr., Eustice,D.C., Darveau,R.P., and Aruffo,A. (1994). CD62/P-selectin binding sites for myeloid cells and sulfatides are overlapping. Biochemistry *33*, 1332-1339.

Bellve,A.R. (1979). Purification, culture, and fractionation of spermatogenic cells. In Guide to Techniques in Mouse Development, P.M.Wassarman, ed. (San Diego, CA: Academic Press, Inc.), pp. 84-112.

Berube,B., Lefievre,L., Coutu,L., and Sullivan,R. (1996). Regulation of the epididymal synthesis of P26h, a hamster sperm protein. Journal of Andrology *17*, 104-110.

Bligh,E.G. and Dyer,W.J. (1959). A rapid method of total lipid estraction and purification. Canadian Journal of Biochemistry and Physiology *31*, 911-917.

Boggs,J.M., Menikh,A., and Rangaraj,G. (2000). Trans interactions between galactosylceramide and cerebroside sulfate across apposed bilayers. Biophysical Journal *78*, 874-885.

Bou,K.M., Chakrabandhu,K., Xu,H., Weerachatyanukul,W., Buhr,M., Berger,T., Carmona,E., Vuong,N., Kumarathasan,P., Wong,P.T., Carrier,D., and Tanphaichitr,N. (2006). Sperm capacitation induces an increase in lipid rafts having zona pellucida binding ability and containing sulfogalactosylglycerolipid. Dev. Biol. *290*, 220-235.

Brogi,A., Presentini,R., Piomboni,P., Collodel,G., Strazza,M., Solazzo,D., and Costantino-Ceccarini,E. (1995). Human sperm and spermatogonia express a galactoglycerolipid which interacts with gp120. J. Submicrosc. Cytol. Pathol. *27*, 565-571.

Brogi,A., Presentini,R., Solazzo,D., Piomboni,P., and Costantino-Ceccarini,E. (1996). Interaction of human immunodeficiency virus type 1 envelope glycoprotein gp120 with a galactoglycerolipid associated with human sperm. AIDS Res. Hum. Retroviruses *12*, 483-489.

Brown,D.A. and London,E. (2000). Structure and function of sphingolipid- and cholesterol-rich membrane rafts. Journal of Biological Chemistry *275*, 17221-17224.

Chen,S. and Cardullo,R. (1994). Characterization and localization of fluorescent zonae pellucidae on mouse sperm. Molecular Biology of the Cell *5*, 224a.

Cheng,C.Y. and Mruk,D.D. (2002). Cell junction dynamics in the testis: Sertoli-germ cell interactions and male contraceptive development. Physiol Rev. *82*, 825-874.

Clermont,Y. (1972). Kinetics of spermatogenesis in mammals: seminiferous epithelium cycle and spermatogonial renewal. Physiol Rev. *52*, 198-236.

Coetzee,T., Fujita,N., Dupree,J., Shi,R., Blight,A., Suzuki,K., Suzuki,K., and Popko,B. (1996a). Myelination in the absence of galactorcerebroside and sulfatide: Normal structure with abnormal function and regional instability. Cell *86*, 209-219.

Coetzee,T., Li,X., Fujita,N., Marcus,J., Suzuki,K., Francke,U., and Popko,B. (1996b). Molecular Cloning, Chromosomal Mapping and Characterization of the Mouse UDP-Galactose:Ceramide Galactosyltransferase Gene. Genomics *35*, 215-222.

Cooper,T.G. and Yeung,C.H. (1997). Physiology of sperm maturation and fertilization. In Andrology: Male Reproductive Health and Dysfunction, E.Nieschlag, ed. (Berlin Heidelberg: Springer-Verlag), pp. 61-78.

Cross,N.L. (1998). Role of cholesterol in sperm capacitation. Biology of Reproduction *59*, 7-11.

Crossin,K.L. and Edelman,G.M. (1992). Specific binding of cytotactin to sulfated glycolipids. Journal of Neuroscience Research *33*, 631-638.

Dacheux,J.L., Gatti,J.L., and Dacheux,F. (2003). Contribution of epididymal secretory proteins for spermatozoa maturation. Microsc. Res. Tech. *61*, 7-17.

de Kretser,D.M. and Kerr,J.B. (1994). The Cytology of the Testis. In The Physiology of Reproduction, E.Knobil and J.D.Neill, eds. (New York: Raven press), pp. 1177-1290.

Dorsett,Y. and Tuschl,T. (2004). siRNAs: applications in functional genomics and potential as therapeutics. Nat. Rev. Drug Discov. *3*, 318-329.

Dym,M. (1977). The male reproductive system. In Histology, L.Weiss, ed. (New York: McGraw-Hill Book Company), pp. 979-1038.

Dym,M. (1994). Spermatogonial stem cells of the testis. Proc. Natl. Acad. Sci. U. S. A *91*, 11287-11289.

Dym,M. and Fawcett,D.W. (1971). Further observations on the numbers of spermatogonia, spermatocytes, and spermatids connected by intercellular bridges in the mammalian testis. Biol. Reprod. *4*, 195-215.

Eddy,E.M. and O'Brien,D.A. (1994). The spermatozoon. In The Physiology of Reproduction, E.Knobil, ed. (New York: Raven Press), pp. 29-77.

Evans,J.P. (1999). Sperm disintegrins, egg integrins, and other cell adhesion molecules of mammalian gamete plasma membrane interactions. Front Biosci. *4*, D114-D131.

Flesch,F.M., Brouwers,J.F., Nievelstein,P.F., Verkleij,A.J., Van Golde,L.M., Colenbrander,B., and Gadella,B.M. (2001). Bicarbonate stimulated phospholipid scrambling induces cholesterol redistribution and enables cholesterol depletion in the sperm plasma membrane. J. Cell Sci. *114*, 3543-3555.

Flesch,F.M. and Gadella,B.M. (2000). Dynamics of the mammalian sperm plasma membrane in the process of fertilization. Biochimica et Biophysica Acta *1469*, 197-235.

Florman,H.M. and Ducibella,T. (2006). Fertilization in mammals. In Knobil and Neil's Physiology of Reproduction, J.D.Neill, ed. (New York: Elsevier), pp. 55-112.

Fluharty,A.L., Stevens,R.L., Miller,R.T., and Kihara,H. (1974). Sulfoglycerogalactolipid from rat testis: A substrate for pure; human arylsulfatase A. Biochemical and Biophysical Research Communications *61*, 348-354.

Fornes,W.M., Sosa,M.A., Bertini,F., and Burgos,M.H. (1995). Vesicles in rat epididymal fluid. Existence of two populations differing in ultrastructure and enzymatic composition. Andrologia *27*, 233-237.

Franca,L.R., Ogawa,T., Avarbock,M.R., Brinster,R.L., and Russell,L.D. (1998). Germ cell genotype controls cell cycle during spermatogenesis in the rat. Biol. Reprod. *59*, 1371-1377.

Frank,M. (2000). MAL, a proteolipid in glycosphingolipid enriched domains: functional implications in myelin and beyond. Prog. Neurobiol. *60*, 531-544.

Frenette,G., Lessard,C., and Sullivan,R. (2002). Selected proteins of "Prostasome-Like Particles" from epididymal cauda fluid are trasferred to epididymal caput spermatozoa in bull. Biology of Reproduction *67*, 308-313.

Frenette,G. and Sullivan,R. (2001). Prostasome-like particles are involved in the transfer of P25b from the bovine epididymal fluid to the sperm surface. Molecular Reproduction and Development *59*, 115-121.

Friedrich,M.V., Gohring,W., Morgelin,M., Brancaccio,A., David,G., and Timpl,R. (1999). Structural basis of glycosaminoglycan modification and of heterotypic interactions of perlecan domain V. J. Mol. Biol. *294*, 259-270.

Fujimoto,H., Tadano-Aritomi,K., Tokumasu,A., Ito,K., Hikita,T., Suzuki,K., and Ishizuka,I. (2000). Requirement of seminolipid in spermatogenesis revealed by UDP-galactose:ceramide galactosyltransferase-deficient mice. Journal of Biological Chemistry *275*, 22623-22626.

Furimsky,A., Vuong,N., Xu,H., Kumarathasan,P., Xu,M., Weerachatyanukul,W., Bou,K.M., Kates,M., and Tanphaichitr,N. (2005). Percoll gradient-centrifuged capacitated mouse sperm have increased fertilizing ability and higher contents of sulfogalactosylglycerolipid and docosahexaenoic acid-containing phosphatidylcholine compared to washed capacitated mouse sperm
2. Biol. Reprod. *72*, 574-583.

Gatti,J.L., Druart,X., Syntin,P., Guerin,Y., Dacheux,J.L., and Dacheux,F. (2000). Biochemical characterization of two ram cauda epididymal maturation-dependent sperm glycoproteins. Biol. Reprod. *62*, 950-958.

Griswold,M.D. (1995). Interactions between germ cells and Sertoli cells in the testis. Biol. Reprod. *52*, 211-216.

Hogan,B., Costantini,F., and Lacy,E. (1994). Manipulating the mouse embryo: a laboratory manual. (Cold Spring Harbor: Cold Spring Harbor Laboratory), pp. 1-497.

Holt,G.D., Krivan,H.C., Gasic,G.J., and Ginsbur,V. (1989). Antistasin, an inhibitor of coagulation and metastasis, binds to sulfatide (Gal(3-SO4)b1-1Cer) and has a sequence homology with other proteins that bind sulfated glycoconjugates. Journal of Biological Chemistry *264*, 12138-12140.

Holt,G.D., Pangburn,M.K., and Ginsburg,V. (1990). Properdin binds to sulfatide [Gal(3-SO4)b1-Cer] and has a sequence homology with other proteins that bind sulfated glycoconjugates. Journal of Biological Chemistry *1990*, 2852-2855.

Honke,K., Hirahara,Y., Dupree,J., Suzuki,K., Popko,B., Fukushima,K., Fukushima,J., Nagasawa,T., Yoshida,N., Wada,Y., and Taniguchi,N. (2002). Paranodal junction formation and spermatogenesis require sulfoglycolipids. Proceedings of the National Academy of Science USA *99*, 4227-4232.

Hsu,L.H., Narasimhan,R., and Levine,M. (1983). Studies of the biosynthesis and metabolism of rat testicular galactoglycerolipids. Can. J. Biochem. Cell Biol. *61*, 1272-1281.

Ida,M., Satoh,A., Matsumoto,I., and Kojima-Aikawa,K. (2004). Human annexin V binds to sulfatide: contribution to regulation of blood coagulation. J. Biochem. (Tokyo) *135*, 583-588.

Iida,N., Toida,T., Kushi,Y., Handa,S., Fredman,P., Svenerholm,L., and Ishizuka,I. (1989). A sulfated glucosylceramide from rat kidney. Journal of Biological Chemistry *264*, 5974-5980.

Ishizuka,I., Suzuki,M., and Yamakawa,T. (1973). Isolation and characterization of a novel sulfoglycolipid, seminolipid, from boar testis and spermatozoa. Journal of Biochemistry *73*, 77-87.

Jegou,B. (1993). The Sertoli-germ cell communication network in mammals. Int. Rev. Cytol. *147*, 25-96.

Joshi,M.S., Anakwe,O.O., and Gerton,G.L. (1990). Preparation and short-term culture of enriched populations of guinea pig spermatocytes and spermatids. J. Androl *11*, 120-130.

Kates,M. (1986). Technique of lipidology: isolation, analysis and identification of lipids. In Laboratory Techniques in Biochemistry and Molecular Biology, R.H.Burdon, ed. (New York: Elsevier), pp. 100-278.

Kerr,C.L., Hanna,W.F., Shaper,J.H., and Wright,W.W. (2002). Characterization of zona pellucida glycoprotein 3 (ZP3) and ZP2 binding sites on acrosome-intact mouse sperm. Biology of Reproduction *66(6)*, 1585-1595.

Kierszenbaum,A.L. (2002). Histology and cell biology: an introduction to pathology. (St. Louis: Mosby, Inc.).

Klugerman,A. and Kornblatt,M.J. (1980). The subcellular localization of testicular sulfogalactoglycerolipid. Can. J. Biochem. *58*, 225-229.

Knapp,A., Kornblatt,M.J., Schachter,H., and Murray,R.K. (1973). Studies on the biosynthesis of testicular sulfoglycerogalactolipid: Demonstration of a golgi-associated sulfotransferase activity. Biochemical and Biophysical Research Communications *55*, 179-186.

Knott,J.G., Kurokawa,M., Fissore,R.A., Schultz,R.M., and Williams,C.J. (2005). Transgenic RNA interference reveals role for mouse sperm phospholipase Czeta in triggering Ca2+ oscillations during fertilization. Biol. Reprod. *72*, 992-996.

Kolter,T. and Sandhoff,K. (2005). Principles of lysosomal membrane digestion: stimulation of sphingolipid degradation by sphingolipid activator proteins and anionic lysosomal lipids. Annu. Rev. Cell Dev. Biol. *21*, 81-103.

Kornblatt,M.J., Knapp,A., Levine,M., Schachter,H., and Murray,R.K. (1974). Studies on the structure and formation during spermatogenesis of the sulfoglycerogalactolipid of rat testis. Can. J. Biochem. *52*, 689-697.

Kreysing,J., Polten,A., Lukatela,G., Matzner,U., van Figura,K., and Gieselmann,V. (1994). Translational control of arylsulfatase A expression in mouse testis. Journal of Biological Chemistry *269*, 23255-23261.

Kurosawa,N., Kadomatsu,K., Ikematsu,S., Sakuma,S., Kimura,T., and Muramatsu,T. (2000). Midkine binds specifically to sulfatide. The role of sulfatide in cell attachment of midkine-coated surfaces. European Journal of Biochemistry *267*, 344-351.

Laemmli,U.K. (1970). Cleavage of structural proteins during the assembly of the head of bacteriophage T4. Nature *227*, 680-685.

Letts,P.J., Hunt,R.C., Shirley,M.A., Pinteric,L., and Schachter,H. (1978). Late spermatocytes from immature rat testis: Isolation, electron microscopy, letin agglutinability and capacity for glycoprotein and sulfogalactoglycerolipid biosynthesis. Biochimica et Biophysica Acta *541*, 59-75.

Lingwood,C., Sakac,K., and Saltiel,A. (1994). Developmentally regulated testicular galactolipid sulfotransferase inhibitor is a phosphoinositol glycerolipid and insulin-mimetic. Molecular Reproduction and Development *37*, 462-466.

Lingwood,C., Schramayr,S., and Quinn,P. (1990). Male germ cell specific sulfogalactoglycerolipid is recognized and degraded by mycoplasmas associated with male infertility. Journal of Cellular Physiology *142*, 170-176.

Lingwood,C.A. (1981). Localization of sulfatoxygalactosylacylalkylglycerol at the surface of rat testicular germinal cells by immunocytochemical techniques: pH dependence of a nonimmunological reaction between immunoglobulin and germinal cells. The Journal of Cell Biology *89*, 621-630.

Lingwood,C.A. (1985). Timing of sulphogalactolipid biosynthesis in the rat testis studied by tissue autoradiography. Journal of Cell Science *75*, 329-338.

Lingwood,C.A. (1986). Colocalization of sulfogalactosylacylalkylglycerol (SGG) and its binding protein during spermatogenesis and sperm maturation. Topology of SGG defines a new testicular germ cell membrane domain. Biochemistry and Cell Biology *64*, 984-992.

Lingwood,C.A., Hay,G., and Schachter,H. (1981). Tissue distribution of sulfolipids in the rat. Restricted location of sulfatoxygalactosylacylalkylglycerol. Can. J. Biochem. *59*, 556-563.

Mamelak,D. and Lingwood,C. (2001). The ATPase domain of hsp70 possesses a unique binding specificity for 3'-sulfogalactolipids. Journal of Biological Chemistry *276*, 449-456.

Marangos,P., Fitzharris,G., and Carroll,J. (2003). Ca2+ oscillations at fertilization in mammals are regulated by the formation of pronuclei. Development *130*, 1461-1472.

Mohan,P.S., Laitinen,J., Merenmies,J., Rauvala,H., and Jungalwala,F.B. (1992). Sulfoglycolipids bind to adhesive protein amphoterin (P30) in the nervous system. Biochem. Biophys. Res. Commun. *182*, 689-696.

Molander-Melin,M., Pernber,Z., Franken,S., Gieselmann,V., Mansson,J.E., and Fredman,P. (2004). Accumulation of sulfatide in neuronal and glial cells of arylsulfatase A deficient mice. J. Neurocytol. *33*, 417-427.

Morales,C.R., Hay,N., El Alfy,M., and Zhao,Q. (1998). Distribution of mouse sulfated glycoprotein-1 (prosaposin) in the testis and other tissues. J. Androl *19*, 156-164.

Moviglia,G.A., Cavicchia,J.C., and Bertini,F. (1982). Lysosomal enzymes in cells separated from rat testis. Journal of Reproduction and Fertility *66*, 123-127.

Needham,L.K. and Schnaar,R.L. (1993). The HNK-1 reactive sulfoglucuronyl glycolipids are ligands for L-selectin and P-selectin but not E-selectin. Proc. Natl. Acad. Sci. U. S. A *90*, 1359-1363.

Newton,S.C., Blaschuk,O.W., and Millette,C.F. (1993). N-cadherin mediates Sertoli cell-spermatogenic cell adhesion. Dev. Dyn. *197*, 1-13.

Nilsson,T. and Warren,G. (1994). Retention and retrieval in the endoplasmic reticulum and the Golgi apparatus. Curr. Opin. Cell Biol. *6*, 517-521.

O'Brien,J.S. and Kishimoto,Y. (1991). Saposin proteins: structure, function, and role in human lysosomal storage disorders. FASEB Journal *5*, 301-308.

Olson,L.D. and Gilbert,A.A. (1993). Characteristics of Mycoplasma hominis adhesion 12. J. Bacteriol. *175*, 3224-3227.

Pancake,S., Holt,G., Mellouk,S., and Hoffman,S. (1992). Malaria sporozoites and circumsporozoite proteins bind specifically to sulfated glycoconjugates. The Journal of Cell Biology *117*, 1351-1357.

Parks,J.E. and Lynch,D.V. (1992). Lipid composition and thermotropic phase behavior of boar, bull, stallion, and rooster sperm membranes. Cryobiology *29*, 255-266.

Pratt,S., Scully,N.F., and Shur,B.D. (1993). Cell surface á1,4 galactosyltransferase on primary spermatocytes facilitates their initial adhesion to sertoli cells in vitro. Biology of Reproduction *49*, 470-482.

Primakoff,P. and Myles,D.G. (2002). Penetration, adhesion, and fusion in mammalian sperm-egg interaction. Science *296*, 2183-2185.

Roberts,D.D. (1988). Interactions of thrombospondin with sulfated glycolipids and proteoglycans of human melanoma cells. Cancer Res. *48*, 6785-6793.

Roberts,D.D., Roa,C.N., Mangani,J.L., Spitalnik,S.L., Liotta,L.A., and Ginsberg,V. (1985). Laminin binds specifically to sulfated glycolipids. Proceedings of the National Academy of Science USA *82*, 1306-1310.

Roberts,D.D., Williams,S.B., Gralnick,H.R., and Ginsburg,V. (1986). von Willebrand factor binds specifically to sulfated glycolipids. Journal of Biological Chemistry *261*, 3306-3309.

Rousset,E., Harel,J., and Dubreuil,J.D. (1998). Sulfatide from the pig jejunum brush border epithelial cell surface is involved in binding of Escherichia coli enterotoxin b. Infect. Immun. *66*, 5650-5658.

Runft,L.L., Jaffe,L.A., and Mehlmann,L.M. (2002). Egg activation at fertilization: where it all begins. Dev. Biol. *245*, 237-254.

Saez,F., Frenette,G., and Sullivan,R. (2003). Epididymosomes and prostasomes: their roles in posttesticular maturation of the sperm cells. J. Androl *24*, 149-154.

Sakac,D., Zachos,M., and Lingwood,C.A. (1992). Purification of the testicular galactolipid: 3'-phosphoadenoisine 5'-phosphosulfate sulfotransferase. Journal of Biological Chemistry *267*, 1655-1659.

Sambrook,J. and Russell,D.W. (2001). Molecular cloning; a laboratory manual. (Cold Spring Harbor: Laboratory Press).

Saunders,C.M., Larman,M.G., Parrington,J., Cox,L.J., Royse,J., Blayney,L.M., Swann,K., and Lai,F.A. (2002). PLC zeta: a sperm-specific trigger of Ca(2+) oscillations in eggs and embryo development. Development *129*, 3533-3544.

Schott,I., Hartmann,D., Gieselmann,V., and Lullmann-Rauch,R. (2001). Sulfatide storage in visceral organs of arylsulfatase A-deficient mice. Virchows Archive *439*, 90-96.

Schulte,S. and Stoffel,W. (1993). Ceramide UDPgalactosyltransferase from myelinating rat brain: purification, cloning, and expression. Proc. Natl. Acad. Sci. U. S. A *90*, 10265-10269.

Shadan,S., James,P.S., Howes,E.A., and Jones,R. (2004). Cholesterol efflux alters lipid raft stability and distribution during capacitation of boar spermatozoa. Biol. Reprod. *71*, 253-265.

Sharpe,R.M. (1994). Regulation of spermatogenesis. In The Physiology of Reproduction, E.Knobil, ed. (New York: Raven Press Ltd.), pp. 1363-1434.

Shi,Y. (2003). Mammalian RNAi for the masses. Trends Genet. *19*, 9-12.

Shirley,M.A. and Schachter,H. (1980). Enrichment of sulfogalactosylalkylacylglycerol in a plasma membrane fraction from adult rat testis. Can. J. Biochem. *58*, 1230-1239.

Simons,K. and Ehehalt,R. (2002). Cholesterol, lipid rafts, and disease. J. Clin. Invest *110*, 597-603.

Sosa,M.A., Barbieri,A.M., and Bertini,F. (1996). Purification and characterization of beta-galactosidase from rat epididymal fluid. Andrologia *28*, 217-221.

Sprong,H., Kruithof,B., Leijendekker,R., Slot,J.W., Van Meer,G., and van der,S.P. (1998). UDP-galactose:ceramide galactosyltransferase is a class I integral membrane protein of the endoplasmic reticulum. J. Biol. Chem. *273*, 25880-25888.

Suzuki,A., Ishizuka,I., Ueta,N., and Yamakawa,T. (1973). Isolation and characterization of seminolipd (1-O-Alkyl-2-O-Acyl-3-[3'-sulfogalactosyl] glycerol) from guinea pig testis and incorporation of {+35}S-sulfate into seminolipid in sliced testis. Japan J. Exp. Japan Journal of Experimental Medicine *43*, 435-442.

Suzuki,Y., Toda,Y., Tamatani,T., Watanabe,T., Suzuki,T., Nakao,T., Murase,K., Kiso,M., Hasegawa,A., Tadano-Aritomi,K., Ishizuka,I., and Miyasaka,M. (1993). Sulfated glycolipids are ligands for a lymphocyte homing receptor, L-selectin (LECAM-1), binding epitope in sulfated sugar chain. Biochemical and Biophysical Research Communications *190*, 426-434.

Tadano-Aritomi,K., Hikita,T., Fujimoto,H., Suzuki,K., Motegi,K., and Ishizuka,I. (2000). Kidney lipids in galactosylceramide synthase-deficient mice. Absence of galactosylsulfatide and compensatory increase in more polar sulfoglycolipids. J. Lipid Res. *41*, 1237-1243.

Tadano-Aritomi,K., Matsuda,J., Fujimoto,H., Suzuki,K., and Ishizuka,I. (2003). Seminolipid and its precursor/degradative product, galactosylalkylacylglycerol, in the testis of saposin A- and prosaposin-deficient mice. J. Lipid Res. *44*, 1737-1743.

Tanphaichitr,N., Bou Khalil,M., Weerachatyanukul,W., Kates,M., Xu,H., Carmona,E., Attar,M., and Carrier,D. (2003). Physiological and biophysical properties of male germ cell sulfogalactosylglycerolipid. In Lipid Metabolism and Male Fertility, S.De Vriese, ed. (Champaign, IL: AOCS Press).

Tanphaichitr,N., Carmona,E., Bou Khalil,M., Xu,H., Berger,T., and Gerton,G.L. (2007). New insights into sperm-zona pellucida interaction: involvement of sperm lipid rafts. Frontiers in Bioscience *12*, 1748-1766.

Tanphaichitr,N., Smith,J., and Kates,M. (1990). Levels of sulfogalactosylglycerolipid in capacitated motile and immotile mouse spermatozoa. Biochem. Cell Biol. *68*, 528-535.

Tantibhedhyangkul,J., Weerachatyanukul,W., Carmona,E., Xu,H., Anupriwan,A., Michaud,D., and Tanphaichitr,N. (2002). Role of sperm sufrace arylsulfatase A in mouse sperm-zona pellucida binding. Biology of Reproduction *67*, 212-219.

Towbin,H. and Gordon,J. (1984). Immunoblotting and dot immunobinding-current status and outlook. Journal of Immunological Methods *72*, 313-340.

Tulsiani,D.R., Skudlarek,M.D., Araki,Y., and Orgebin-Crist,M.C. (1995). Purification and characterization of two forms of beta-D-galactosidase from rat epididymal luminal fluid: evidence for their role in the modification of sperm plasma membrane glycoprotein(s). Biochem. J. *305 (Pt 1)*, 41-50.

Tupper,S., Wong,P.T.T., Kates,M., and Tanphaichitr,N. (1994). Interaction of divalent cations with germ cell specific sulfogalactosylglycerolipid and the effects on lipid chain dynamics. Biochemistry *33*, 13250-13258.

van der Spoel,A.C., Jeyakumar,M., Butters,T.D., Charlton,H.M., Moore,H.D., Dwek,R.A., and Platt,F.M. (2002). Reversible infertility in male mice after oral administration of alkylated imino sugars: a nonhormonal approach to male contraception. Proc. Natl. Acad. Sci. U. S. A *99*, 17173-17178.

von Figura,K., Gieselmann,V., and Jaeken,J. (2001). Metachromatic Leukodystrophy. In The Online Metabolic & Molecular Bases of Inherited Disease, The McGraw-Hill Companies), pp. 3695-3724.

Walkey,C.J., Donohue,L.R., Bronson,R., Agellon,L.B., and Vance,D.E. (1997). Disruption of the murine gene encoding phosphatidylethanolamine N-methyltransferase. Proc. Natl. Acad. Sci. U. S. A *94*, 12880-12885.

Wassarman,P.M. (2005). Contribution of mouse egg zona pellucida glycoproteins to gamete recognition during fertilization
4. J. Cell Physiol *204*, 388-391.

Weber,J.E., Russell,L.D., Wong,V., and Peterson,R.N. (1983). Three-dimensional reconstruction of a rat stage V Sertoli cell: II. Morphometry of Sertoli--Sertoli and Sertoli--germ-cell relationships. Am. J. Anat. *167*, 163-179.

Weerachatyanukul,W., Probodh,I., Kongmanas,K., Tanphaichiatr,N., and Johnston,L.J. (2007). Visualizing the localization of sulfoglycolipids in lipid raft domains in model membranes and sperm membrane extracts. Biochim. Biophys. Acta *in press*.

Weerachatyanukul,W., Rattanachaiyanont,M., Carmona,E., Furimsky,A., Mai,A., Shoushtarian,A., Sirichotiyakul,S., Ballakier,H., Leader,A., and Tanphaichitr,N. (2001a). Sulfogalactosylglycerolipid is involved in human gamete interaction. Molecular Reproduction and Development *60(4)*, 569-578.

Weerachatyanukul,W., Sobhon,P., and Tanphaichitr,N. (2001b). Localization of arylsulfatase-A in mouse testicular germ cells and epididymal sperm. Biology of Reproduction *64, Suppl. 1*, 220, Abstract.

Weerachatyanukul,W., Xu,H., Anupriwan,A., Carmona,E., Wade,M., Hermo,L., da Silva,S.M., Rippstein,P., Sobhon,P., Sretarugsa,P., and Tanphaichitr,N. (2003). Acquisition of arylsulfatase A onto the mouse sperm surface during epididymal transit. Biol. Reprod. *69*, 1183-1192.

White,D., Weerachatyanukul,W., Gadella,B., Kamolvarin,N., Attar,M., and Tanphaichitr,N. (2000). Role of sperm sulfogalactosylglycerolipid in mouse sperm-zona pellucida binding. Biology of Reproduction *63*, 147-155.

Williams,C.J. and Schultz,R.M. (2006). Transgenic RNAi: a tool to study testis-specific genes. Mol. Cell Endocrinol. *247*, 1-3.

Wong,V. and Russell,L.D. (1983). Three-dimensional reconstruction of a rat stage V Sertoli cell: I. Methods, basic configuration, and dimensions. Am. J. Anat. *167*, 143-161.

Wu,A., Anupriwan,A., Iamsaard,S., Chakrabandhu,K., Santos,D.C., Rupar,T., Tsang,B.K., Carmona,E., and Tanphaichitr,N. (2007). Sperm surface arylsulfatase A can disperse the cumulus matrix of cumulus oocyte complexes. J Cell Physiol *213*, 201-211.

Yamato,K., Handa,S., and Yamakawa,T. (1974). Purification of arylsulfatase a from boar testis and its activities toward seminolipid and sulfatide. Journal of Biochemistry *75*, 1241-1247.

Yanagimachi,R. (1994). Mammalian fertilization. In The Physiology of Reproduction, E.Knobil, ed. (New York: Raven Press Ltd.), pp. 189-317.

Yanagimachi,R., Kamiguchi,Y., Mikamo,K., Suzuki,F., and Yanagimachi,H. (1985). Maturation of spermatozoa in the epididymis of the Chinese hamster. Am. J. Anat. *172*, 317-330.

Yeung,C.H., Schroter,S., Wagenfeld,A., Kirchhoff,C., Kliesch,S., Poser,D., Weinbauer,G.F., Nieschlag,E., and Cooper,T.G. (1997). Interaction of the human epididymal protein CD52 (HE5) with epididymal spermatozoa from men and cynomolgus monkeys. Mol. Reprod. Dev. *48*, 267-275.

APPENDIX I

Mouse CGT peptide was scored for their antigenicity, hydrophilicity, and structure using MacVector software program version 7.0.

Antigenicity Profiles

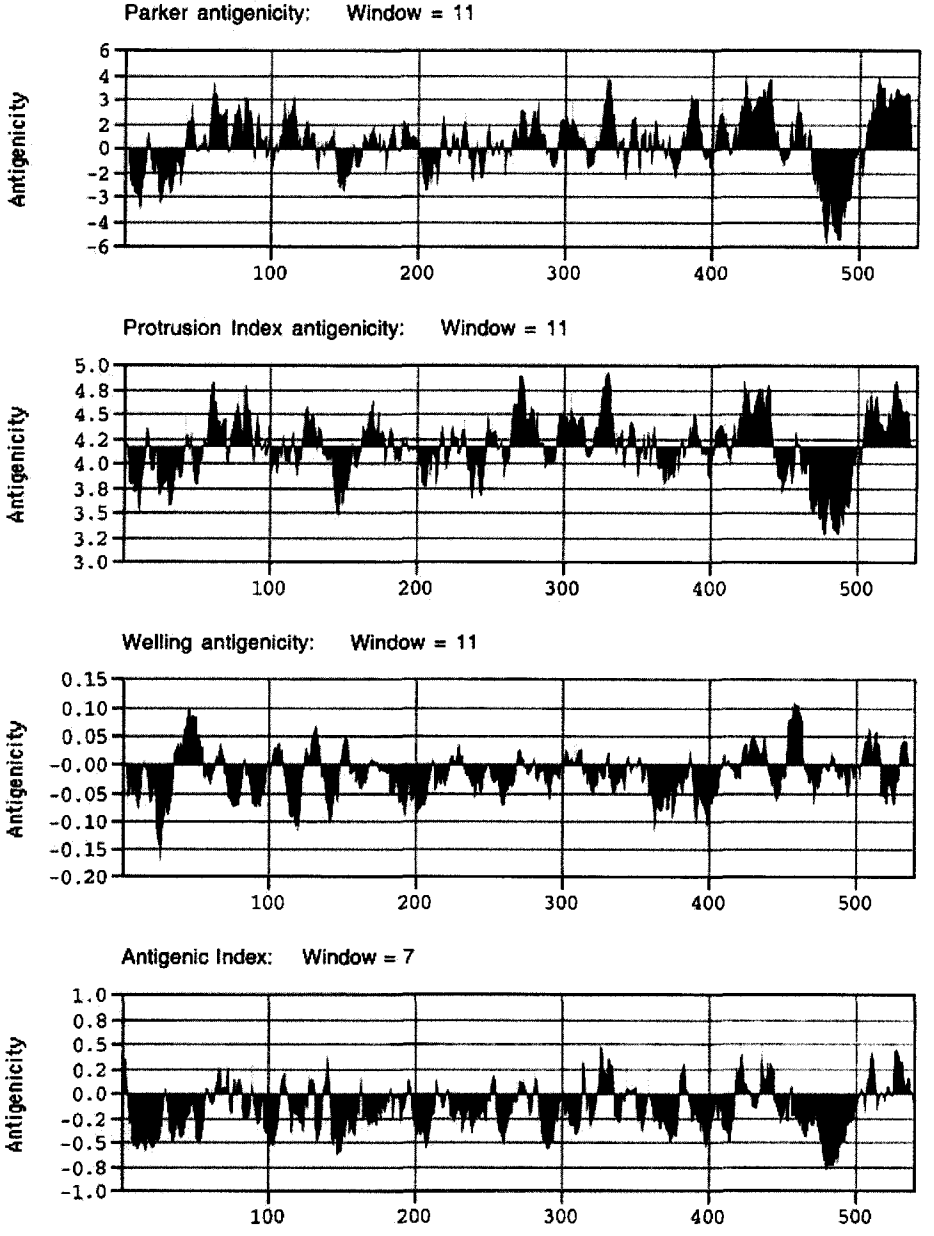

Hydrophilicity Profiles

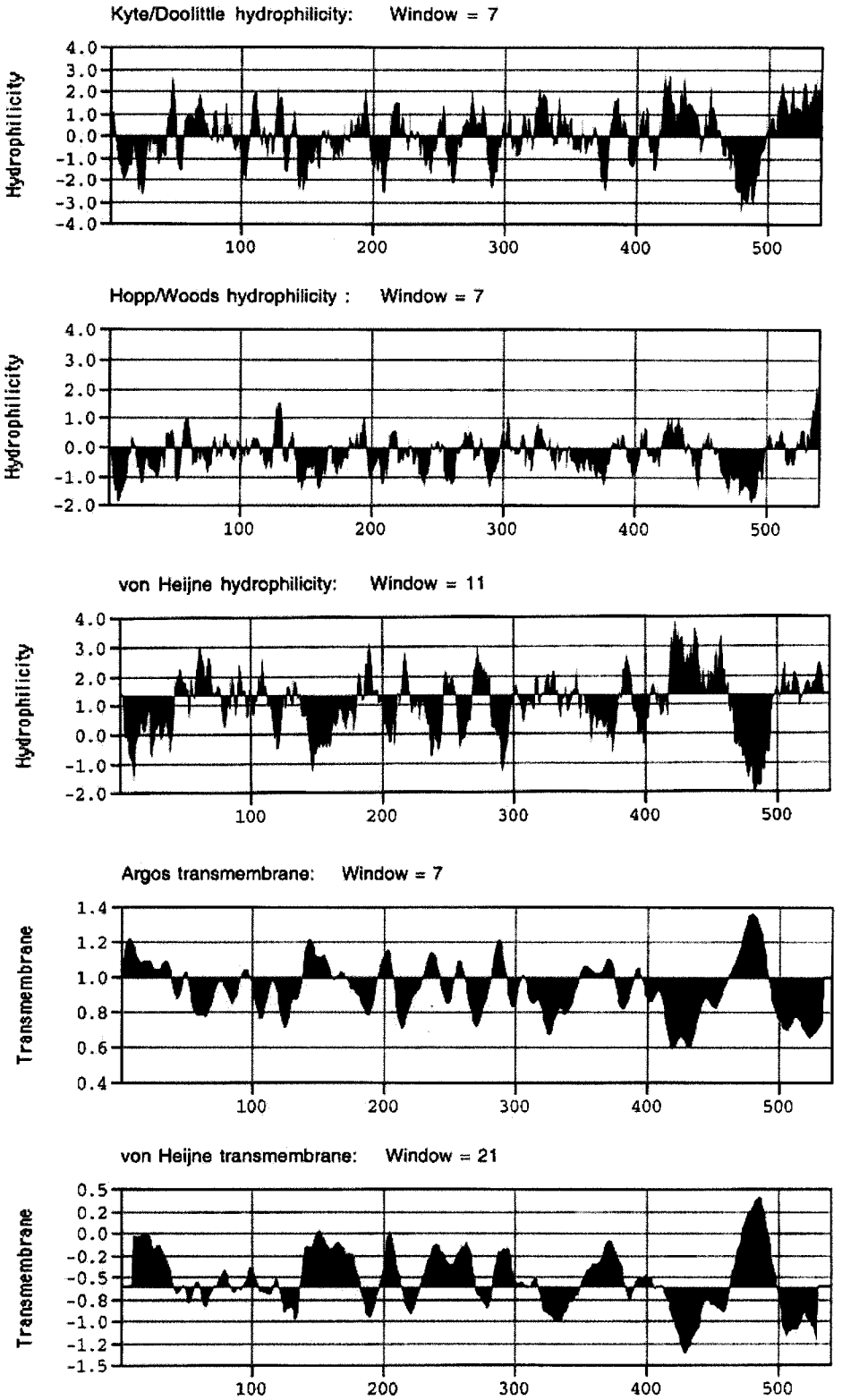

Structure Analysis Profiles

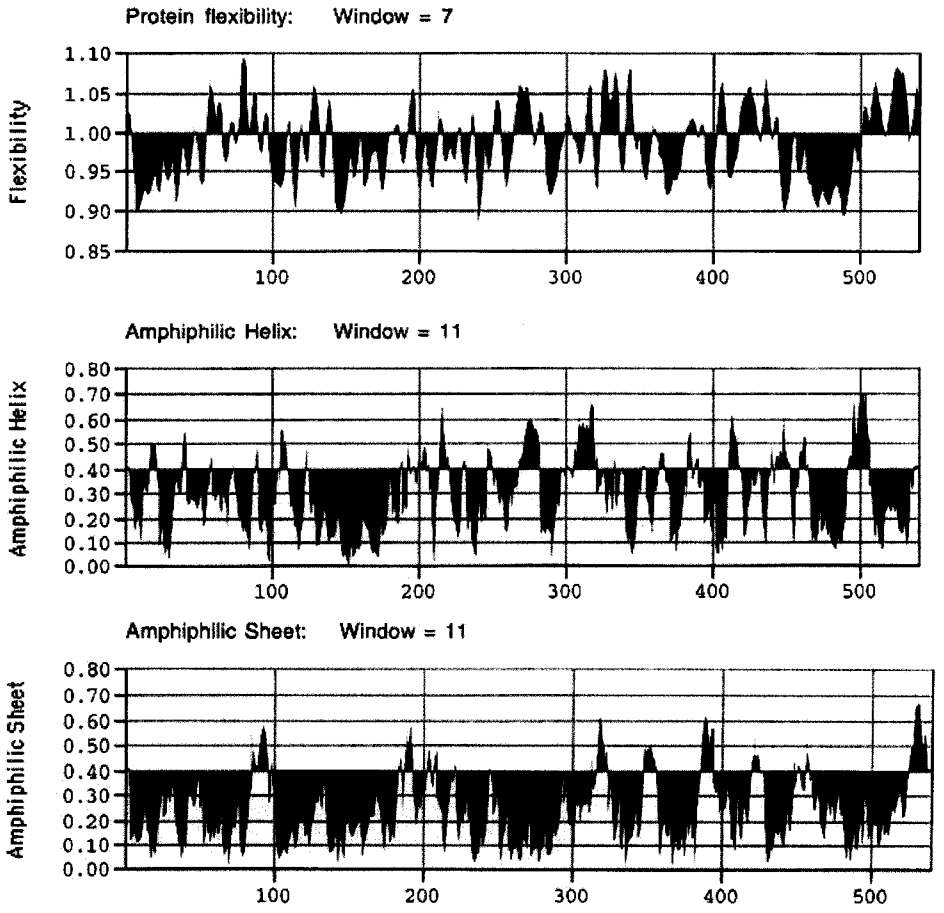

APPENDIX II

Quantification of SGG in wild type and *Cgt*$^{+/-}$ testes by ESI-MS using deuterated SGG as the internal standard

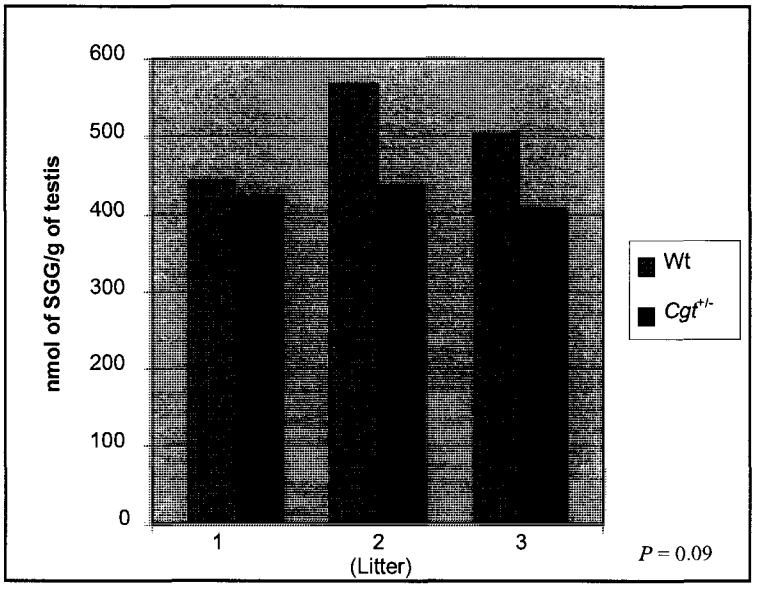

The average SGG levels in *Cgt*$^{+/-}$ and wild type testes were 421.50 ± 14.54 and 503.11 ± 64.25 nmol/g of wet tissue, respectively. The Student's *t*-test analysis revealed no significant difference between the two sets of data ($P = 0.09$).

CURRICULUM VITAE

KESSIRI KONGMANAS

Work Address:
Ottawa Health Research Institute
Civic Campus
725 Parkdale Avenue
Ottawa, ON
K1Y 4E9
Tel. (613)798-5555x13511

Home Address:

E-mail address:

PERSONAL DATA:

Birth date:	September 4, 1982
Birthplace:	Kanchanaburi, Thailand
Marital Status:	Single

EDUCATION:

2006-Present	A M.Sc. student in the Department of Biochemistry/Microbiology/Immunobiology, Faculty of Science, University of Ottawa [Courses taken: Advanced Topics in Systems Biology (BCH 8110) and Advanced Topics in Structure and Function of Plasma Proteins (BCH 8107)]
2004 – 2006	A special student in the Department of Biochemistry/Microbiology/Immunobiology, Faculty of Science, University of Ottawa [Courses taken: General Intermediary Metabolism (BCH 3120), Special Topics in Biochemistry I&II (BCH 8165, BCH 8166), Macromolecules (BCH 4122) and Cell Regulation and Control (BCH 4125)]
2004 (Fall)	A graduate student in the Department of Biochemistry/Microbiology/Immunobiology, Faculty of Science, University of Ottawa [Course taken: Macromolecules (BCH 4122)]

2000-2004	An undergraduate student in the Department of Zoology, Faculty of Science, Kasetsart University, Thailand, graduated with a B.Sc. (Hons), valedictorian, G.P.A. 3.84
1997-1999	GRADE 10-12, Sriboonyanon School, Nonthaburi, Thailand, G.P.A. 3.96
1994-1996	GRADE 7-9, Thamakawittayakom School, Kanchanaburi, Thailand, G.P.A. 3.78
1988-1993	GRADE 1-6, Siriwittayanubal School, Kanchanaburi, Thailand, G.P.A. 4.00

SCHOLARSHIPS AND AWARDS:

In Canada

- The first prize for poster presentation in the M.Sc. student category at the Ottawa Reproductive Biology Workshop in May 2006

- The Larry Ewing Memorial Trainee Travel Fund (LEMTTF) for the Society for the Study of Reproduction meeting held on July 29 – August 1, 2006 at Omaha, Nebraska, USA

In Thailand

- "The Development and Promotion of Science and Technology Talented Project (DPST)", Thailand, scholarship for 6 years (2004-2010) of graduate study abroad covering all tuition and fees, textbooks, stipend, travel expenses and research bench fees. This scholarship project is jointly administered in Thailand by the Ministry of Education, the Ministry of Science, Technology and Environment and the Institute for the Promotion of Teaching Science and Technology (IPST).

- The DPST scholarship for high school and undergraduate study in Thailand (1997-2003). DPST scholarships are awarded annually to 60 grade 9 students and 120 grade 12 students who have demonstrated outstanding talent in science and technology.

- The award from the Commission on Higher Education, Ministry of Education, Thailand entitled "The Best and the Brightest" Project. This award was given to 90 selected students who were divided into three groups. Each group visited organizations in a different part of the USA. The third group (my group) visited government organizations, private companies and universities in San Francisco and Los Angeles, California, USA, 2004

- The annual award from the Faculty of Science, Kasetsart University, for outstanding science students in each department, based on the highest G.P.A. The students trained for two weeks in the laboratories of the Faculty of Science, University of Strathclyde, in collaboration with the Faculty of Science, Kasetsart University, 2003

- The award from the Faculty of Science, Kasetsart University, for the best poster presentation in the senior project poster presentation contest, 2004

- The award from the Department of Zoology, Faculty of Science, Kasetsart University, for the best oral and poster presentation in the annual departmental seminar, 2004

- Medal awards from Kasetsart University (2001-03), given each year to high-ranking students in each Faculty

- "The Professor Dr. Tab Nilanidhi Foundation" medal award for the highest ranking senior science student at Kasetsart University, 2004

- "The Professor Dr. Tab Nilanidhi Foundation" medal award for the highest ranking freshman science student at Kasetsart University, 2000

- Medal for high moral value from the Buddhist Association of Thailand, under the patronage of the King of Thailand, 1999

RESEARCH PROJECT:

Current M.Sc. research project (under Dr. Nongnuj Tanphaichitr's supervision):
Significance of Sulfogalactosylglycerolipid (SGG) in Male Fertility: Studies Using *Cgt* Heterozygous Mice.
(The thesis has been submitted for evaluation.)

In Thailand
Defining Suitable Conditions for Sperm Reactivity of the Freshwater Pearl Mussel, *Hyriopsis* (*Hyriopsis*) *bialatus* Simpson, 1900
(This was my 4th year senior project at Kasetsart University.)

PUBLICATIONS:

Weerachatyanukul W, Probodh I, Kongmanas K, Tanphaichitr N, and Johnston L. Visualizing the Localization of Sulfoglycolipids in Lipid Raft Domains in Model Membranes and Sperm Membranes Extracts. *Biochimica et Biophysica Acta* 1768 (2007):299-310.

Anupriwan A, Schenk M, Kongmanas K, Vanichviriyakit R, Santos DC, Wu A, Yaghoubian A, Berger T, Nyholm P-G, Faull KF, Sretarugsa P, Tanphaichitr N. Presence

of Arylsulfatases in Mouse Ovaries: Localization of Arylsulfatase A to the Corpus Luteum. *Endrocrinology,* provisionally accepted.

Franchini L, Panza L, Kongmanas K, Tanphaichitr N, Faull KF, Ronchetti F. An Efficient and Convenient Synthesis of Deuterium-labelled Seminolipid Isotopomers and Their ESI-MS Characterization. *Chem Phys Lipids*, provisionally accepted.

OTHER INTERNATIONAL EXPERIENCE:

2004 (19 Apr-31 Aug)	Trained in research as a summer student at the Ottawa Heath Research Institute, Canada, for 4.5 months
2003 (9-23 Nov)	Visited government organizations, private companies and universities in San Francisco and Los Angeles, California, USA (e.g., California Department of Transportation, NASA Jet Propulsion Laboratory, University of California at Berkeley, Stanford University, and Caltech University). The aim of these visits was to widen the vision of the high-potential Thai students and give them the opportunity to apply new ideas for further development in Thailand. These visits were part of the award, "The Best and the Brightest" Project of the Commission on Higher Education, Ministry of Education, Thailand, which was given to 90 selected students from 4th year undergraduate and graduate students from both private and public universities in Thailand.
2003 (13-26 Oct)	Trained in determination of monosaccharides of the serum glycoprotein, alpha-1-acid glycoprotein (AGP), by using high pH anion exchange chromatography at the Department of Bioscience, University of Strathclyde, Scotland. This training was part of the award for outstanding science students of the Faculty of Science, Kasetsart University.
1998 (5-12 Dec)	Represented Thailand at the SUNBURST Youth Camp in Singapore for academic and cultural exchange among students from ASEAN countries.

EXTRACURRICULAR ACTIVITIES:

2003	Vice President, Faculty of Science student committee, Kasetsart University
2002	President, Department of Zoology student committee, Faculty of Science, Kasetsart University
2002	President, Thai Classical Music Club, Kasetsart University